NOTICE

The quality of this microform is heavily dependent upon the quality of the original thesis submitted for microfilming. Every effort has been made to ensure the highest quality of reproduction possible.

If pages are missing, contact the university which granted the degree.

Some pages may have indistinct print especially if the original pages were typed with a poor typewriter ribbon or if the university sent us an inferior photocopy.

Reproduction in full or in part of this microform is governed by the Canadian Copyright Act, R.S.C. 1970, c. C-30, and subsequent amendments.

AVIS

La qualité de cette microforme dépend grandement de la qualité de la thèse soumise au microfilmage. Nous avons tout fait pour assurer une qualité supérieure de reproduction.

S'il manque des pages, veuillez communiquer avec l'université qui a conféré le grade.

La qualité d'impression de certaines pages peut laisser à désirer, surtout si les pages originales ont été dactylographiées à l'aide d'un ruban usé ou si l'université nous a fait parvenir une photocopie de qualité inférieure.

La reproduction, même partielle, de cette microforme est soumise à la Loi canadienne sur le droit d'auteur, SRC 1970, c. C-30, et ses amendements subséquents.

ISBN 0-315-53854-6

IN-PLANE SHEAR PROPERTIES OF ADVANCED COMPOSITE MATERIALS FOR AEROSPACE APPLICATIONS

STEPHEN KIM-LON LEE

A Thesis submitted to the Faculty of Graduate
Studies and Research in partial fulfillment
of the requirement for the degree of
Master of Applied Science

Department of Mechanical Engineering
University of Ottawa
Ottawa, Canada

ABSTRACT

The thesis begins with a comprehensive literature review of all the commonly used in-plane shear test methods for advanced composite materials. Four criteria (cost of fabrication, cost of testing, data reproducibility and accuracy of experimental results) are used to assess each test method . Using a decision analysis technique, Iosipescu, ±45° off-axis tensile and 10° off-axis test methods are identified for use in this study. A brief survey of the micromechanical analysis techniques which have been proposed by various investigators to predict the in-plane shear moduli and strengths is also presented.

Three relatively new polymer matrix systems(Narmco Rigidite 5245C. Hexcel F584 and American Cyanamid Cycom 1806 epoxy resins) reinforced with high strain-to-failure, intermediate modulus, Hercules IM6 carbon fibres were investigated as well as an older system (Narmco Rigidite 5208 reinforced with T300 carbon fibres) which formed a baseline for this study. Processing techniques and specimen preparation and testing procedures are described in detail. Machining of the notches of the Iosipescu specimen and the development of testing techniques for this specimen are highlighted.

Results obtained from three test methods are compared with the theoretical predicted values. The Halpin-Tsai's approach is the most desirable technique for predicting the in-plane shear modulus of these advanced composite materials. The Iosipescu shear test method is the most appropriate test method for determining the in-plane shear modulus required for the classical laminate analysis of these composites . Further research efforts are needed for developing more accurate predictive theories for the in-plane shear strength of advanced composite materials.

ACKNOWLEDGEMENT

The author wishes to express special appreciation to Dr. M. Munro for his valuable supervision and guidance through the course of this study. Also, he wishes to extend his very sincere thanks to Dr. W. Wallace and Mr. R.F. Scott of the Structures and Materials Laboratory, National Aeronautical Establishment, National Research Council of Canada, for their support of this study and permit him to use part of the in-house research project on advanced composite materials for his graduate study. Further , the author would like to thank the staff of the composite materials group of the Structures and Material Laboratory for their technical help.

Table of Contents

List of Figures

List of Tables

Chapter 1

INTRODUCTION

1.1 Advanced Composite Materials

Composites are considered to be a combination of materials differing in composition or form on a macro-scale. The constituents retain their identities in the composite; that is , they do not dissolve or otherwise merge completely into each other, although they act in concert. Normally, the components can be physically identified and lead to an interface between components. They usually exhibit the best qualities of their constituents and often some qualities that neither constituent possesses. The main advantages of the composite materials are: high strength-to-density, high stiffness-to-density, formable to complex shapes and tailorable mechanical and thermal properties.

Composite materials are normally classified into three types:

1. Fibrous composites which consist of long or short fibres in a matrix;

2. Particulate composites which are composed of particles in a matrix;

3. Laminated composites which consist of layers of unidirectional fibrous composite materials (Figure 1.1).

The composite materials used in this study are so-called "advanced composite materials" since the reinforcements are carbon fibres which have greater strength and stiffness properties than those of glass fibres. At present, the application of advanced composite

materials in secondary and primary structures for civil and military aircraft are mostly made with laminated composites (Figure 1.1). Basically secondary structures (e.g. access doors and wing body fairings) are not flight critical. Primary structures (e.g. wing and rudder)are safety critical and failure may lead to loss of the aircraft.

1.2 Problem Definition

The efficient use of advanced composite materials for primary structures of aerospace vehicles requires the accurate determination of the composite materials' response to thermal and mechanical loads (tensile, compressive and shear) . Basic material properties which are required for micromechanical analysis, structural design and analysis and quality control are determined by mechanical testing. The testing of advanced composite materials is generally more complicated than for the more common homogeneous, isotropic materials because composites behave in much more complicated fashion due to a macroscopic anisotropic effect (properties depending upon orientation), and lamination effects(various other coupling effects-linking a side effect to a principal effect). Additional required tests arise from the anisotropic and heterogeneous nature of composites. Even for the simplest case of a homogeneous orthotropic material (the assumption made for the individual layer of a laminated fibrous composite material), a minimum of four independent elastic constants (E_{11} ,E_{22} ,ν_{12} and G_{12}) must be determined for complete in-plane characterization (Figure 1.2). The complete characterization of in-plane elastic constants and strength properties of a fibre composite may also require a large number of tests because the behaviour in tension of heterogeneous materials is frequently very different from that in compression. The determination of in-plane shear modulus (G_{12}) and strength (τ_{12}) of fibre composites requires an independent test.

It is well known that accurate determination of shear properties for advanced composite materials (elastic modulus,nonlinear stress-strain behaviour and shear strength) presents a particular problem. The problem stems from a difficulty in obtaining a pure shear stress state for a defined specimen geometry and loading condition. There have been

numerous attempts to develop reliable test methods (Chapter 2) to determine the in-plane shear stress-strain response for fibre composites. Some of these tests are appropriate for determining the in-plane shear modulus but not the ultimate shear strength. Each of these test methods has its relative advantages, disadvantages and areas of validity. From an applied mechanics point of view, the thin-walled tube appears to be the most desirable specimen for shear tests. On the practical side, however, the tube is too expensive and often difficult to fabricate and test . Because of these disadvantages of the tube, considerable efforts have been made to develop flat shear specimens for fibre composites. It is generally recognized that an ideal shear test method is one which is relatively simple to conduct, requires small, easily fabricated specimens, and is capable of measuring both shear strength and shear modulus simultaneously. It is difficult, however, to devise a test method which incorporates all of above.

The overall purpose of this work was to evaluate the in-plane shear test methods in order to determine which technique is best suited for measuring the shear properties of four composite material systems. Three relatively new polymer matrix systems (Narmco Rigidite 5245C, Hexcel F584 and American Cyanamid Cycom 1806 toughened epoxy resins) reinforced with high strain-to- failure, intermediate modulus, Hercules IM6 carbon fibres were selected, as well as an older system (Narmco Rigidite 5208 reinforced with T300 carbon fibres) which formed a baseline for material mechanical property data. A common characteristic of the tougher resin systems is their greater ductility and higher strain to failure compared to the currently used 5208 epoxy resin. Composite materials made with these epoxy resins have improved resistance to impact damage and delamination as compared with the baseline material.

1.3 Thesis Overview

In Chapter 2 all the commonly used in-plane shear test methods for advanced composite materials are examined and discussed. Four criteria (cost of fabrication, cost of testing, data reproducibility and accuracy of experimental results) are used to assess each test

method. Using a decision analysis technique, three test methods ($\pm 45^{\circ}$ off-axis tensile , 10° off-axis tensile and Iosipescu) are identified for use in the experimental phase of this study.

In Chapter 3 three basic micromechanical approaches (strength-of-materials, semi-empirical and elasticity) for predicting the in-plane shear modulus of advanced composite materials are reviewed and seven predictive techniques are presented and discussed. Two methods for predicting the in-plane shear strength are also briefly reviewed.

In Chapter 4 fabrication procedures , processing and vacuum bagging techniques and curing cycle for each composite material are presented and described in detail. The machining of specimens is described including the development of machining techniques for the Iosipescu specimen which are presented in detail.

In Chapter 5 experimental procedures and data reduction techniques are presented. This chapter also describes in detail how the testing procedures for the Iosipescu specimen were developed.

In Chapter 6 theoretically predicted results and experimental results for in-plane shear modulus and strength are compared and discussed.

Chapter 7 contains the conclusions of the study and some recommendations for further investigation.

Chapter 2

EVALUATION OF THE IN-PLANE SHEAR TEST METHODS BY THE DECISION ANALYSIS TECHNIQUE

2.1 Introduction

Of the many shear test methods available, some provide qualitative data while others provide quantitative data. Qualitative shear test methods are mainly for quality control and material screening. They generally provide comparative values of shear modulus and shear strength. Qualitative shear test methods are used to accurately determine the complete shear stress-strain response of composite materials.

The ideal quantitative shear test method should provide a region of pure, uniform shear stress. In addition, there should be a unique relationship between the applied load and the magnitude of the shear stress in the test section. Further, for accurate determination of the shear stress-strain response, the test section should be one of maximum shear stress relative to all other regions of the specimen.

Based on the published literature, all the existing in-plane shear test methods are

examined and discussed in detailed in this chapter. This chapter also gives an assessment (using a decision analysis technique) of all the shear test methods and concludes that three test methods are worthy of further study. The results of this analysis have also been published [1].

2.2 In-Plane Shear Test Methods

2.2.1 Introduction

The following sections present detailed descriptions and discussions of the major papers for each in-plane shear test method. Many investigators have evaluated and compared the various in-plane shear test methods for fibre composite materials. Since the various authors have not all compared the same test methods, some overlap occurs between the following sections.

2.2.2 Two and Three Rail Shear

The 2-rail shear specimen test and fixture (Figure 2.1) has been used quite extensively for advanced fibre composite materials in the aerospace industry. This method consists of clamping or bolting the long sides of a rectangular specimen to steel rails while the remaining sides are not constrained. The load is introduced at the ends of the rails to displace one rail parallel to the other.

Whitney et al[2] conducted an extensive theoretical stress analysis of the 2-rail specimen using a Fourier series solution. they concluded that this test method is valid for measuring the shear modulus of laminated composites provided that the length/width ratio is at least 10. For determining the in-plane shear strength, they found that an additional necessary condition was that the effective Poisson's ratio of the laminate with respect to the specimens edges should be less than unity. In the case of laminates having a high effective Poisson's ratio (such as $\pm 45°$ angle- ply composites) the shear stress distribution is very irregular and leads to extremely low values of shear strength as determined by

this test method. They recommended that if this test method is used to obtain design allowables in shear, it must be used in conjunction with the proper laminate orientations or the designer will pay an unnecessary penalty by using values which are far too conservative thus resulting in over design of the structure.

A two-dimensional linear elastic finite element model was used by Garcia et al [3] to analytically determine how various geometric parameters influenced the magnitude and distribution of in-plane normal and shear stresses in a 2-rail shear specimen. They concluded that: (1) the direction of loading (axial or diagonal) has little effect on the stress distribution within the specimens, (2) the aspect ratio of the specimen can have a major effect on the stress distribution (this varies according to the laminate) and(3) very high normal stresses occur perpendicular to the filaments in the 0° oriented specimen and, in fact, initiate premature failures relative to the 90° specimen.

Sims [4] believed that a better approximation to a state of pure shear can be obtained using the 3-rail shear test method (Figure 2.2), since the compressive load is applied parallel to the clamped edges of the specimen. Another advantage of this configuration is that two independent calculations of the shear stress-strain response can be made from one specimen.

Bergner et al[5] investigated the 3-rail shear test method using finite element analysis and concluded that the rail configurations produce regions of uniform shear stress over most of the test sections for all laminates studied. However, this area of uniform shear stress was often accompanied by significant normal stresses depending upon the stiffness of the rails, the method of load application, and the laminate properties. Significant axial stress was always present in the test section for elastic rails axially loaded. The magnitude of this axial stress was approximately inversely proportional to the stiffness of the rails. Stress concentrations in the vicinity of the corners were found in all specimens.

Based on the results of the ASTM round robin on the 2 and 3-rail shear tests for laminated fibre composites [6], reported in 1981, Subcommittee D-30.04 on Composites made the following conclusions: (1) the variation in averages was great enough to cast doubt on the validity of the data as the tests are now run and (2) the spread of the data

between the two test systems(2 or 3 rails) did not indicate a preferred test system.

2.2.3 ±45° Off-Axis Tensile

The ±45° off-axis tension coupon is a simple test specimen for obtaining the linear and nonlinear shear stress- strain response in the lamina co-ordinate axes. The specimen is a [±45°]s (+45°/ − 45°/.../ − 45°/+45°) tension coupon [ASTM D-3518](In-plane shear stress-strain response of unidirectional reinforced plastic) usually with end tabs (Figure 2.3). Through the use of relations derived from laminated plate theory, Rosen[7] developed expressions which allow the in-plane 0° shear stress-strain curve to be generated from the longitudinal and transverse stress-strain curves obtained from a uniaxial tension test of the ±45° laminate.

The stress-strain results of a ±45° laminate test have been compared to those from the cross-beam test by Petit [8] (see para 2.5). He found close agreement between the two tests except for the nonlinear portion of the curve beyond the design allowable. He pointed out though that there were two approximations which were inherent with this test method. Firstly, since the laminate Poisson's ratio is not exactly 1.0 and hence ϵ_x is not quite equal to the negative of ϵ_y , the strain state at ±45° to x-y axes is not quite pure shear. Secondly, small tensile strains exist in addition to the relatively large shear strains in the principal directions of the laminae. This results in tensile stress existing in the longitudinal and transverse directions of the laminae. Rosen[7] also suggested that the existence of an edge effect problem in the ±45° laminate requires care in the choice of the specimen width in order to obtain the desired accuracy of measurement.

Sims [4] found good agreement between the stress-strain response of ±45° tensile and 3-rail shear test specimens with glass fibre/epoxy composites. There was reasonably good agreement between the results of ±45° tensile tests and torsional tube tests (see para 2.7) performed by other workers for carbon fibre/epoxy composites.

Hahn [9]pointed out that the practice of equating $\frac{1}{2}\sigma$ to τ_{12} can be allowed only if there is no shear coupling (linear or nonlinear) even for symmetric laminates. He also concluded that the simple ±45° angle-ply will produce acceptable results provided that the layers are

stacked in as homogeneous an arrangement as possible.

Chiao et al [10] strongly recommended the $\pm 45^{\circ}$ specimen for determining the stress-strain response curve. They found good agreement with the tubular specimen up to failure. Based on the experimental results obtained in the study, they concluded that the $\pm 45^{\circ}$ tensile specimen has the following merits: good reproducibility, simple to make, is a conventional tensile test, economical in material, requires simple data reduction and is easy to test at high or low temperatures. Most of the above advantages were also verified by Greszczuk [11], Terry [12] and Yeow and Brinson [13].

2.2.4 10° Off-Axis Tensile

The 10° off-axis tension coupon is another simple specimen similar in geometry to the $[\pm 45^{\circ}]_s$ tension coupon. The laminate is unidirectional with fibres oriented at 10° to the tensile load axis (Figure 2.4). A biaxial stress state occurs when a 10° off-axis specimen is subjected to a uniaxial tensile load. This biaxial stress state consists of three stresses: longitudinal, transverse and in-plane shear on the 10° plane. Chamis and Sinclair's [14], [15] theoretical and experimental investigations led to the conclusion that when the 10° off-axis tensile specimen fails, the in-plane shear stress is near its critical value and he recommended the 10° off-axis tensile specimen for measuring in-plane shear strength of unidirectional fibres composites. Based on their study, they listed the following advantages of this test method: (1) specimens have uniform shear stress through the thickness, (2) can be adapted to testing for environmental and elevated temperature effects, (3) can be readily used for fatigue testing and dynamic and impact loading characterization, (4) specimens are free of laminate residual stresses and (5) the in-plane shear strain reaches or approaches its maximum value when the angle between the load and fibre directions is about 10° for graphite/epoxy composites.

The in-plane shear stress of the 10° off-axis tensile specimen is very sensitive to small misorientation errors. It is generally recommended that fibre direction, strain-gage positioning and load alignment be kept within $\pm 1^{\circ}$. However, the misorientation is not critical if the fracture in- plane shear strain is sought since the strain peaks at a load angle of

about 10° and is insensitive to small errors about this angle.

Yeow and Brinson [13] have made a comparison of the shear responses for various test methods and concluded that a 10° off-axis test together with incremental lamination theory calculations is a reasonable approach to shear property determination. They suggested that the 10° off-axis test represents the best method of those investigated for the determination of the shear response of a ply or lamina.

Chiao et al [10] evaluated this method with aramid fibre/epoxy composite material and found that the 10° off-axis tensile shear test resulted in significant shear coupling and that it gave a higher shear modulus, lower failure stress, and lower failure strain than the ±45° off-axis laminate tensile shear test.

A theoretical investigation of the 10° off-axis tensile test method was conducted by Chamis and Sinclair [15] to study the fracture characteristics of unidirectional fibre composites subjected to an off-axis tensile load. The predicted results using composite mechanics were in very good agreement with measured data for modulus, Poisson's ratio, and shear coupling coefficient. However, the results obtained using the finite element method indicated that the axial strain variation is very sensitive to out-of-plane bending and twisting eccentricities as small as about one ply thick. They recommended that the in-plane and out-of-plane effects should be taken into account in interpreting experimental data.

2.2.5 Cross-Beam Sandwich

The cross-beam shear specimen has been used for determining shear stress-strain response as well as ultimate shear strength values for fibre composite laminates. The cross-beam shear specimen is loaded in positive and negative values of bending to produce a biaxial state of tension and compression over the test area at the centre of the specimen. The composite material facings are thin relative to the honeycomb core and thus are located at a large distance, relative to the facing thickness, from the mid- plane of the sandwich plate. The composite material is presumed to be subjected to an in-plane shear over the test section. Laminates commonly used with the cross beam are [0°/90°], and [±45°], (Figure 2.5).

Fibre orientation and core reinforcement significantly influence the stress distribution present in the test section. The actual stress state predicted by analysis by Duggan et al [16] can deviate considerably from predictions based upon an elementary bending moment analysis. In a pure shear condition, the maximum shear stress planes must be free of normal stresses. Analysis of the $[\pm 45°]_s$ laminates of the cross- beam test revealed significant normal stresses, resulting in errors of 13 to 20 percent in shear strength. Surprisingly, the normal stresses are greater in the test section than those applied away from that region. Duggan attributes this phenomenon to corner effects.

2.2.6 Picture Frame Panel

The specimen (see Figure 2.6) for this shear test consists of one or two thin flat square panels bonded to a honeycomb core material for stability. A rigid four-bar linkage frame is then bolted or bonded to the panel for load introduction. In order to reduce high corner stresses, these areas are usually cut out and have doublers bonded on or near the resulting free edges. The load is introduced by a combination of tension and/ or compression forced in pairs on opposite corners. Thus, the specimen is subjected to shear loading along planes at 45° to the diagonals.

Bryan [17]made a photoelastic investigation of the stress distribution in the panels and found that the stress distribution deviated substantially from pure shear, thus the method is not appropriate for measuring the in-plane shear modulus. However, Bryan showed that at the critical region (which is along the edge) the stress state was essentially uniform pure shear and thus he recommended that this should be an accurate method for determining the in-plane shear strength.

Using a finite element analysis that included frame and nonlinear effects, Hadcock and Whiteside [18] tested boron/epoxy and boron/aluminium picture frame specimens and reported that the corner stress concentration nevertheless remained significantly high in both experiments. Dastin et al[18] reported that reliable initial shear modulus and ultimate strength values could be obtained from the picture frame specimen for fibreglass $[0°/90°]_s$ laminates.

The panel must be sized to avoid buckling. The following expression for the applied diagonal force, necessary to buckle the panel, has been derived by Davenport and Bert [20].

$$P_{cr} = 1.414\pi^2 K D_y / a \tag{2.1}$$

where a = length of panel side, D_y = transverse flexural rigidity of the panel and K is a dimensionless buckling coefficient which depends upon D_x/D_y.

2.2.7 Thin-Walled Torsion Tube

Whitney and Halpin [21] stated that the torsion tube is the most desirable specimen for determining shear stress/strain response from an applied mechanics standpoint. In this test, a thin-walled circumferentially wound cylindrical tube is subjected to a pure torque about its longitudinal axis (see Figure 2.7). This subjects the wall of the specimen to a pure shear stress which is uniform around the circumference and along the length of the specimen. Since the wall thickness is small compared with the mean radius of the tube, the shear strain gradient through the thickness is negligible. In addition, the specimen has minimal normal stresses in the test section.

The stress distribution of the torsion tube specimen is very desirable, however, Rizzo and Vicario [22] reported that strength values may be influenced by gripping the ends of the tube. Care should be taken to ensure that only pure torque is applied to the specimen; therefore to prevent the development of bending moments, the specimen must be mounted concentrically. Axial forces that result as the specimen undergoes shearing deformation can be prevented by allowing one end of the specimen to move axially. The uniformity of the state of stress produced for tubular laminated specimen depends on the anisotropy as well as the geometry. Hahn and Erikson[23] found that the wall thickness to diameter ratio should be less than 0.03 to ensure fairly uniform stress distribution.

The main drawback to this specimen is the difficulty associated with fabricating and subsequently testing tubular specimens since a sophisticated testing apparatus is required which is not available in most laboratories.

2.2.8 Slotted-Tensile Specimen

Duggan et al [16] proposed a new technique for determining the in- plane shear properties for arbitrary laminae orientations. In this test, standard tensile coupons are modified to provide shear specimens by adding two thin axially oriented slots which terminate 25.4 mm apart along the centreline of the specimen(see Figure 2.8). Tensile and compressive stresses are provided by applying axial and transverse loads in a ratio governed by the specimen width and the distance between slots. The authors used the finite element method to calculate the slotted- tension coupon stresses resulting from mechanical loading and compared the results with those from the cross-beam specimen which was previously analysed for two orthotropic cases. For the $[\pm 45°]_s$ case, the authors reported that the shear stress in the slotted-coupon test section is much closer to the ideal case. The strain gauge result is within 2% of the stress calculated from the applied load. The analysis indicates a shear stress concentration near the edge of the compression load pad, however, the error is less than expected for the cross-beam specimen. The authors found that when a $[0°/90°]_s$ laminate was tested the material failed in tension so the value obtained is not a valid shear result. Very little data is available for evaluation of this new shear test method, thus more studies are required.

2.2.9 Iosipescu's Method

This test method is relatively simple to conduct ,employs small, easily fabricated specimens, and is capable of measuring both shear strength and stiffness. Nicolne Iosipescu of Rumania first proposed this test method in 1967 [24].

The Iosipescu shear test(see Figure 2.9) achieves a state of pure shear stress at specimen mid-length by applying two counteracting moments produced by force couples. A state of constant shear force is induced through the middle section of the test specimen and the induced moments exactly cancel at the mid-length of the test specimen, thus producing a pure shear loading state at that location. The minimum section would have to be at the centreline to obtain maximum shear stress at that location. Such a condition was achieved

by Iosipescu [24] in metal specimens machined with 90° vee-notches at the top and bottom edges, leaving a net section depth at the specimen centreline of one-half of the overall depth. Iosipescu confirmed the uniform state of pure shear by means of photo-elastic stress field measurement on Plexiglass models. The uniform stress state apparently results from the coincidence of the principal stress direction at ±45° to the specimen axis with the 90° notch angle in the region of zero bending stress. There is not a stress singularity at the notch root because of the absence of normal stresses at this point.

Iosipescu's investigation was concerned only with homogeneous, isotropic materials. Finite element analysis carried out by Slepetz et al [25] confirmed that the parabolic and uniform stress distributions deviate somewhat from ideal conditions and may in fact be dependent on material properties. There is a significant stress concentration found at the notch root in unidirectional laminates and it is believed that shear coupling deformations along the notch flank impose a redistribution of stresses at the notch section, resulting in concentration at the root. Bergner et al [5] reported that bonding suitable doublers to the corners and rounding the notch tips can reduce the stress concentrations in critical areas.

Adams and Walrath's results [26] for sheet moulding compound (SMC) composite materials showed that the Iosipescu shear test works well for determining the in-plane and through-the-thickness shear strength of SMC. The shear modulus results obtained for the various SMC materials tested agreed well with values obtained by other investigators using different test methods. Shear strength results obtained with the Iosipescu shear test were somewhat higher than those obtained with rail shear tests.

This test method is not limited to in-plane shear measurements of composite materials. It could be used to determine interlaminar shear properties of laminates and would also appear to be useful for measuring the shear strength of adhesive joints.

2.3 Evaluation of Test Methods by the Decision Analysis Technique

2.3.1 Introduction

The objective of this review is to evaluate the more commonly used test methods for measuring the in-plane shear stress-strain response of advanced composite materials. It is generally recognized that an ideal test method is one which is relatively simple to conduct, requires small, easily fabricated specimens, and is capable of measuring both shear strength and shear stiffness simultaneously. It is difficult, however, to devise a test method which incorporates all of the above.

The detailed discussion of the major test methods for measuring in-plane shear properties in the previous sections indicates the types of problems which may be encountered and the limitations of each test method. Comparing these factors is very difficult in some aspects. Factors which are less important for some test methods become dominant for others. Considering other factors such as the cost of materials, cost of testing, specimen fabrication, and testing equipment required leads to the conclusion that no one test method can be considered best for all applications.

In order to evaluate the test methods for this study from as wide a base as possible, a decision analysis technique has been used. This technique is very useful for the difficult task of evaluating a large number of solutions against a large number of criteria. It allows for assignment of quantitative ratings based upon subjective evaluations. In this section the nine major in- plane shear test methods have ben evaluated with respect to eleven criteria covering the major areas of cost of fabrication, cost of testing, data producibility and accuracy of experimental results. Each test method is numerically rated on a relative basis from 0 to 10 for each criterion. Each criterion is assigned a weight between 0 and a maximum of 200 depending upon how important the authors consider each criterion relative to the others. The criterion score for a test method is the product of the numerical rating and the weight; the total score for the test method is the sum of all of these products.

The actual ratings for this study are given in Table 2.1. The next section discusses the reasons for selecting the individual criteria, their respective weights, and the more critical relative rankings for each test method with respect to individual criteria.

2.3.2 Decision Analysis

Criteria Weighting

At present, advanced composite materials are more expensive than conventional metallic materials. However, the quantities required for making the experimental test coupons are usually small, so the material costs are not a significant factor compared with other factors. Thus, the material quantity criterion is assigned a weight of 20. There are two major processes to manufacture advanced composite materials: prepreg lay-up and wet filament winding. The prepreg materials cured in an autoclave always yield laminates with better controlled thickness and lower void contents. The physical properties of advanced composites made with wet filament winding technique are more difficult to control. The processing equipment criterion was assigned a higher weighting of 50. Because of the differences in the specimen geometry of the different test methods, special processing techniques are required for fabrication. Some of these are costly and time-consuming with the result that specimen processing is weighted at 40. The quality of the machined specimen is important and critical as any damage to the specimen (micro-cracking or delamination) during preparation can lead to unreliable test results. Since the test specimens for all test methods are different in geometry, special machining equipment and techniques are usually required for preparing the specimen with, in some cases, special trimming fixtures. Thus, the specimen preparation criterion also received a weight of 40. Testing equipment plays a very important role in in-plane shear testing. For some types of specimens, the universal test machines are simply not adequate to perform the testing because of the requirement of non-standard loading directions. The testing equipment criterion received a weight of 100. In order to conduct the testing using universal test machines, special testing fixtures are required for some test methods so that loads can be applied at certain areas of the spec-

imen. Handling test procedures and testing time for different test methods vary greatly. Auxiliary instrumentation is required for most test methods in order to obtain the desired measurements. Each of these three final criteria were assigned a weight of 50.

Since the primary objective of all the in-plane shear test methods is to measure the strengths and the stiffness of advanced composite materials, these two criteria are essentially the most important and they are each weighted at 150.

Any useful or meaningful results obtained from experimental work not only rely on the accuracy of measurement and the interpretation of the test data but also depend on the reliability of the test method. It is generally agreed that the thin-wall tube torsion test method is one of the most desirable test methods to determine the in-plane shear properties of composite materials. It is used as a reference by many investigators to evaluate other shear test methods. The accuracy of the experimental results (with respect to the thin-wall tube specimen results) was thus assigned a weight of 200.

Test Method/ Criteria Rating

The rating assigned to each of the nine test methods for each of the 11 criteria are given in Table 2.1. In the following sections on cost of fabrication, cost of testing, data producibility and accuracy of experimental results, some of the more noteworthy ratings are discussed.

Cost of Fabrication

Material Quantity: The thin-walled tube specimen was assigned a very low rating of 1 for the material quantity criterion because the amount of material required for the tube specimen is much more than for the others. The tubes must be long enough to permit the attachment of end plugs for load application and thick enough to minimize handling damage. Due to the size of the complete cross-beam sandwich specimen, a considerable amount of material is required for the specimen, with the result that it was rated at 2. The 10° off-axis tensile shear specimen requires the least amount of material and was assigned a rating of 10.

Processing Equipment: The thin-walled tube and the cross- beam shear test methods

were rated at 8 because of their more complicated geometrical configurations. The remainder of the other test methods were rated at 10.

Specimen Processing: Filament winding or special lay-up techniques are required to fabricate the thin-walled tube specimens, therefore, the tube specimen was rated at 2. The other flat specimens fabricated with conventional hand lay-up techniques were rated at 9 or 10.

Specimen Preparation: In the rail shear tests, specimens are clamped or bolted to the test fixture. To properly align the specimen with the loading direction, a pattern of holes is introduced to the specimen using a special drilling fixture and tools, thus, the rail shear specimen was rated at 6. Because of the relatively simple preparation required, the flat coupon type specimens were rated at 10. The remainder of the test methods were rated a 7 or 8 depending on the test fixture configurations.

Cost of Testing

Testing Equipment: The thin-walled tube specimen was rated at 2 because of the requirement of a torsion device to perform the testing while the other test methods require only a universal test machine.

Special Fixture: The 10° off-axis tensile shear and the $\pm 45°$ tensile shear test do not require any testing fixture and were each rated at 10 in the special fixture criterion. The others were rated differently depending on the complexities of their testing fixtures.

Specimen Testing: The thin-walled tube specimen, cross-beam sandwich specimen, and both the slotted-tensile and the picture frame specimen were rated at 2,3,and 4, respectively, because of the set-up and actual testing time required are much more than for the rest.

Auxiliary Instrumentation: Most of the test methods were rated at 10 in the auxiliary instrumentation criterion except for the thin-walled tube and the slotted-tensile specimens. Dial gauges and strain gauges are usually required for these two test methods.

Data Producibility

The nature of the shear stress state induced in each test method is dependent on the geometry of the specimen. Based on the data published in past years (reviewed in detail earlier in the chapter), each in-plane shear test method is now briefly summarized. For the rail-shear test, Lockwood [6] reported that the spread between the two and three rail test methods did not indicate a preferred system and the wide variation in the average values casts doubt on the validity of the data. For the 10° off- axis tensile method [10] the shear modulus is about 19 % higher and the fracture stress is about 38% lower than that of the thin-walled tube torsion test. Whitney et al [2] found that this test resulted in significant shear coupling. Chamis [14] indicated that the test results from the 10° off-axis tensile specimen are within the range of the values reported elsewhere. He also pointed out that the spread in the available data is due to variation in fibre volume ratio. Chiao et al[10] evaluated the ±45° off-axis laminate tensile shear test with aramid/epoxy material and found a shear modulus about 10% higher and a shear failure stress about 6% lower than that of the thin-walled tube torsion. They concluded that the ±45° off-axis laminate tensile shear test was simple and reproducible. The cross-beam sandwich laminate test [16] revealed significant normal stresses resulting in errors of 13 to 20%. Due to corner effects, the stresses are greater in the test section than those applied away from that regions, so the data obtained from this test are not reliable. Several investigators reported that the corner stress concentrations are significantly high and only the initial shear modulus and ultimate strength values are reliable from the picture frame specimens. Results for the slotted-tensile test being studied by Duggan et al [16] indicate that this test method works well for a certain number of materials. However, further analytical studies are required to fully investigate the effect of specimen geometry. Since the torsional shear of a thin-walled tube can produce the desirable state of pure shear, many researchers have used this test method as a reference base for the shear test methods. On the other hand, it is not a simple test that can be easily used. The Iosipescu test method has been studied in detailed by Bergner et al [5] with the finite element method. They found that the specimen is one of the most suitable for the determination of the in-plane shear response of composite laminates.

Adams and Walrath [26]also reported that the shear modulus results obtained for various sheet moulding composite materials agreed with values obtained by other investigators using different test methods. Also, shear strength results obtained with the Iosipescu test method were somewhat higher than results obtained with the rail-shear test.

From an applied mechanics point of view, torsion of a thin-walled tube provides a means of directly applying pure shear to the specimen. The thin-walled tube specimen was therefore rated at 10 for the stiffness and strength criteria. The two-rail shear and cross-beam sandwich test methods were each rated at 6 in the strength criterion, mainly because of the free edge and corner effects, respectively. Most of the test methods were assigned of a rating of 7 or 8 in the stiffness criterion except for the picture frame specimen. The picture frame specimens usually experience buckling under load and thus give unreliable data.

Accuracy of Experimental Results

There are a number of test methods available for the determination of the shear stress/strain response of advanced composite materials and most of the aforementioned are frequently used today. However, many produce quantitative results which are questionable. The uncertainty of obtaining a state of pure shear is the main problem. It is generally agreed that torsion of a hoop-wound, thin-walled tube produces the desired state of stress and strain and provides accurate shear strength and stiffness data [27],[28],[29]. Since the hoop-wound, thin-walled tube is considered to be the most reliable test method for determining the shear stress/strain response, investigators often use the results of this test method as a standard for comparison. Some of the published experimental results for various shear tests tested are again reviewed.

Sims [4] determined graphite/epoxy shear properties by using the rail-shear test method and compared the results to those of the torsion-tube test. He found that the shear stress/strain response agreed well in the useful strain level (below the allowable design limit). Garcia et al[3]reported that the rail-shear test method gives a conservative ultimate strength. Chiao et al [10] compared the $\pm 45^{\circ}$ off-axis tensile shear test results for

aramid/epoxy composites with those of the thin-walled tube torsion test and found that the ±45° off-axis tensile shear test results in a 10% higher shear modulus and a lower ultimate strength. Sims [4] also compared the ±45° off-axis tensile shear test method with published thin-walled tube torsion data for graphite/epoxy composites and found good agreement in shear stress/strain responses. For the 10° off-axis tensile test, Chamis and Sinclair [14] compared the experimental results with several shear test methods including the thin-walled torsion tube and concluded that the shear stress/strain responses were in good agreement . Lenoe [30] used several shear test methods to characterize graphite epoxy composite materials and reported that the shear strength obtained from the cross-beam shear test is 30% lower than that of the thin-walled torsion test. No specific experimental data for the picture frame shear test compared with the torsion-tube shear test could be found in the literature. Dastin et al [18] found that reliable initial shear modulus and ultimate strength values could be obtained from the picture frame test method. Duggan et al [16] reported that the shear modulus determined by the slotted-tension test method differed by 10% compared with the thin-walled tube torsion test. He pointed out that a final assessment of the validity and accuracy of this technique must be further studied. Adams and Walrath [26],[31] have used the Iosipescu shear test to determine the shear properties of several different composite materials.They found that the shear modulus agreed well with the values obtained by other investigators using different test methods. The shear strength results obtained with the Iosipescu shear test were somewhat higher than results obtained with the rail-shear tests.

In light of the above discussion, the thin-walled tube torsion test was assigned a rating of 10 and the other tests are evaluated with respect to it. The ±45° off-axis tensile, 10° off-axis tensile and Iosipescu all received very good ratings of 9 with the remainder of other test methods evaluated at 7 or 8.

Total Rating Scores

Table 2.1 provides the details of the decision analysis rating where high total scores indicate promising test methods for this study. The top three are Iosipescu, ±45° off- axis tensile

and 10° off-axis, respectively. They have very similar scores with the test methods of the next group (three-rail shear, slotted-tensile) significantly lower.

2.4 Conclusions

This chapter was concerned with the review and subsequent evaluation of essentially all available in-plane shear test methods. By using a decision analysis technique, 9 methods were evaluated against 11 criteria and the three most promising test methods were identified for use in this study.

Chapter 3

A REVIEW OF THEORETICAL PREDICTIONS OF IN-PLANE SHEAR PROPERTIES OF UNIDIRECTIONAL COMPOSITE MATERIALS

3.1 Introduction

It is generally agreed that a unidirectional composite is the fundamental unit from which composite structures are constructed. If the stiffness and strength properties of the unidirectional material are known or can be predicted in terms of material and geometric properties of the constituents , then the structural designer has data available for predicting structural behavior. This chapter assesses some of the analytical techniques for predicting the in-plane shear behavior of a unidirectional composite.

Currently, mechanics analyses of composite material behavior are classified into two broad areas, commonly termed macromechanics and micromechanics. Within this definition, macromechanical analysis does not recognize individual filaments and the material is

considered as homogeneous. The values of the elastic constants,C_{ij}, in the general constitutive equation (3.1). are assumed to be known initially.

$$\sigma_i = C_{ij}\epsilon_j \tag{3.1}$$

$[ij = 1,2,3,...6]$

Also, since most practical composites are uniformly constructed within each layer, each layer of the material can usually be assumed to be quasi-homogeneous on the macro scale. The basic "building block" of a macromechanics analysis is the individual layer; thus its material properties must be known initially. The purpose of the analysis is to predict the behavior of a structure constructed in some arbitrary manner using these building blocks. The values of the elastic coefficients,C_{ij}, required for a macromechanics analysis are often determined experimentally. However, attempts have been made in the past to determine these composite properties analytically based upon known constituent material properties and geometrical considerations such as filament cross-sectional shape, packing array, spacing between filaments,etc. This analytical approach is called " micromechanics".

3.2 Micromechanics

Micromechanics is the study of interactions between individual filaments, matrix, and any interfacial zone existing between each filament and the surrounding matrix material. Thus, the basic material properties utilized in a macromechanics analysis are the properties of the constituent materials, i.e., the filament, matrix, and interface zone. Typically these materials are, in themselves, isotropic and homogeneous and hence the appropriate approach is an isotropic analysis. An isotropic, heterogeneous analysis would be associated with a composite consisting of isotropic filaments in an isotropic matrix (a typical combination) in which an interface reaction has occurred, creating a zone of isotropic material but having material properties varying from essentially those of the filaments at the inner boundary to those of the matrix at the outer boundary.

Given a group of filaments and matrix materials, it is desired to predict the composite properties obtainable for various combinations and for different filament packing densities,

i.e., to predict the properties which are required for subsequent structural analysis applications. Since a micromechanics analysis does recognize individual constituents within the composite and these constituents are typically isotropic, most of the analyses follow conventional isotropic analysis concepts. The principal problem is to accurately describe the boundary conditions existing between each constituent within the material. Because the state of strain (or stress) will, in general, be complex and completely unknown initially, an elasticity analysis is required to solve the prescribed boundary value problem. Usually many assumptions and approximations are introduced in the analyses such as:

1. The matrix and fibres are both homogeneous and isotropic;

2. The matrix and fibres, and hence the composite, exhibit linear elastic behavior;

3. The fibres are uniform, regularly spaced, and perfectly aligned;

4. The composite is free of voids and perfect bonding exists between the fibres and the matrix.

3.3 Prediction of In-Plane Shear Modulus

In structural composites the fibres are strong and stiff, and serve as the load bearing constituent. On the other hand,the matrix is weak and compliant, and its direct load bearing is negligible. However, the role of the matrix is very important for structural integrity of composites as the matrix protects fibres from hostile environments, transfers load to the fibres predominantly through longitudinal shear loading at the interface and localizes the effect of broken fibres.

Micromechanics involves the study of mechanical properties of unidirectional composites in terms of those of constituent materials. In this section, the property to be discussed is the in-plane shear modulus.

There are three basic approaches in the micromechanics of composite materials for predicting the in-plane shear modulus:

1. Strength of Materials;

2. Semi-Empirical;

3. Elasticity

3.3.1 Strength of Materials

Method 1

In analyzing composite properties it is important to define a volume element which is small enough to show the microscopic structural details, yet large enough to represent the overall behavior of the composite. Such a volume element is called the representative volume element. A simple representative volume element can consist of a fibre embedded in a matrix block. A set of prescribed boundary conditions must be chosen to represent the in-situ states of stress and strain within the composite.

A prediction of composite properties follows from the boundary value problem. Although the procedure involved is conceptually simple, the actual solution is rather difficult and the derivation of the expression for predicting the shear modulus has been adapted from Tsai and Hahn [35].

Consider a composite of mass M and volume V. V is the volume of a representative volume element. Since the composite is made of fibres and matrix, the mass M is the sum of the total mass M_f of fibres and the mass of matrix M_m :

$$M = M_f + M_m \tag{3.2}$$

or

$$m_f + m_m = 1 \tag{3.3}$$

in mass fraction

and

$$V = V_f + V_m + V_v \tag{3.4}$$

or

$$v_f + v_m + v_v = 1 \tag{3.5}$$

in volume fraction

V_f, V_m, and V_v are volumes of fibres, matrices and voids, respectively. Where the subscripts f, m, and v are used to denote fibres, matrix and void, respectively in this chapter.

The composite density ,ρ, is:

$$\rho = \frac{M}{V} = \frac{(\rho_f V_f + \rho_m V_m)}{V} \tag{3.6}$$

$$= \rho_f \nu_f + \rho_m \nu_m \tag{3.7}$$

In terms of mass fraction,ρ , becomes

$$\rho = \frac{M}{V} = \frac{M}{V_f + V_m + V_v} \tag{3.8}$$

$$= \frac{1}{m_f/\rho_f + m_m/\rho_m + V_v/\rho} \tag{3.9}$$

So, the composite density, ρ, is seen to be equal to the densities of the constituents averaged over the composite volume. And, the composite stresses and composite strains are defined similarly. The stress field is σ_i and the composite stress, $\bar{\sigma}_i$, is defined by:

$$\bar{\sigma}_i = \frac{1}{V}\int_v \sigma_i dv = \frac{1}{V}\left[\int_{V_f} \sigma_i dv + \int_{V_m} \sigma_i dv + \int_{V_v} \sigma_i dv\right] \tag{3.10}$$

The volume-average stress in the fibres and matrix are $\bar{\sigma}_{fi}$ and $\bar{\sigma}_{mi}$, respectively.

$$\begin{aligned} \bar{\sigma}_{fi} &= \frac{1}{V_f}\int_{V_f} \sigma_i dv \\ \bar{\sigma}_{mi} &= \frac{1}{V_m}\int_{V_m} \sigma_i dv \end{aligned} \tag{3.11}$$

Since no stress is transmitted in the voids i.e., $\sigma_i = 0$ within V_v.

$$\bar{\sigma}_i = V_f \bar{\sigma}_{fi} + V_m \bar{\sigma}_{mi} \tag{3.12}$$

The composite stress, $\bar{\sigma}_i$, is expressed in terms of the average constituent stress as $\bar{\sigma}_{fi}$ and $\bar{\sigma}_{mi}$.

Similarly to the composite stress, the composite strain is defined as the volume-average strain, and is

$$\bar{\epsilon}_i = \nu_f \bar{\epsilon}_{fi} + \nu_m \bar{\epsilon}_{mi} + \nu_m \bar{\epsilon}_{vi} \tag{3.13}$$

or

$$\bar{\epsilon}_i = \nu_f \bar{\epsilon}_{fi} + \nu_m \bar{\epsilon}_{mi} \tag{3.14}$$

The void strain is defined in terms of the boundary displacement of the voids. Usually, the void fraction is less than 1 % and is negligible.

Consider a composite laminate with fibres in the x-direction, Figure 3.1. The fibre is assumed to have a rectangular cross-section with the same thickness as that of the matrix plate. Therefore, the width ratio, $W_f/(W_f + W_m)$, is chosen to be the same as the fibre volume fraction of the composite itself.

The imposed boundary conditions for the determination of the shear modulus are:

$\bar{\sigma}_x = 0$ on AB and CD

$\bar{\sigma}_y = 0$ on AD and BC

$\sigma_s = \bar{\sigma}_s$ on all boundaries

So,

$\bar{\sigma}_x = \bar{\sigma}_{fx} = \bar{\sigma}_{mx} = 0$

$\bar{\sigma}_y = \bar{\sigma}_{fy} = \bar{\sigma}_{fm} = 0$

$\bar{\sigma}_s = \bar{\sigma}_{fs} = \bar{\sigma}_{ms}$

Therefore the composite shear strain ,$\bar{\epsilon}_s$, is given by

$$\begin{aligned} \bar{\epsilon}_s &= V_f \bar{\epsilon}_{fs} + V_m \bar{\epsilon}_{ms} \\ &= \left(\frac{V_f \bar{\sigma}_{fs}}{G_f} + \frac{V_m \bar{\sigma}_{ms}}{G_m}\right) \\ &= \left(\frac{V_f}{G_f} + \frac{V_m}{G_m}\right)\bar{\sigma}_s \end{aligned}$$

$$\frac{1}{E_s} = \left(\frac{V_f}{G_f} + \frac{V_m}{G_m}\right) \tag{3.15}$$

where

$E_s = G_{12}$

3.3.2 Semi-Empirical

Method I

In the previous section the representative volume element consisted of the fibre and matrix of the same thickness. However, in actual composites, fibres are completely surrounded by the matrix. Thus a more realistic representative volume element will be a concentric cylinder. Also, the boundary conditions should be changed to simulate the in-situ state of stress and the new representative volume element.

Noting that matrix is softer than fibre, it is assumed that

$$\bar{\sigma}_{ms} = \eta_s \bar{\sigma}_{fs} \tag{3.16}$$

$$0 < \eta_s \leq 1 \tag{3.17}$$

where η_s = the stress partitioning parameter

The equation for the modulus can be derived following the previous procedure:

$$\frac{1}{E_s} = (\frac{V_f}{G_f} + \eta_s \frac{V_m}{G_m}) \tag{3.18}$$

where,

$$E_s = G_{12} \tag{3.19}$$

The modulus increases as the stress partitioning parameters decreases. Decreasing parameter indicates an increasing load sharing by fibres. Since the fibre is stiffer than the matrix, the resulting composite modulus therefore increases.

Hashin [33] used the concentric cylinder model to show that η_s is independent of V_f, and that η_s can be expressed as :

$$\eta_s = \frac{1}{2}(1 + \frac{G_m}{G_f}) \tag{3.20}$$

Method II

In the fabrication of composites , the fibres are often somewhat randomly placed rather than being arranged in a regular array, i.e., that fibres touch each other rather than being

entirely surrounded by matrix material. But, the fibres do not touch in many instances. Chamis [34] introduced the degree of contiguity K_f, into the following equation

$$G_{12} = \frac{G_m}{1 - \sqrt{K_f}(1 - G_m/G_f)} \qquad (3.21)$$
$$K_f = 0.785$$

3.3.3 Elasticity

Method I

Hashin and Rosen [36] attempted to obtain estimates of in-plane shear modulus of fibre composite materials by using the strain-energy approach. The fibres can be hollow (see Figure 3.2) and have a circular cross-section (Figure 3.3). Two cases were studied: (1) identical fibres in hexagonal array (Figure 3.4),(2) fibres of various diameters in a random array. In both cases, the basic analysis element is a set of concentric cylinders with their axis in the fibre direction. For the random array, the concentric cylinder model consists of the fibre with matrix material around it in proportion to the volume content of matrix in the total volume.

Because of the resulting complexity of the problem , advanced techniques and numerical solution procedures are required to obtain the solutions. A closed-form solution for this micromechanics approach was derived and described in detail in [36]. In this study, an expression for the random array (Figure 3.5) approach is highlighted and presented as follows:

$$G_{12} = G_m \frac{G_f(1 + C) + G_m(1 - C)}{G_f(1 - C) + G_m(1 + C)} \qquad (3.22)$$

Where $C = V_f$= Volume fraction of fibres,

G_m= shear modulus of matrix,

G_f= shear modulus of fibre.

Method II

Previous analyses are based on models in which fibres are isolated. But in practice, a linear combination of (1) a solution in which all fibres are isolated from one another (Figure 3.6) and (2) a solution in which all fibres contact each other provides a more realistic solution, (see Figure 3.7). Tsai [37] proposed a contiguity factor ,C, to Hashin's equation.

$$G_{12} = (1 - C)G_m\frac{2G_f - (G_f - Gm)V_m}{2G_m + (G_f - G_m)V_m} + CG_f\frac{(G_f + G_m) - (G_f - G_m)V_m}{(G_f + G_m) + (G_f - G_m)V_m} \tag{3.23}$$

where $C = 0$ corresponds to isolated fibres, see Figure 3.6.

$C = 1$ corresponds to fibres in contact, see Figure 3.7.

Experimental results obtained by Tsai indicated that C is 0.2 for fibre-glass/epoxy.

Method III

The Halpin-Tsai Unified Equation

All of the theoretical equations in predicting the shear modulus are complicated and somewhat awkward to use. Halpin and Tsai [38] developed an approximate representation of more complicated micromechanics

$$\frac{G_{12}}{G_m} = \frac{1 + \varsigma\eta V_f}{1 - \eta V_f} \tag{3.24}$$

$$\eta = \frac{(G_f/G_m - 1)}{(G_f/G_m + \varsigma)}, \varsigma = 1 + 40V_f{}^{10}[39] \tag{3.25}$$

The advantages of the above equations are:

1. It is simple and can be used in the design process.

2. It generalizes micromechanics results. According to some of the published results, the predicted results are quite accurate if the fibre volume ,V_f, does not approach one.

Method IV

Adams and Doner[40] used the theory of elasticity analysis to formulate the problem of a doubly periodic rectangular array of parallel elastic filaments in an elastic matrix material

subjected to shear stress components in the direction of the filament axis. A finite difference technique was ultilized to obtain a solution. They also studied the local stress distribution in the composite and provided a mean of predicting shear strength as well as stiffness as function of the material properties of the constituents and their geometry.

3.4 Prediction of In-Plane Shear Strength

The prediction of the ultimate strengths of advanced composite material is more complex than the prediction of the modulus and is less developed and successful. One of the main reasons is that failure is likely to initiate in a region because of the local influence of the constituents' properties and the geometry in that region. This dependence upon local characteristics makes the analysis of the composite failure mechanisms much more complex. It is difficult to establish accurate micromechanics equations for prediction of in-plane shear strength. Little work has been done in this area to date. In this study, two theorectical predictions of in-plane shear are reviewed and presented.

3.4.1 Strength-of-Materials: Stress Concentration Factor

The model used to predict the in-plane shear strength, τ_{12}, is depicted in Figure 3.8. The equation derived by Greszczuk [41] is based on the following assumptions:(1) perfect interfacial bond, (2) uniform array of fibre distribution ,(3) linear stress-strain relationship ,(4) identical bulk and in-situ constituent material properties,(5) neglection of residual stress, and (6) equal elastic properties in tension and compression. For the maximum stress concentration in the matrix, the equation has the following form:

$$SCF = \frac{1 - V_f(1 - (G_m/G_f)}{\sqrt{(1 - (4V_f/\pi))(1 - (G_m/G_f)}} \tag{3.26}$$

Where SCF= Stress Concentration Factor,

V_f=Fibre volume fraction

The in-plane shear strength is given by:

$$\tau_{12} = \tau_m / SCF \tag{3.27}$$

Where τ_m = ultimate shear strength of the matrix

3.4.2 Advanced Method

Adams and Doner[40] used the finite difference method to solve the plane elasticity problem. Stress concentration factor results from this analysis are shown in Figure 3.9. The SCF value can be substituted into equation (3.27) to obtain the in-plane shear strength for a particular composite material system at a certain fibre volume percentage.

3.5 Concluding Remarks

From an engineering design point of view, an explicit formula such as the one given by Hashin and Rosen[4] would be highly desirable. For this reason, an empirical correction factor C was introduced in Hashin and Rosen's formula by Tsai in order to make their results coincide with experimental results. The Halpin-Tsai equation is equally applicable to fibre, ribbon, or particulate composites. The only difficulty in using the equation is the need to accurately determined the value of ς. Hewitt and DeMalherbe [39] pointed out that the Halpin- Tsai equation (with $\varsigma = 2$) yields an underestimate of shear modulus, G_{12}, of composites with circular fibres in a square array for fibre volume fractions greater than 0.5. They developed, again using finite difference methods, a better estimate of ς as $(1 + 40 v_f^{10})$. The Halpin-Tsai equations are used by designers still to this day.

Predicting unidirectional composite strengths in term of the properties of their constituents is a complex task. There are a multitude of factors which influence strengths. These factors range from the constituents' mechanical properties to the fabrication process and environment. Strength values usually exhibit a larger scatter than modulus because the former depends much more on defects within a material than the latter. Equations

reviewed in this chapter will be verified with experimental results in the latter part of this study.

Chapter 4

MATERIALS AND SPECIMEN PREPARATION

4.1 Introduction

The fibre composite materials used in this study were so-called "advanced composite materials ". The fibres (e.g. carbon,kevlar,boron ...etc.) are high-strength , high -stiffness fibres, generally having tensile strength and stiffness properties greater than glass fibre. In this study, carbon fibres were used to reinforce $177°C$ $(350°F)$ temperature cure epoxy resins.

The most widely accepted method of making advanced composite materials (Figure 4.1) for aerospace application is from layers of prepreg (fibres pre-impregnated with resin) which are made by either arranging fibres bundles parallel to each other (unidirectional) or in fabric form. The resin in the prepregs is normally in the so-called B- stage, i.e. an intermediate stage in the reaction of a thermosetting resin in which the cure has advanced to a point which facilitates handling and processing. In the B-stage, the resin melts at a slightly elevated temperature enabling the prepreg to conform to the required shape. The prepreg manufacturers formulate resin systems to have a specific viscosity at the recommended cure temperature, so that a particular resin will have a desired degree of flow under the cure pressure.

4.2 Materials

Four unidirectional carbon fibre prepreg systems (Narmco Rigidite T300/5208 and Rigidite IM/5245C, Hexcel's IM/F584, American Cyanamid's Cycom IM/1806) were characterized at room temperature during this study. Rigidite T300/5208 has been commercially available since the early seventies and has been one of the most widely used prepreg systems in the aerospace industry. This material was included in this study as the base line for comparison. The other three systems are newly developed resins reinforced with high strength, intermediate modulus Hercules IM6 carbon fibres manufactured by the Hercules Corp. Utah, and have a modulus of 278 GPa (40.4 MSI) and a failure strain of 16000 microstrain. Cycom 1806, Narmco 5245C and Hexcel F584 resins were selected for this study since they represented modified epoxy resin systems with improved toughness.

A common characteristic of the tougher resin systems is their greater ductility and higher strain to failure compared to the currently used 5208 epoxy resin. All materials were procured to the Structures and Materials Laboratory Specifications, see Table 4.1. Each prepreg material system was from a single batch (lot number) and was delivered in good condition packed in dry ice. Quality test results from the supplier for the materials accompanied the shipments. After checking the packing, the identification, marking and the supplier's certificate of compliance for the material was stored at $-18°C$. At that temperature all the prepreg systems were guaranteed by the manufacturers for six months.

4.3 Fabrication Procedures

The unidirectional prepreg material, purchased as 305 mm (12 inches) wide tape for all the systems, was cut to the required size and ply orientation. Each panel was assigned a number so that all information and data pertaining to a particular panel could be retained on file.

Fabrication of high-quality advanced composite material is not only dependent on the prepreg, but also on the care in processing the prepreg materials. Hand lay-up and vacuum

bagging techniques have been developed for fabricating a variety of aerospace components and structures. Complex shapes, have included double contours and relatively large parts such as the space shuttle cargo door. This bagging technque is primarily suited to prepreg materials. The essential steps in the process are the lay-up ,preparation of a bleeder system (optional) and the bagging operation. A bleeder system is required for some resin systems to absorb excess resin and permit the escape of volatiles. Bleed out may be through the surfaces or edges. In this study , a surface bleedout technique was used to process Narmco T300/5208 prepreg material and a dam was located peripherally to prevent edge bleeding (Figure 4.2). The other three resin systems were processed with a non-bleeding technique (Figure 4.4). Typical handling, lay-up and bagging procedures for laminate panels from each material system are now described.

4.3.1 Laminate Lay-up Procedures

The roll of prepreg was removed from the freezer and allowed to warm up to room temperature before opening the air-tight protective bagging. The required number of plies for a lay-up were pre-cut to size and orientation. The first ply of prepreg was placed face down (with the backing material up) on a flat metal surface coated with either a release agent or parting film. Each ply was worked to remove trapped air and wrinkles. The prepreg plies were gently smoothed with a piece of Teflon and occasionally moderate heat from a heat gun was applied to improve the tack. The backing material was then removed. The lay- up was vacuum-bagged and placed in the autoclave for curing.

NARMCO T300/5208

During the lay-up, every four to eight plies of laid-up prepreg were compacted using a temporary vacuum bag for 20 minutes. The T300/5208 prepreg material required a bleeding system to extract resin as well as any volatile during the cure. The bleeder system comprised of a sheet of perforated Teflon and the required number of plies of style 181 and 120 fibreglass cloth which were placed over the laminate. The lay-up was dammed with sealing tape prior to bagging (see Figure 4.2) to control resin flow. A pressure plate was placed on top of the lay-up to provide a flat surface on the bag side of the cured

laminate. The cure cycle employed is described in Table 4.2 and is presented in Figure 4.3.

NARMCO IM6/5245C The IM6/5245C prepreg material was relatively dry and lacked adequate tackiness for the lay-up. To ensure trapped air and wrinkles were removed, the prepreg plies were smoothed with a piece of Teflon and also moderate heat from a heat gun was applied to improve tack. During the lay-up, every four to eight plies were compacted for 20 minutes. The bagging technique was simple for this material(Figure 4.4) as neither bleeding nor dams were required since the material was a no-bleed and low flow system. The bagging procedure for this material is similar to that described in detail in Section 4.3.2. The cure cycle can be found in Table 4.2 and is represented in Figure 4.5.

HEXCEL IM6/F584

This material was also a no-bleed and low flow system. The bagging technique was similar to that used for Rigidite 5245C material. The tack of this prepreg material was also low. The backing paper of prepreg had to be carefully removed so that the prepreg lamina would stay in place. To ensure that the laid-up plies were well compacted, the temporary vacuum was applied every three plies for over 30 minutes instead of 20. After the application of vacuum, the laminate was well compacted and had a relatively smooth surface. The manufacturer's recommended cure cycle for this material required a constant heat-up rate until the cure temperature plateau was reached. The cure cycle is described in Table 4.2 and is represented in Figure 4.6.

AMERICAN CYANAMID IM6/1806

The IM6/1806 material exhibited good handling characteristics, particularly, the tack property of the material which was excellent for lay-up. To be consistent in the processing procedures with the other materials, every three plies were compacted for approximately 20 minutes. Since this material was a no-bleed and low flow system, the bagging technique was similar to the previous two. The cure cycle employed for this material was identical to that used for the Hexcel F584 material.

4.3.2 Vacuum bagging of a lay-up

The purpose of vacuum bagging the lay-up is to eliminate wrinkles and evacuate trapped gases in the laminate. The method of bagging utilized depends on the specific prepreg material. The following steps provide a general method for bagging no-bleed prepreg materials and this method is illustrated in Figure 4.4.

1. Four strips of breather cloth are rolled and placed around. but not touching, the lay-up to form an edge breather.

2. At one corner of the lay-up, a strand off fibreglass yarn is placed between the edge of the lay-up and the edge breather to allow evacuation off any trapped air from the lay-up.

3. The lay-up is covered with a sheet of parting film to prevent sticking.

4. A pressure plate is usually placed on the top of a lay- up top to produce a smooth, even surface on the bag-side of the cured laminate.

5. Fibreglass cloth is laid over the pressure plate covering any sharp edges.

6. A layer of heavy-duty breather cloth is placed over the lay-up and reaches the edge breather.

7. Sealing tape is put slightly beyond the edge breather on the plate or mandrel.

8. The base of a vacuum valve is placed on one of the edge breathers. A nylon sheet (vacuum bag) is spread over the lay-up and sealed at the edges with the sealing tape.

9. A small slit is made in the vacuum bag and the top of the vacuum valve is fitted through the slit into the base. The vacuum hose is attached and a vacuum drawn. The vacuum bag is checked for leaks before curing in an autoclave.

This method was used for processing the Narmco IM6/5245C, American Cyanamid IM6/1806 and Hexcel IM6/F584 carbon/epoxy material systems at a curing temperature

of $177°C(350°F)$. A similar method was used to process the high flow and bleed material system such as Narmco T300/5208, however, surface bleeder material was used to absorb excess resin during cure,(Figure 4.2).

4.3.3 Autoclave curing

The bagged lay-up was cured in an autoclave (Baron-Blakeslee Co., Model-BAC-46) by the simultaneous application of heat and pressure. Most cure processes also use vacuum to remove trapped air or other volatiles. The vacuum and autoclave pressure cycles are designed to permit maximum removal of air or volatile without incurring excessive resin flow. Vacuum is usually applied only in the initial stages of the curing cycles, while autoclave pressure may be maintained during the entire heating and cooling cycles. Four curing cycles have been developed and used in processing the laminate panels in this work. The detailed curing steps of each cure cycles are listed in Table 4.2.

4.4 Nondestructive Inspection of Cured Laminates

After fabrication , each panel was inspected by ultrasonic C-scan at the National Aeronautical Establishment using a reflection plate technique. Copies of the C-scan plots were retained on file. Once the panels had passed C-scan inspection, the end tabs were bonded to the panels(Figure 4.7) , as specified, prior to cutting into specimens. In some cases, small defects in the panels were traced out using the C-scan plots as the reference to ensure that specimens prepared from the panels were free of defects.

4.5 Test-Matrix and Specimen Configuration

The in-plane shear test matrix for these four material systems is shown in Table 4.3 . Specimen configurations and strain gauge locations on the specimens used for 10° off-axis tensile, $\pm 45°$ off-axis and Iosipescu tests are shown respectively in Figure 4.8, Figure 4.9 and Figure 4.10. All specimens for a particular test method and material were machined

from a single panel. Ten specimens were prepared for each combination of test method and material, resulting in a total of 120 specimens.

4.6 Specimen Preparation

4.6.1 $\pm 45^{\circ}$ and 10° Off-axis Specimen

The shear test specimens were cut from each of the 12 panels made from 4 different materials with a Star Lite Magni-wheel, diamond grit 60/80, mounted in a special table saw designed for cutting composites in the Structures and Materials Laboratory. This cutting wheel produced relatively smooth edges without any damage to the composite material. For the 10 degree off-axis specimens, the specimens were carefully prepared so that the fibre direction was at angle of 10 degrees with the axis of the specimen.

4.6.2 Iosipescu Specimen

After the specimens were cut with the fibres oriented 90 degree to the longitudinal axis (Figure 4.10) by the diamond saw to a size of 51 mm(2 in) long,12.7 mm(0.5 in) , each specimen was then ground on the long edges to a width tolerance of 0.025 mm(0.001 in). The quality of the machined surface on the specimen is important when determining the mechanical properties of a composite material. Carbon/epoxy composites pose certain difficulties in attaining good machined surfaces, especially for a 90 degree notch. The type of cutting tools, feed rate and rotational speed are all important and affect the quality of the machined surfaces. It was not know if the material at the root of the notch would suffer any micro-damage from machining, thus, two different machining techniques were evaluated for machining the 90 degree notches. The final procedures are described in detail as follows: in the first method (A), a stack of specimens with backing material were held in a vise on a milling machine (Figure 4.11). A 45 degree side-faced steel slitting saw with an outside diameter of 152 mm (6 in) was positioned such that a single pass would cut a notch in each specimen. The cutting operation was performed at a rotational speed of 600

RPM and a feedrate of 0.4 m/minute (1 ft/minute). Since all the specimens were ground on both edges, the notches on the other side were cut using the same procedure. A finished specimen is shown in Figure 4.12. The small portion of vertical flank which can be seen at the top of the notch was due to the insufficient thickness of the saw. In the second method (B), a 2-flute silicon carbide tipped end mill with a diameter of 12.7 mm(.5) was positioned at a 45 degree angle to the workpiece (Figure 4.13). Again, backing material was used to prevent delamination at the end of the cut. The rotational speed of the end mill was 3,500 RPM in combination with a feedrate of approximately 0.4 m/minute (1 ft/minute). A finished specimen is shown in Figure 4.14.

In order to initially evaluate the effects of the two machining procedures, the roots of the notches were examined for each batch of specimens using a low power microscope (50X) . In general, the machined surfaces prepared from methods A and B showed no visible damage and appeared quite smooth. In order to learn more about the effects of these two machining techniques on the quality of the notch, especially at the root of the notch, SEM examinations were carried out on samples which included the root of the notch. As shown in Figure 4.15, the specimen prepared from method A had a micro-crack which extended along the notch root in the thickness direction. The specimen prepared from method B had no micro-cracks in the machined area (Figure 4.16). Therefore, method B was used to prepare all the Iosipescu specimens for this study.

Chapter 5

EXPERIMENTAL CONSIDERATIONS AND TESTING PROCEDURES

5.1 Introduction

In this study, three selected shear test methods(±45° off-axis tensile, 10° off-axis tensile and Iosipescu) were used to determine in-plane shear stress-strain behaviour of four composite materials. These three test methods feature different loading conditions and data reduction techniques and they are described in detail in the following sections.

5.2 Data Reduction Techniques

±45° TENSILE SPECIMEN

A simple expression for the shear modulus of ±45° composite has been derived by Rosen [7]. The shear stress at 45° is half the applied tensile stress and is uniform through the specimen except at the edges. The overall shear strain is given by

$$\gamma_{xy} = \epsilon_x - \epsilon_y \tag{5.1}$$

But for 45° fibre orientations the shear strain of the individual lamina γ_{12} is given by

$$\gamma = \epsilon_x(1 + \nu_{xy}) \tag{5.2}$$

therefore

$$\gamma_{12} = \epsilon_x - \epsilon_y \tag{5.3}$$

The difference between the two strains ϵ_x and ϵ_y can be determined and the shear modulus is given by

$$G_{12} = \frac{\sigma_x}{2(\epsilon_x - \epsilon_y)} \tag{5.4}$$

where $\tau_{12} = \frac{\sigma_x}{2}$. The anaylsis for a $\pm 45_o$ specimen to obtain in-plane shear properties of fibre reinforced composite material is therefore quite simple.

10° OFF-AXIS TENSILE SPECIMEN

The detailed derivation of equations required to generate shear stress-strain behaviour are also described in Reference [14]. For the sake of completeness, the derivation of these equations is also presented in this section. Assuming that the applied stress is uniformly distributed over the test section, the ply stresses in a unidirectional specimen are given by the following stress transformation laws:

$$\sigma_1 = \sigma_x cos^2\theta \tag{5.5}$$

$$\sigma_2 = \sigma_x sin^2\theta \tag{5.6}$$

$$\tau_{12} = -\sigma_x sin\theta cos\theta \tag{5.7}$$

Where σ_x is the uniaxially applied stress and θ is the angle of the unidirectional fibre direction with respect to the load direction.

In order to generate material principal strains from the rosette strains, three-element rosette transformation equations in matrix form were employed as follows:

$$\begin{Bmatrix} \epsilon_a \\ \epsilon_b \\ \epsilon_c \end{Bmatrix} = \begin{bmatrix} cos^2\theta_a & sin^2\theta_a & \frac{1}{2}sin2\theta_a \\ cos^2\theta_b & sin^2\theta_b & \frac{1}{2}sin2\theta_b \\ cos^2\theta_c & sin^2\theta_c & \frac{1}{2}sin2\theta_c \end{bmatrix} \begin{Bmatrix} \epsilon_x \\ \epsilon_y \\ \epsilon_{xy} \end{Bmatrix} \tag{5.8}$$

or in compact form

$$\{\epsilon_G\} = [R]\{\epsilon_C\} \tag{5.9}$$

where $\epsilon_a, \epsilon_b, \epsilon_c$ are the true strains for gauge elements A,B,C and $\theta_a, \theta_b, \theta_c$ are corresponding orientation angles of gauges A,B,C measured from the load direction,(Figure 5.1). The equation relating the ply in-plane shear strain to loading-axis strain for any θ orientation is

$$\epsilon_{12} = (\epsilon_y - \epsilon_x)sin2\theta + \epsilon_{xy}cos2\theta \tag{5.10}$$

And the loading-axis strains $\{\epsilon_C\}$ are obtained from equation (5.9) as follows:

$$\{\epsilon_C\} = [R]^{-1}\{\epsilon_G\} \tag{5.11}$$

The expanded form of equation (5.11) for a rectangular rosette (θ_a=0 degree; θ_b= 45 degree and θ_c= 90 degree) is

$$\epsilon_x = \epsilon_a \quad \epsilon_y = \epsilon_b \quad \epsilon_{xy} = -\epsilon_a + 2\epsilon_b - \epsilon_c \tag{5.12}$$

The in-plane shear strain along the 10 degree plane is obtained by substituting the loading-axis strain from equation (5.12) into equation (5.10) and setting θ = 10°. The resulting equation is:

$$\epsilon_{12} = -1.282\epsilon_a + 1.879\epsilon_b - 0.598\epsilon_c \tag{5.13}$$

And the equation relating the in-plane shear stress to the loading axis stress is:

$$\tau_{12} = 0.171\sigma_x \tag{5.14}$$

IOSIPESCU SPECIMEN

The in-plane shear stress for this test shown in Figure (5.2) is simply the shear force (p) divided by the net-cross sectional area. i.e.,

$$\tau_{12} = \frac{p}{wt} \tag{5.15}$$

where w is the net width between the notches and t is the thickness of the test specimen.

The shear strain in the Iosipescu shear test is measured with biaxial strain gauges. Strain gauges oriented at ±45° to the longitudinal axis of the test specimen are bonded at

the specimen midlength, as shown in Figure (5.3), and the in-plane shear strain is obtained by the following equation:

$$\gamma_{12} = |\epsilon_1| - |\epsilon_2| \tag{5.16}$$

5.3 Testing Procedures

±45° and 10° OFF-AXIS SPECIMEN TEST

The tests were conducted in accordance with ASTM D3518-76(In-plane shear stress-strain response of unidirectional fibre reinforced plastics). Specimens were installed in the Instron Universal Testing Machine (Model 1125 equipped with a 90 kN load cell) using wedge grips. A typical test set is shown in Figure 5.4 . Biaxial strain gauges or three-axis rectangular rosette strain gauges and the Instron load cell were connected to a data acquisition system interfaced to an HP 85 mini-computer. A crosshead loading rate of 1.0 mm/minute(0.004 inches/minute) was used. For the ±45° degree specimens, the loading rate was increased to 5 mm/minute after the microstrain level of 30,000 was reached to shorten the testing time. Above this level of 30,000 microstrain, cracks tended to develop which cast doubt on the values of strain measured by the gauges.

IOSIPESCU SHEAR SPECIMEN TEST

Since this test method had not been used at NAE before . a preliminary study was conducted before the actual testing study was carried out. The following paragraphs describe the step-by-step procedure that was undertaken to establish testing procedures for the Iosipescu shear test method.

An initial specimen was instrumented with a 90 degree biaxial rosette of strain gauges (Micro-measurement-CEA 06-062WT-120) in the section between the notches at 45 degrees to the loading axis of the specimen (Figure 5.3). The specimen was inserted into the loading fixture(Figure 5.5) and centered using an alignment bar in the upper specimen notch. Teflon shims were placed in the vertical slots between the fixture and the specimen and were pressed against the specimen by tightening the horizontal screws. An Instron Testing Machine (Model 1125) equipped with a 90 KN load cell was used for testing at

crosshead loading rate of 0.5 mm/minute (0.02 in/minute) and a typical test set-up is shown in Figure 5.5. The strain gauges and load cell were again connected to the data acquisition system interfaced to an HP 85 mini-computer.

During the initial stage of testing, the load was applied and then removed as a discrepancy was observed in the strain readings as shown in Case(1)of Table 5.1. The absolute value of the compressive strain was more than 200 % of the tensile strain value, instead of being equal (pure shear). When the same specimen was rotated 180 degrees (top-to-bottom) and re-tested, the discrepancy in the values of strain reading still existed. It initially appeared that the loading had introduced some local compressive stresses into the specimen, thus a state of pure shear stress did not exist between the two notches.

In order to have a better understanding of the strain distribution on both front and back surfaces in the test section, a pair of 90 degree biaxial rosette strain gauges (Micro-measurement-CEA06-062WT-120) were bonded in a back-to-back configuration in the test section of a trial specimen. The test set-up was the same as shown in Figure 5.5. At a load of 120 N (27lb),the back-to-back strain readings did not agree with each other as shown in Case 2 of Table 5.1. These discrepancies were possibly caused by torsion of the specimen in addition to the induced compressive stresses. This torsion could result from improper seating of the specimen due to the roughness of the machined loading surfaces as depicted in Figure 5.6. It was decided to analytically investigate the sensitivity of the results to a reasonable value of torsion. This value was determined by assuming a nominal load of 100 N applied as shown in Figure 5.6. The values of the strains in the direction of the strain gauges i.e., at 45° to the longitudinal axis were calculated using the LAMCAL laminate analysis code [42]. Three of the required elastic constants(E_{11}, E_{22} and ν_{12}) for the individual lamina had been previously determined for the same prepreg material and curing cycle. A value of 5.2 GPa was assumed for the shear modulus (G_{12}). The calculated linear strains in the strain gauge directions were approximately 10,700 microstrain in magnitude. This was an approximate value since the effects of the notches and edges were ignored and it was well above shear strain design value of 4000 microstrain. The result is significant though since the magnitude was very large in comparison to the

strain values recorded during the test. This indicates that even a slight misalignment in the seating of the specimen could have a significant effect on the results. In an attempt to reduce the previously discussed torsional effect, the clearance between the fixture and the specimen was shimmed with smooth hard steel razor blades of thickness 0.18 mm (0.007in.) and brass shims of thickness 0.08mm(0.003in.) on the four loading surfaces (Figure 5.7). The specimen with the two shear pair strain gauges(Case 2) bonded in a back-to-back configuration, was re-installed in the fixture. The test set-up and procedure were the same as the previous one. At a load of 149 N (31lb), the back-to-back strain readings agreed quite well (Case 3 of Table 5.1), however, the absolute values of tensile and compressive strain readings from the same surfaces did not agree. Thus, it appeared that the torsional loading due to improper seating had been eliminate by shimming, but the localized compressive stress induced by the loading points still existed. A close examination of the loading surfaces of the fixture revealed that the machined surfaces had some knurls and that these knurls might not provide even and parallel surfaces for the specimens even when the shims were used. It was then decided that loading surfaces on the fixture would be ground parallel to permit uniform shimming and subsequently proper loading. When retested, the strain readings from gauges 1 ,2, 3 and 4 from both surfaces were now consistent(case 4 of Table 5.1). This implied that shimming on ground parallel surfaces was needed to provide a close tolerance fit. The actual fitting procedures were based upon judgement and usually a preloading was required to verify the gauge readings prior to the actual testing. It is interesting to note that the re-designed Iosipescu fixture by Adams and coworkers [43] incorporates a height adjustment that eliminates the need for shimming.

5.4 Concluding Remarks

The testing procedures for $\pm 45°$ off axes tensile specimens has been adopted by ASTM and incorporated in D 3518-76. The testing procedure in this study was conducted according to that specification and was quite straight-forward. For the $10°$ off- axis tensile test, the test procedure was similar to the $\pm 45°$ off-axis, however, since the shear stress of the specimen

is sensitive to small misorientation errors, extra care have been taken in strain gauge positioning and load alignment. The Iosipescu test fixture did impose some problems during testing. The loading faces in the fixture require close dimensional and flatness tolerances to prevent torsional and local compressive loading effects. It is important to ensure that the four loading faces are parallel to one another.

Chapter 6

EXPERIMENTAL RESULTS AND DISCUSSION

6.1 Introduction

The results from the experimental phases of this study are presented in this chapter. In order to facilitate data comparison of four materials with the discussions of the influence of each test method, the results are presented in section format for each test method. The second section of this chapter presents the test results for four materials using the $\pm 45^{\circ}$ tensile specimen. The third and fourth sections deal with 10° off-axis tensile and Iosipescu shear specimens,respectively. The fifth section presents the comparison of the in-plane properties of the four materials obtained by three shear test methods with the theoretical predicted values.

6.2 Test Results For The $\pm 45^{\circ}$ Tensile Specimen

The $\pm 45^{\circ}$ shear test results of the four materials are summarized in Table 6.1, 6.2, 6.3 and 6.4,respectively. Typical shear stress-strain curves of each specimen made from four materials are shown in Figure 6.1. Photographs of the typical failed specimens are shown in Figure 6.2. Most of the specimens failed in the vicinity of the bonded end tabs which

may have been caused by the combination of the Poisson's effect and constraint in the end tabs. This phenomenon was especially pronounced in the toughened resin material systems. During the testing the specimens gave audible sounds at the first indication of damage. Beyond that region numerous sharp drops in the load curve were observed. Post examination of the specimens indicated extensive delamination and interply failure prior to separation (complete failure).

6.3 Test Results For The 10° Off-Axis Specimens

The test results for four material systems are summarized in Table 6.5,6.6, 6.7 and 6.8, respectively. Typical shear stress-strain curves for the T300/5208, IM6/5245C, IM6/1806 and IM6/F584 specimen are presented in Figure 6.3. Photographs of typical failed specimens for each material system are shown in Figure 6.4. As can be seen in this figure, the fracture occurred in the gauge section parallel to the fibres indicating in-plane shear fracture. The fracture surfaces of the Narmco T300/5208 and American Cyanamid IM6/1806 were generally smooth, indicating brittle fracture. For the Narmco IM6/5245C and Hexcel IM6/F584, the fracture surfaces were irregular and featured some fibre pull out.

6.4 Test Results For The Iosipescu Shear Specimens

Average ultimate shear strength and shear moduli for the four material systems are presented in Table 6.9, 6.10, 6.11 and 6.12, respectively. Typical shear stress-strain plots of each specimen made from four materials are presented in Figure 6.5. Photographs of typical failed specimens of each material system are shown in Figure 6.6. Basically, all four material specimens exhibited a similar failure mode, i.e. fractures occurred within the gauge section of the specimens and ran from notch tip to notch tip.

6.5 Comparison of Experimental Values of In-plane Shear Moduli With The Theoretically Predicted Values

6.5.1 Comparisons With The Lamination Analysis

The main purpose in obtaining the shear stress-strain response of a lamina using any procedure is to provide correct values of shear modulus and strength for lamination analysis in order to predict laminate response characteristics under arbitrary boundary loads. Thus, in the present study it was decided to use the shear results obtained from three shear test methods in conjunction with the other pre-determined properties to predict the responses of several laminates under a tensile load. A lamination analysis code [42]was used to calculate the modulus of a 48 ply laminate with a lay-up configuration of $|+45°/0°/-45°/90°|_{6s}$ (Figure 6.7). The four required elastic constants (E_{11}, E_{22}, ν_{12} and G_{12}) for the individual lamina of each material system for the analysis have been previously determined and are listed in Table 6.13. The predicted results for laminate tensile modulus using the shear modulus for three test methods are compared with the experimentally measured laminate tensile modulus in Table 6.14. In order to verify the predicted values, tensile tests of three laminate specimens for each material sytem were performed according to NASA specifications [45]. It is interesting to note that the highest coefficient of variation of four average test results is 1.2% for Narmco T300/5208. As can be observed the Iosipescu shear test results gave on averagethe most accurate predictions for the tensile response of all four laminates although the predictions using the $\pm 45°$ tensile results were also very accurate. It appeared though that the Iosipescu shear test would provide the most accurate data among the three test methods for the three new resin systems.

6.5.2 Comparisons With The Micromechanical Predictions

The micromechanical models for shear modulus are now evaluated. The properties of the Hercules IM6 fibre, Toray T300 fibre and the resins were not measured as part of the present study, the data were taken from the material manufacturers' literature. The values used in the predictions of moduli are listed in Table 6.15. Seven techniques for predicting the in-plane shear modulus of advanced composite materials were reviewed and examined in chapter 3. All of them are used to predict the shear modulus for each material and the predicted values are presented in Table 6.16 with the detailed calculations for predictions presented in Appendix A. The predicted values obtained by the strength-of-material technique are quite low and these values are in doubt for representing any meaningful predictions. For two semi-empirical prediction techniques, a discrepancy was observed in the data obtained by these two predictions. The values obtained from technique (b) were consistently 68% greater than technique (a). Again, this casts doubt on the reliability of this approach. The values predicted by the elasticity approach ,Halpin-Tsai theory and the Adams-Doner's prediction for four materials are in reasonable agreement and the deviation is only a few percentage points . From an engineering design point of view, the Halpin-Tsai equation is the most desirable because it is a simple explicit formula and is easy to use. It permits easy determination of effective shear moduli for a variety of matrix properties, fibre properties and volume fraction with sufficient engineering accuracy. This equation was also highly rated by Jones [46]. As found in the previous section, the Iosipescu shear test provides the most accurate shear test results for the laminate analysis. Therefore, data obtained by this test method was used to compare with the theoretically predicted values in Table 6.16. The elasticity, Halpin-Tsai and the Adams-Doner' predictions gave reasonable agreement with the Iosipescu shear test results except for the American Cyanamid IM6/1806 material. It is interesting to note that the American Cyanamid IM6/1806 had the lowest modulus in all three test methods. A fractographic examination of Iosipescu specimens indicated considerable interfacial debonding between fibres and matrix in the American Cyanamid IM6/1806 which is a possible reason for the generally weak performance of this material(see Figure 6.8 and Figure 6.9).

6.6 Comparison of Experimental Values of In-plane Shear Strengths With The Theoretical Predicted Values

Since the shear strength data for these four neat resin systems was not available in the literature and it was practically impossible to determine them in this study, it was decided to use an estimate which has been commonly used for homogeneous, isotropic materials to obtain the shear strength. This estimate assumes that shear strength of the resin is approximately equal to 60% of the tensile strength of the resin. The properties of the Hercules IM6 fibres, Toray T300 fibre and the estimated neat resin shear properties are listed in Table 6.17. The detailed calculations for obtaining the predicted shear strengths are presented in Appendix B. The micromechanics predictions of in-plane shear strengths and experimental results are summarized in Table 6.18. The predicted values obtained by both techniques are much lower than the experimental values in all three cases. It appeared that these these predicted values do not represent any meaningful predictions at all. As previously discussed, these strength predictions are highly dependent on the local failure mechanisms and the matrix material properties . Therefore, it is very difficult to establish micromechanics equations to predict the shear strength accurately. This suggests that much more work needs to be done in this area so that more accurate prediction theories can be developed.

Chapter 7

CONCLUSIONS AND RECOMMENDATIONS

By using a decision analysis technique, three in-plane shear test methods (Iosipescu , $\pm 45^{\circ}$ off-axis tensile and 10° off-axis) were identified for this study. These three test methods were used to characterize the in-plane shear properties of four advanced composite materials and test results were compared with the micromechanical predictions. Based on the data discussed in this study, the following conclusions and recommendations are made concerning testing techniques , material properties and theoretical predictions.

1. The Narmco 5245C, Hexcel F584 and American Cyanamid 1806 resins were more easily processed than the Narmco 5208 resin system since these materials were low-flow,no-bleed resin system.

2. The carbide end-mill cutter with appropriate feedrate and cutting speed appeared to provide good quality machined notches for the Iosipescu specimens.

3. The placing of the Iosipescu specimen into the test fixture was complicated and required care. In addition, the loading faces of the fixture and specimens must be ground parallel and smooth.

4. The strain gauge readings for the final test procedure confirmed that strain distributions in the test section on the Iosipescu specimen are of pure shear.

5. Using pre-determined material properties, laminate analyses were performed to predict the tensile moduli of laminates .The Iosipescu test data provided the best predictions.

6. The Iosipescu test is a viable test method for determining the in-plane shear stress-strain response of advanced composite materials, providing the specimen preparation and testing procedures are carefully executed.

7. The Halpin-Tsai's equation is the simplest one and provides reasonably accurate predictions of the in-plane shear modulus as compared with the test results obtained by the Iosipescu test.

8. Theories for more accurately predicting the shear strength of advanced composite materials need to be developed.

References

[1] Lee,S. and Munro,M.,*Evaluation of In-plane shear test methods for advanced composite materials by the decision analysis technique*,Composites,Vol.17, no.1,(January 1986) pp 13-22

[2] Whitney,J.M., Stansbarger,D.L. and Howell,H.B., *Analysis of the rail shear test: applications and limitations*,Journal of Composite Materials 5 (January 1971) pp 24-34

[3] Garcia,R., Weisshaar,T.A. and McWithey,R.R., *An experimental and analytical investigation of the rail shear test method as applied to composite materials*,Experimental Mechanics 20 No 8 (August 1980) pp 273-279

[4] Sims,D.F., *In-plane shear stress strain response of unidirectional composite materials*,Journal of Composite Materials 7 (January 1973) pp 124-128

[5] Bergner,H.W.,Davis,J.G. and Herakovich,C.T., *Analysis of shear test methods for composite laminates*, Report VPI-E-77-14 (Virginia Polytechnic Institute and State University)

[6] Lockwood,P.A., *Results of the ASTM round-robin on the rail shear test for composites*, Composite Technology Review 3 No2 (summer 1981) pp 83-86

[7] Rosen,B.W., *A simple procedure for experimental determination for the longitudinal shear modulus of unidirectional composites*, Journal of Composite Materials 6 (October 1972) pp 552-554

[8] Petit, P.H., *A simplified method of determining the in-plane shear stress-strain response of unidirectional composites*, ASTM STP 460 (American Society For Testing and Materials .1969) pp 83-93

[9] Hahn,H.T., *A note on determination of the shear stress-strain response of unidirectional composites*, Journal of Composite Materials 7 (July 1973) pp 383-386

[10] Chiao,C.C., Moore,R.L. and Chiao,T.T., *Measurement of shear properties of fibre composites*, Composites 8 No 3 (July 1977) pp 161-169

[11] Greszczuk, L.B., *New test technique for shear modulus and other elastic constants of filamentary composites*, Report AD 801 547 (January 1967)

[12] Terry,G., *A comparative investigation of some methods of unidirectional, in-plane shear characterization of composite materials*, Composites 10 No 4 (October 1979) pp 233-237

[13] Yeow,Y.T. and Brinson,H.F., *A comparison of simple shear characterization methods for composites laminates*, Composites 9 No 1 (January 1978) pp 49-55

[14] Chamis,C.C. and Sinclair, J.H.,10° *off-axis test for intralaminar shear characterization of fiber composites*, Report NASA TN D-8215 (April 1976)

[15] Chamis,C.C. and Sinclair, J.H., 10° *off-axis test for shear properties in fiber composites*, Experimental Mechanics 17 No 9 (September 1977) pp 339-346

[16] Duggan,M.F., McGrath,J.T. and Murphy, M.A., *Shear testing of composite materials by a simple combined-loading technique*, AIAA 78-508 (1978) pp 311-319

[17] Bryan,E.L., *Photoelastic evaluation of the panel shear test for plywood*, ASTM STP 289 (American Society for Testing and Materials 1961) pp 90-94

[18] Hadcock, R.N. and Whiteside, J.B.,*Special problems associated with boron-epoxy mechanical test specimens*, ASTM STP 460 (American Society for Testing Materials, 1969) pp 27-36

19 Dastin.S., Lubin. G., Munyak, J. and Slobodzinski.A., *Mechanical properties and test techniques for reinforced plastic laminates.* ASTM STP 460 (American Society for Testing and Materials,1969) pp 13-26

20 Davenport,O.B. and Bert.C.W.,*Buckling of orthotropic, curved, sandwich panels subjected to edge shear loads.* Journal of Aircraft 9 No 7 (1972) pp 477-480

21 Whitney,J.M. and Halpin,J.C., *Analysis of laminated anisotropic tubes under combined loading.* Journal of Composite Materials 2 No 3 (1968) pp 360-367

22 Rizzo.R.R. and Vicario.A.A., *A finite element analysis for stress distribution in gripped tubular specimens.* ASTM STP 497 (American Society for Testing and Materials. 1972) pp 68-88

23 Hahn.H.T. and Erikson.J., *Characterization of composite laminates using tubular specimens.* Report AFML-TR-77-144 Air Force Material Laboratory, Wright-Patterson Air Force Base.OH. USA. 1977

24 Iosipescu. N., *New accurate procedure for single shear testing of metals.* Journal of Materials 2 No 3 (September 1967) pp 537-565

25 Slepetz. J.M., Zagaeski. T.F. and Novello,R.F., *In-plane shear test for composite materials.* AMMRC TE 78-30 (Army Materials and Mechanics Research Center. Watertown. Ma. USA. July 1978)

26 Adams.D.F. and Walrath. D.E., *Iosipescu shear properties of SMC composite materials.* ASTM STP 787 (American Society for Testing and Materials. 1982) pp 19-33

27 Pagano.N.J. and Whitney.J.M., *Geometric design of composite cylindrical characterization specimens.* Journal of Composite Materials 4 (July 1970) pp 360-378

28 Feldmen.A., Tasi.J. and Stang.D.A., *Experimental determination of stiffness properties of thin-shell composite cylinders.* Experimental Mechanics 6 No 8 (August 1966) pp 385-394

[29] Swanson,S.R., Tombes, G.R. and Beckwith, S.W., *In-plane shear properties of composites using torsion test of thin-wall tubes*, 29th SAMPE Symp (April 1984) pp 567-577

[30] Lenoe,E.M., *Testing and design of advanced composites materials*, Journal of Engineering Mechanical Division (December 1970) pp 809-823

[31] Adams,D.F. and Walrath,D.E., *Damage mechanism/failure mechanics of carbon-carbon composite materials*, Report UWME-DR-904-101-1 (Department of Mechanical Engineering , University of Wyoming ,Laramie, WY,USA. 1979)

[32] Whitney,J.M. Daniel,I.M. and Pipes,R.B., *Experimental mechanics of fiber reinforced composite materials*, Society for Experimental Stress Analysis Monograph No 4 (1982) pp 193-196

[33] Hashin,Z., *Theory of fibre reinforced materials*, NASA CR- 1974,(1972)

[34] Chamis,C.C., *Simplified composite micromechanics equations for hygral, thermal and mechanical properties*, SAMPE Quarterly (April 1984) pp 14-23

[35] Tsai,S.W. and Hahn,H.T.,*Introduction to composite materials*, Technomic Publishing Co., In., 1980

[36] Hashin,Z. ar.d Rosen,B.W., *The elastic moduli of fibre reinforced materials*, Journal of Applied Mechanics vol 31 No 2 (1964) pp 1-10

[37] Tsai,S.W., *Structural behaviour of composite materials*, NASA CR-71 (July 1964)

[38] Halpin,J.C. and Tsai,S.W., *Effects of environmental factors on composite materials*, AFML-TR-69-432 (June 1969)

[39] Hewitt,R.L. and DeMalherbe, M.C., *Approximation for the longitudinal shear modulus of continuous fibre composites*, Journal of Composite Materials (April 1970) pp 280-282

[40] Adams,D.F. and Doner,D.R., *Longitudinal shear loading of a unidirectional composites*, Journal of Composite Materials, vol.1, (1967) pp 4-17

41 Greszczuk,L.B. SPI Annual Conference 22nd. Sect.20-A, Washington D.C. (1967)

42 Hall,S.R., *Lamcal: an iterative design package for performing a laminated plate theory analysis of composite materials*, LTR-ST-1656, NAE. NRC Canada (November 1987)

43 Adams,D.F. and Walrath,D.E., *Further development of the Iosipescu shear test method*, Experimental Mechanics ,Vol. 27, no.1 (1987) pp 113-119

44 Pindera,M.J., Choksi,G.,Hidde,J.S. and Herakovich,C.T., *A methodology for accurate shear characterization of unidirectional composites*, Journal of Composite Materials 21(12) (December 1987) pp 1164-1184

45 NASA-RP-1092, *Standard tests for toughened resin composite, revised edition*, (July 1983)

46 Jones,R.M., *Mechanics of Composite Materials, McGraw-Hill Company*, 1975 edition.

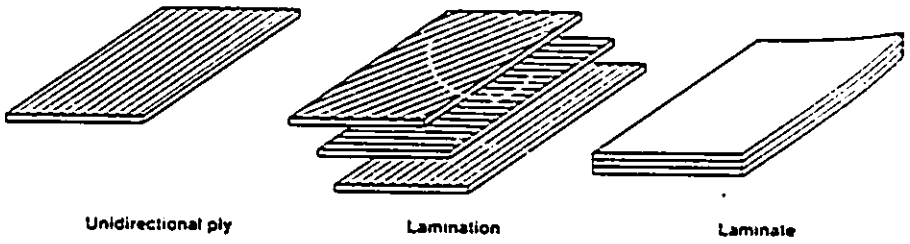

FIGURE 1.1: LAMINATE CONSTRUCTION

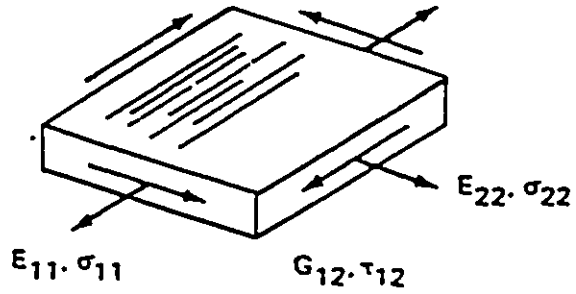

$$\upsilon_{12} = \frac{\varepsilon_2}{\varepsilon_1}$$

FIGURE 1.2: ELASTIC CONSTANTS OF A LAMINA

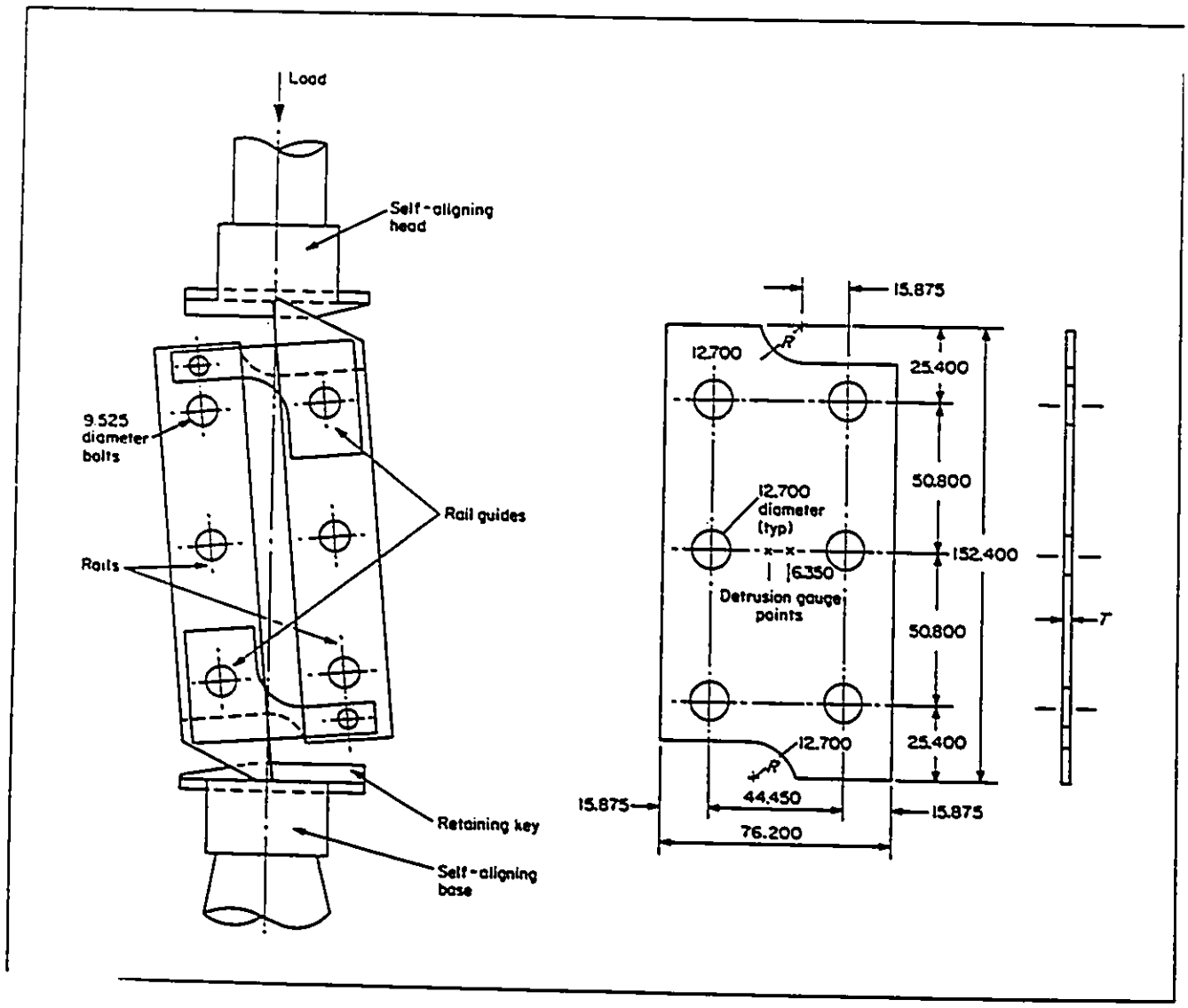

FIGURE 2.1: TWO-RAIL SHEAR APPARATUS AND SPECIMEN (REF. 32)
ALL DIMENSIONS IN mm

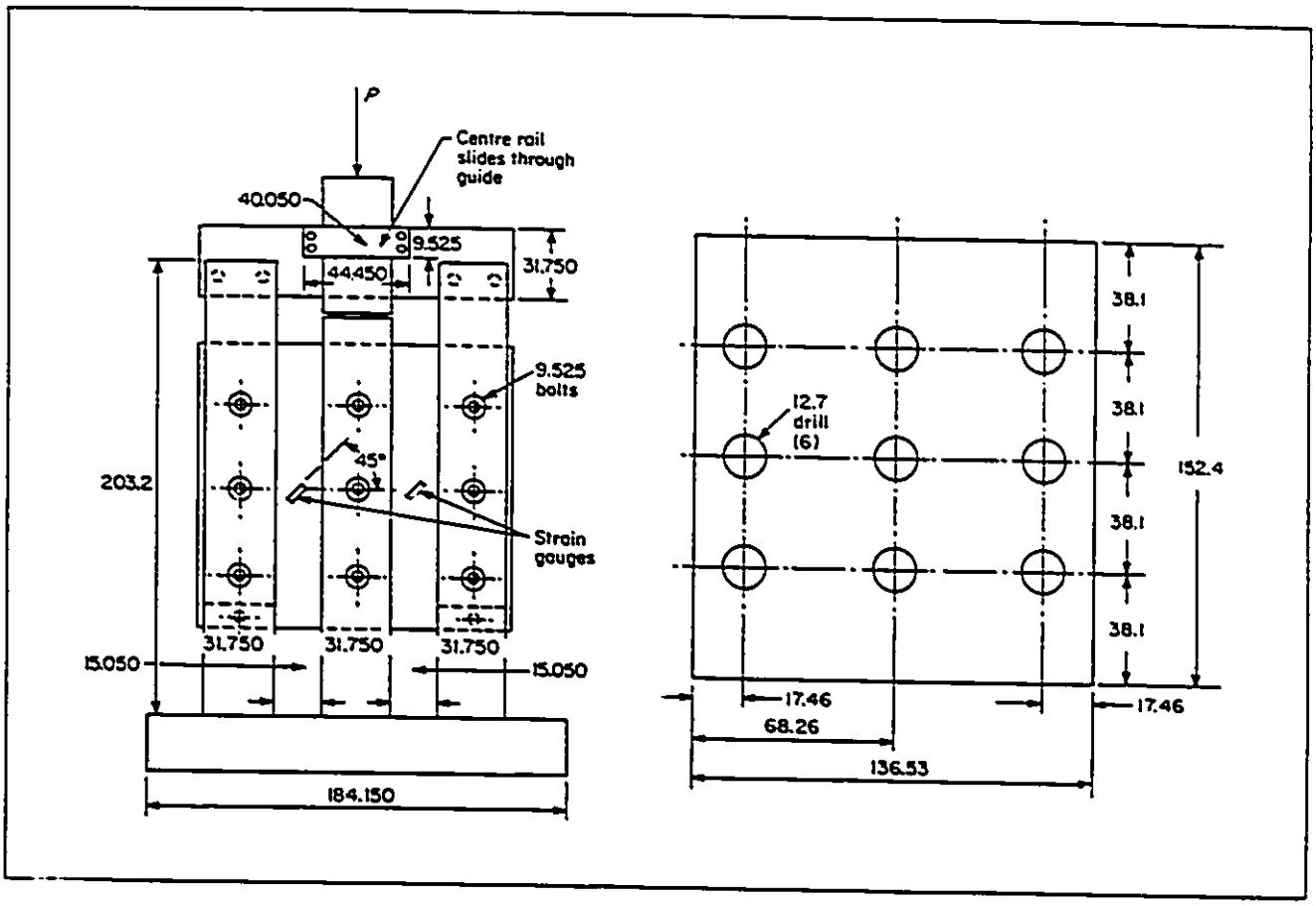

FIGURE 2.2: THREE-RAIL SHEAR APPARATUS AND SPECIMEN (REF. 32)
ALL DIMENSIONS IN mm

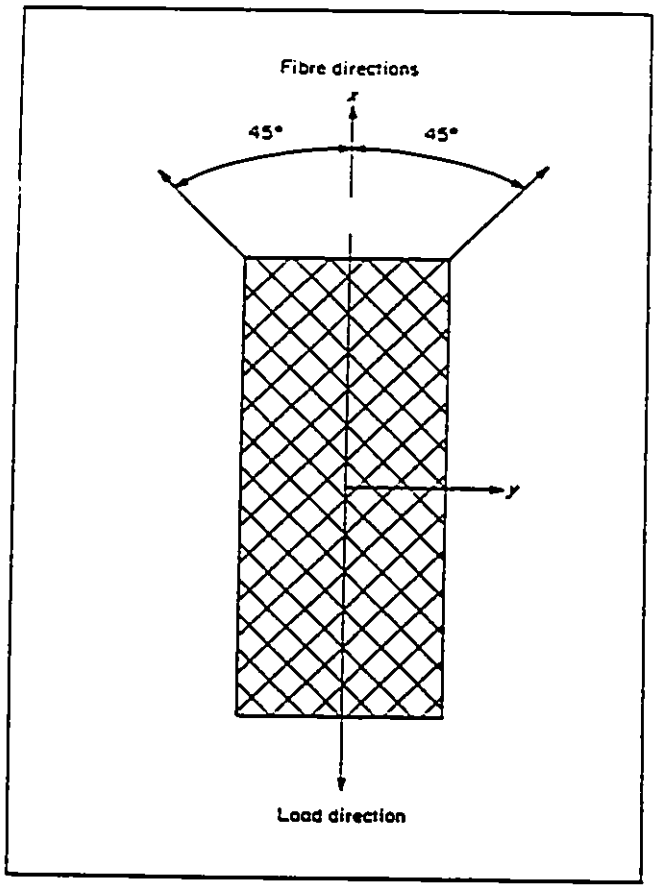

FIGURE 2.3: ±45° OFF-AXIS TENSILE SPECIMEN

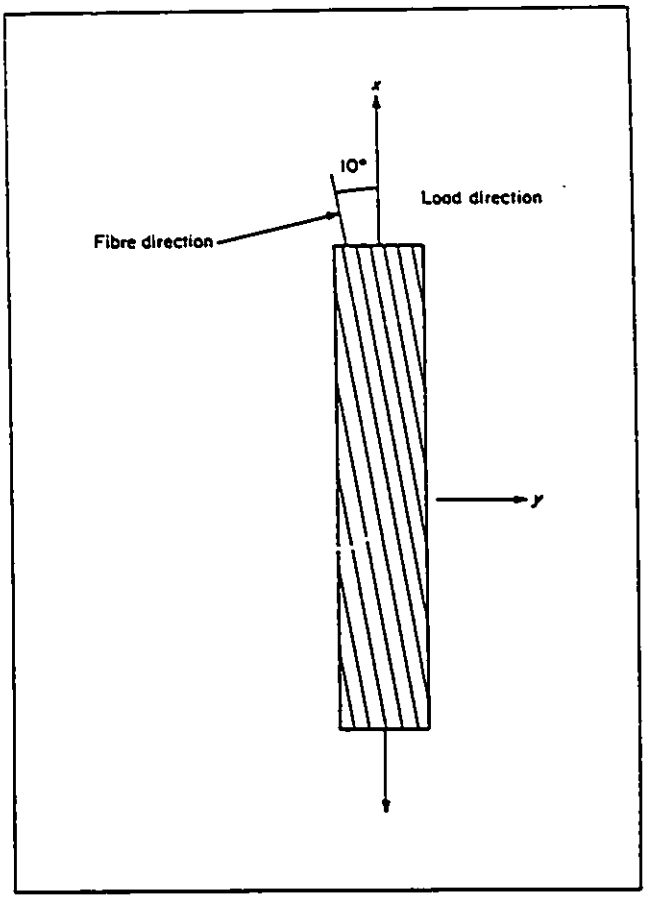

FIGURE 2.4: 10° OFF-AXIS TENSILE SPECIMEN

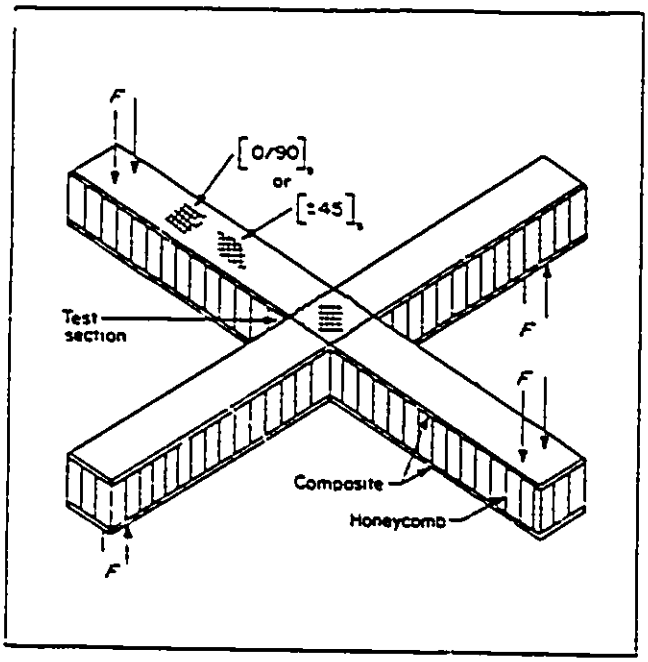

FIGURE 2.5: CROSS-BEAM SANDWICH SPECIMEN (REF. 16)

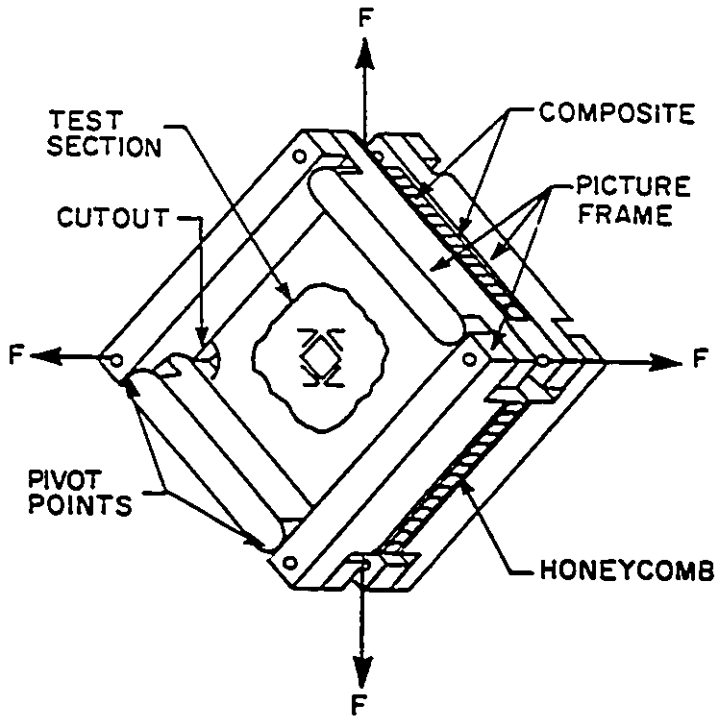

FIGURE 2.6: PICTURE FRAME PANEL LOADING FIXTURE AND SPECIMEN (REF. 17)

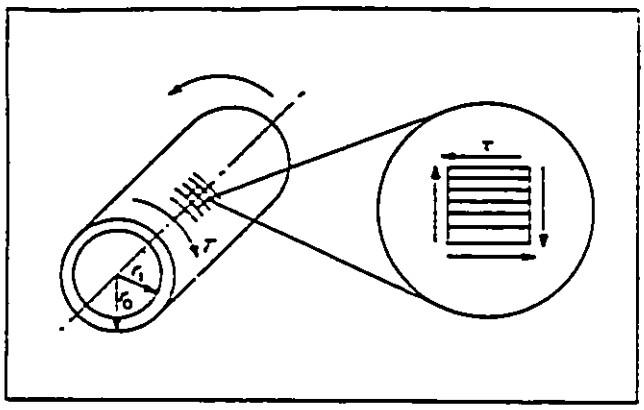

FIGURE 2.7: THIN-WALLED TORSION TUBE

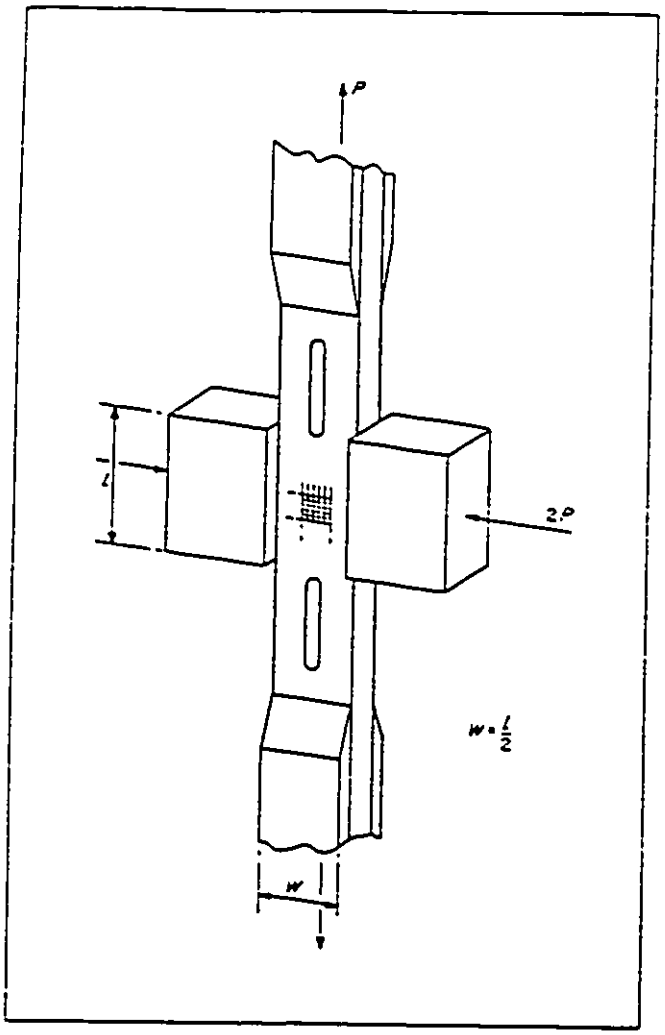

FIGURE 2.8: SLOTTED-TENSILE SPECIMEN (REF. 16)

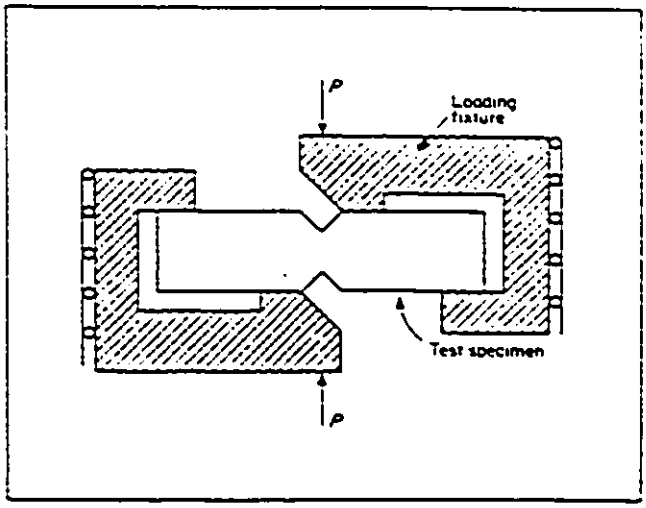

FIGURE 2.9: SCHEMATIC OF IOSIPESCU TESTING FIXTURE AND SPECIMEN

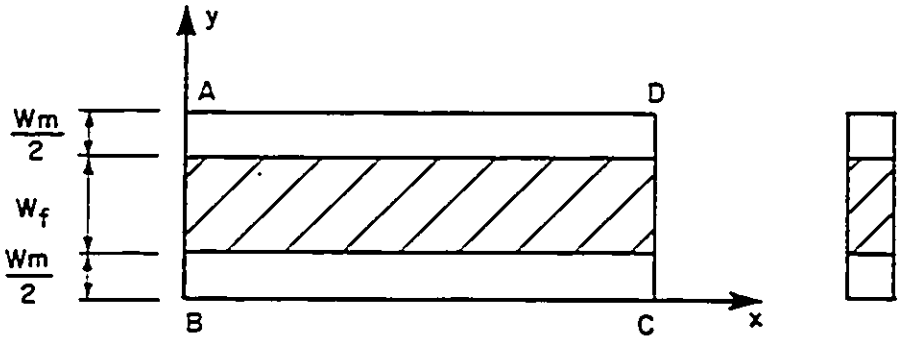

FIGURE 3.1: TYPICAL COMPOSITE MATERIAL SEGMENT

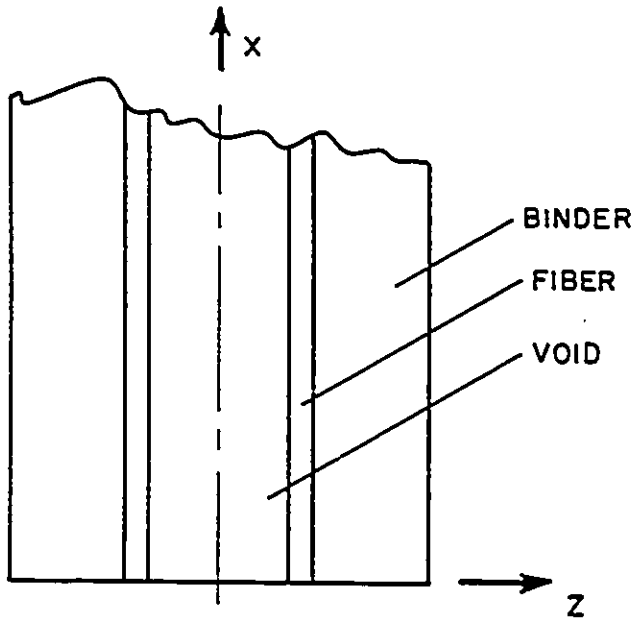

FIGURE 3.2: SECTION VIEW OF COMPOSITE MATERIAL SEGMENT (REF. 36)

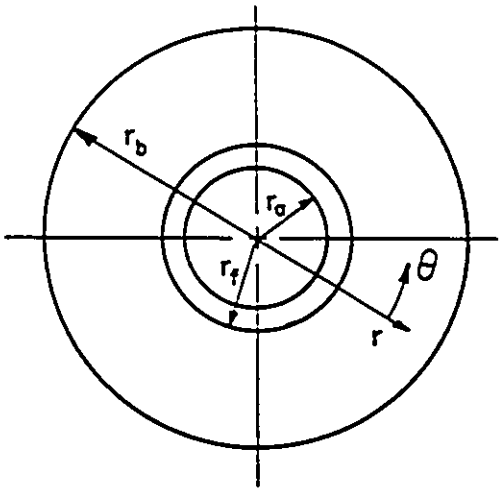

FIGURE 3.3: END VIEW OF COMPOSITE MATERIAL SEGMENT (REF. 36)

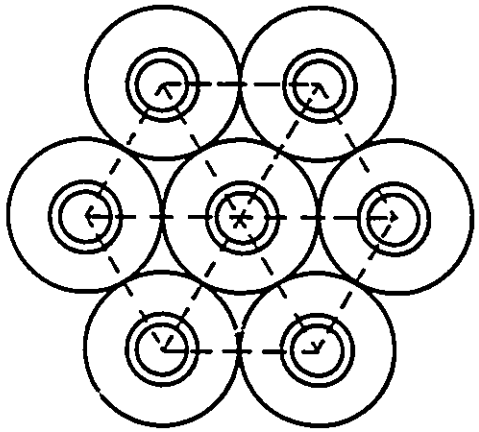

FIGURE 3.4: FIBRES IN HEXAGONAL ARRAY

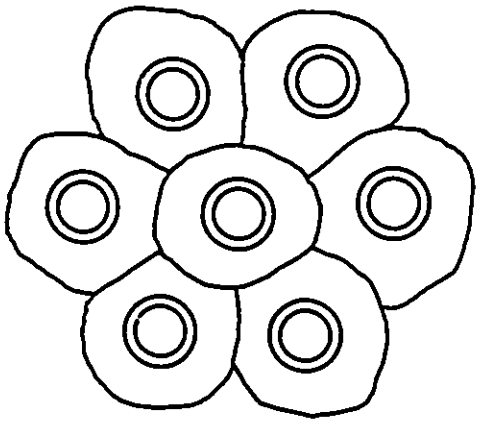

FIGURE 3.5: FIBRES IN RANDOM ARRAY

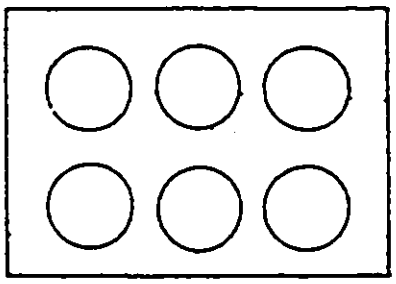

C=0

FIGURE 3.6: ISOLATED FIBRES
(RESIN CONTIGUOUS)

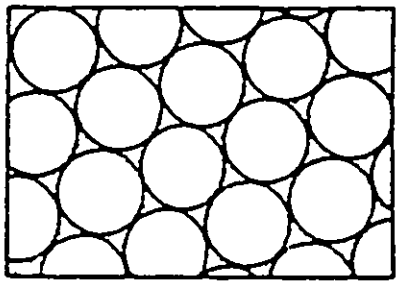

C=1

FIGURE 3.7: ISOLATED MATRIX
(FIBRES CONTIGUOUS)

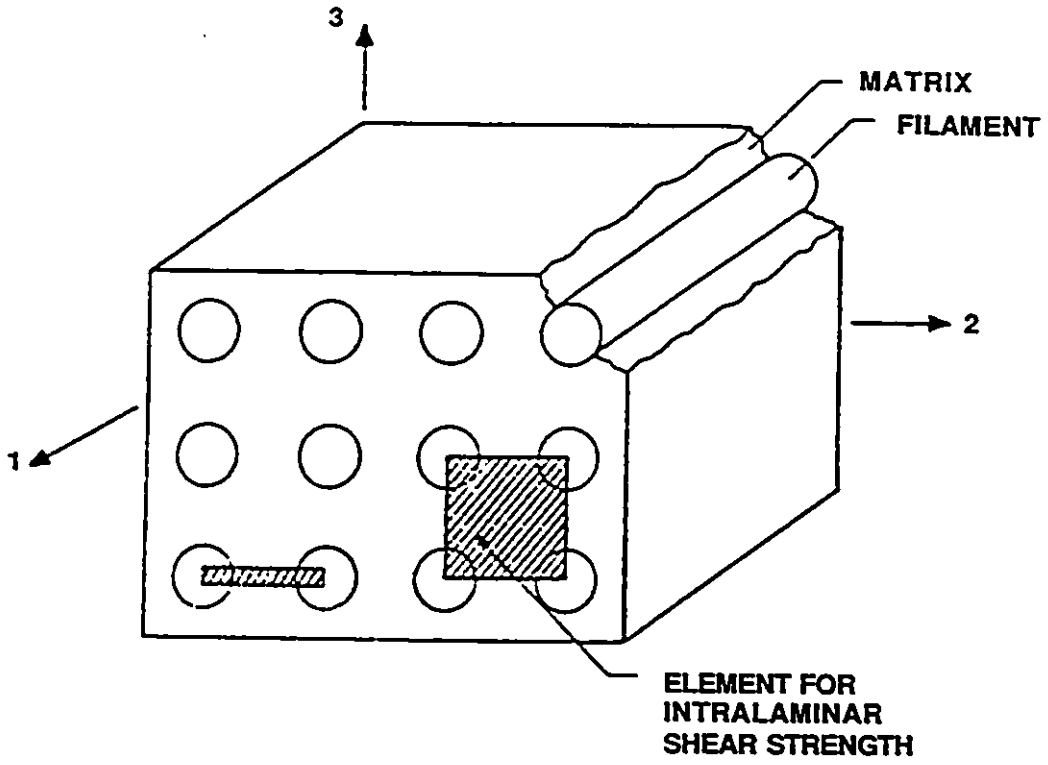

FIGURE 3.8: SCHEMATIC OF SQUARE ARRAY
(REF. 39)

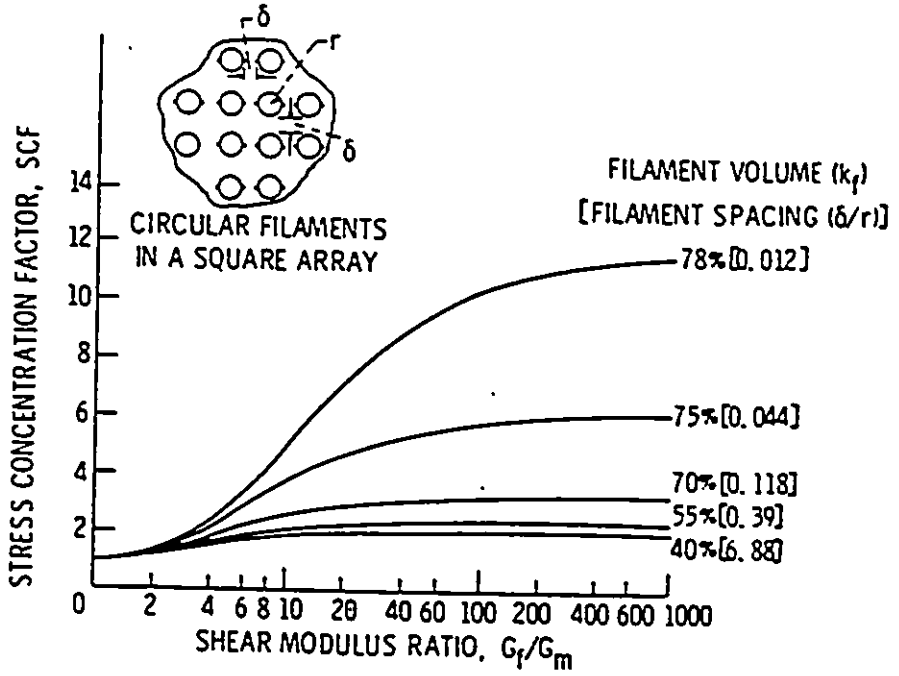

FIGURE 3.9: STRESS CONCENTRATION FACTOR (SCF) FOR CIRCULAR FILAMENTS IN A SQUARE ARRAY SUBJECTED TO INTRALAMINAR SHEAR LOADING (REF. 40)

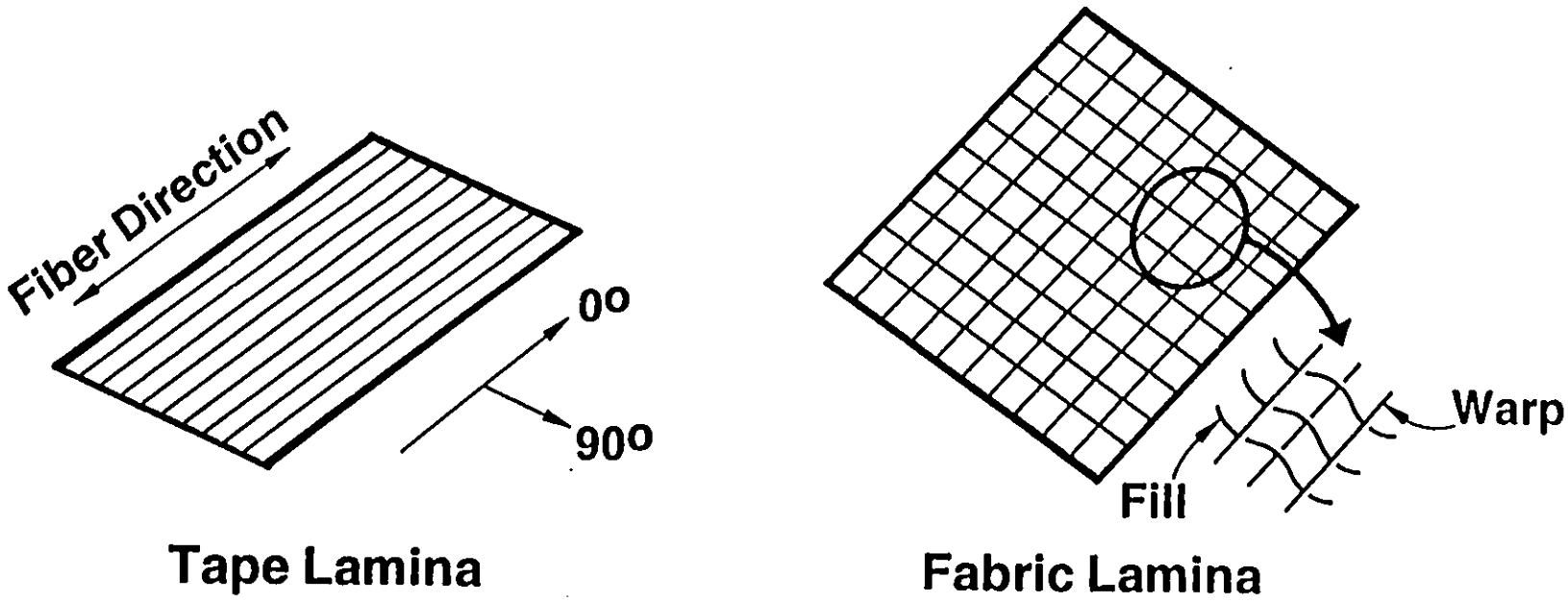

FIGURE 4.1: PREPREG IN UNIDIRECTIONAL AND FABRIC FORMS

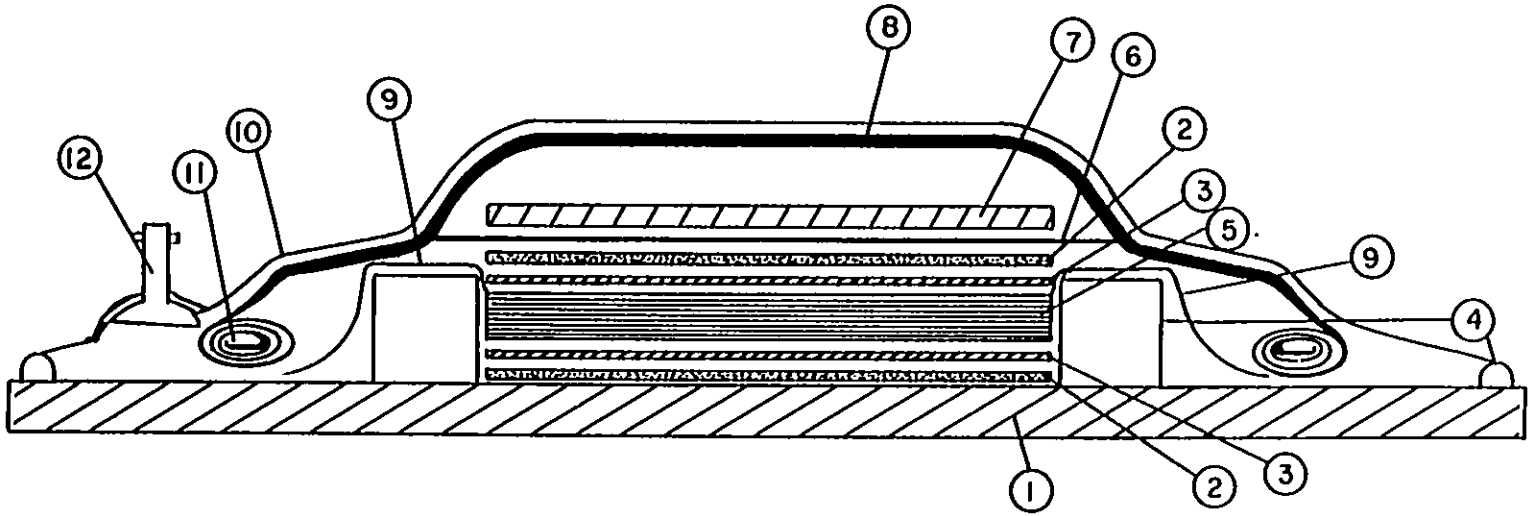

(1)	PLATE COATED WITH RELEASE AGENT	(7)	PRESSURE PLATE
(2)	LAYERS OF FIBREGLASS BLEEDER	(8)	BREATHER CLOTH
(3)	PERFORATED PARTING FILM	(9)	FIBREGLASS YARN
(4)	EDGE DAM (SEALING TAPE)	(10)	VACUUM BAG
(5)	COMPOSITE LAY-UP	(11)	EDGE BREATHER
(6)	NON-PERFORATED PARTING FILM	(12)	VACUUM SOURCE

FIGURE 4.2: SURFACE BLEED VACUUM BAGGING OF T300/5208

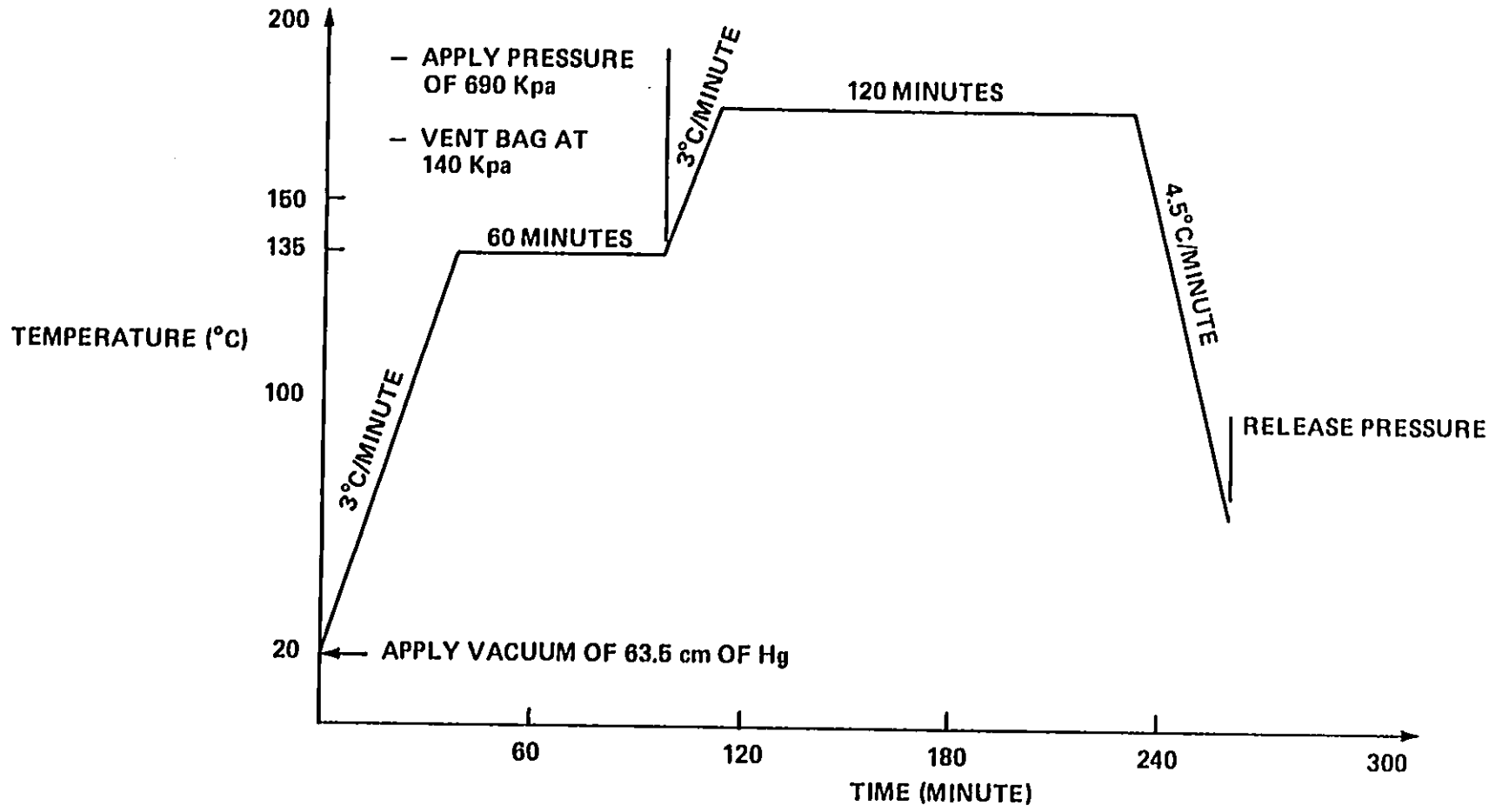

FIGURE 4.3: TYPICAL CURING CYCLE FOR NARMCO 5208 EPOXY RESIN

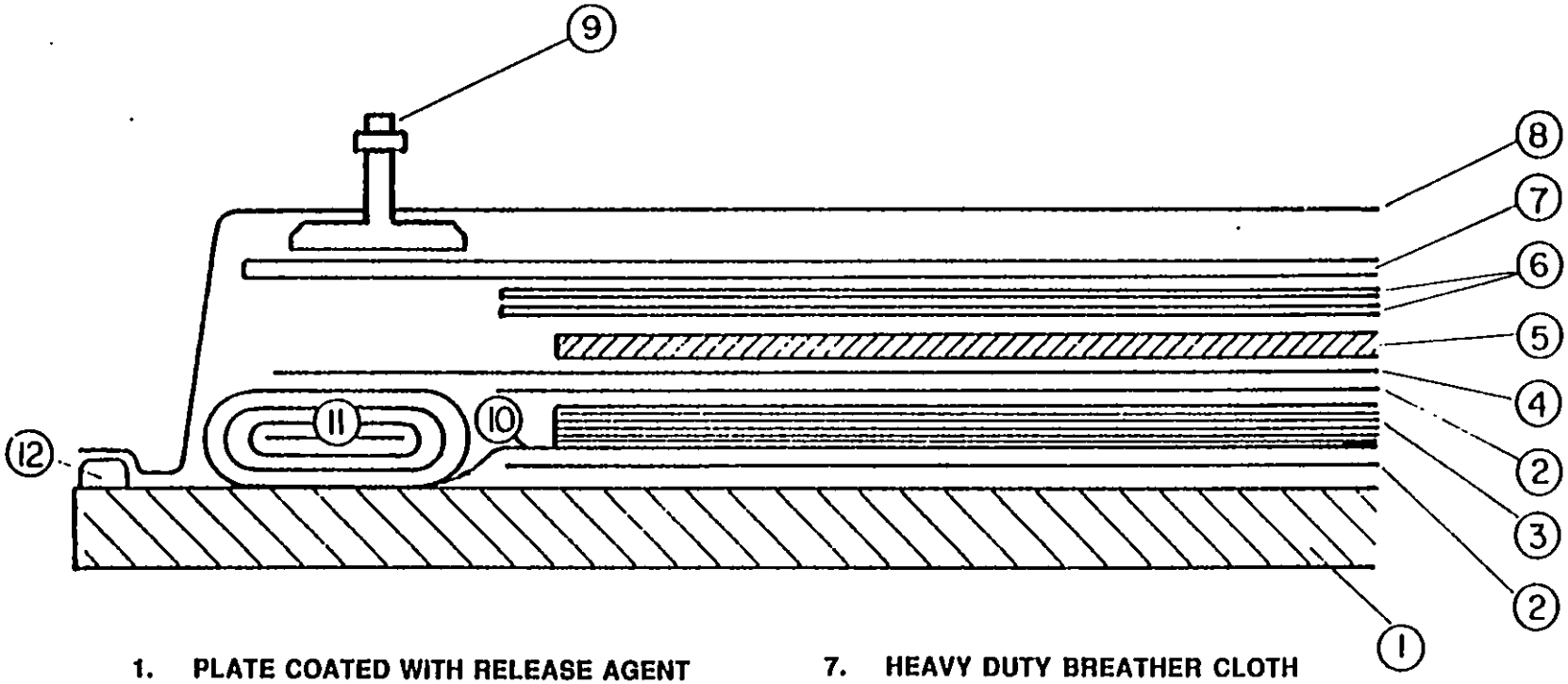

1. PLATE COATED WITH RELEASE AGENT
2. PEEL-PLY (OPTIONAL)
3. COMPOSITE LAY-UP
4. PARTING FILM
5. PRESSURE PLATE
6. 120 FIBRE GLASS (2 LAYERS)
7. HEAVY DUTY BREATHER CLOTH
8. VACUUM BAG
9. VACUUM SOURCE
10. FIBREGLASS YARN
11. BREATHER CLOTH
12. SEALING TAPE

FIGURE 4.4: VACUUM BAGGING A NON-BLEED LAY-UP

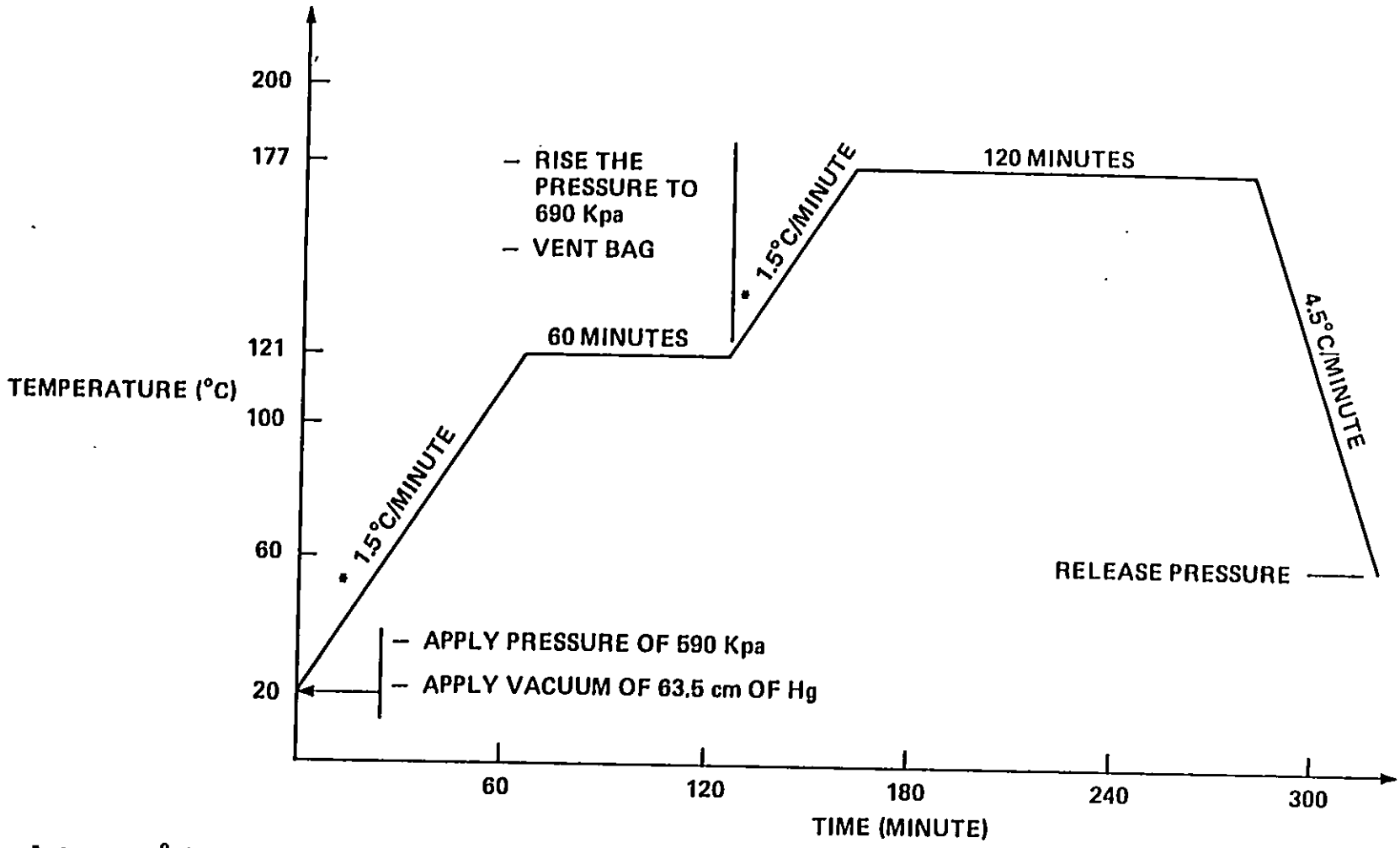

FIGURE 4.5: TYPICAL CURING CYCLE FOR NARMCO 5245C EPOXY RESIN

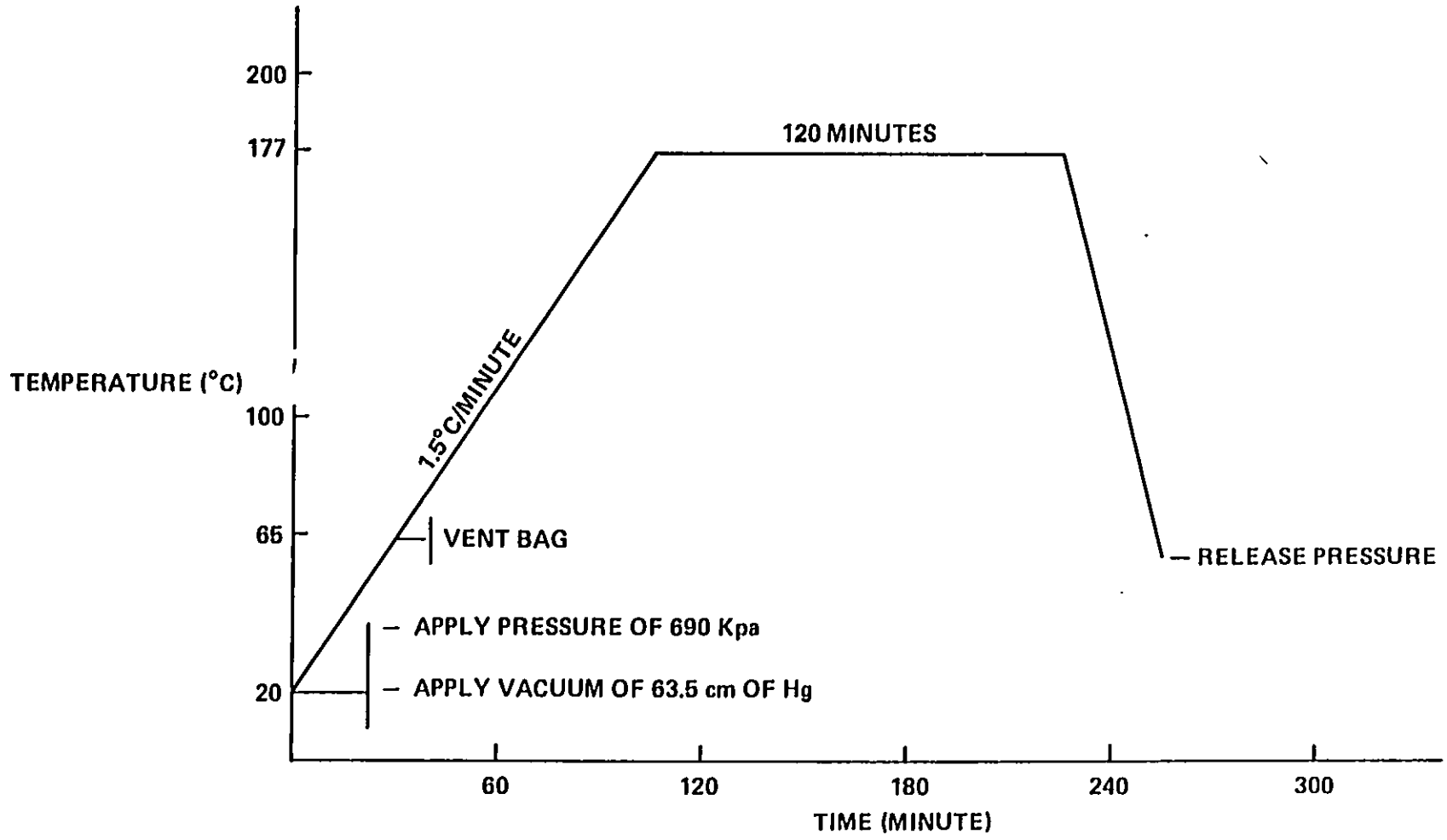

FIGURE 4.6: TYPICAL CURING CYCLE FOR HEXCEL F584 AND AMERICAN CYANAMID 1806 EPOXY RESINS

FIGURE 4.7: PANEL BONDED WITH END TABS

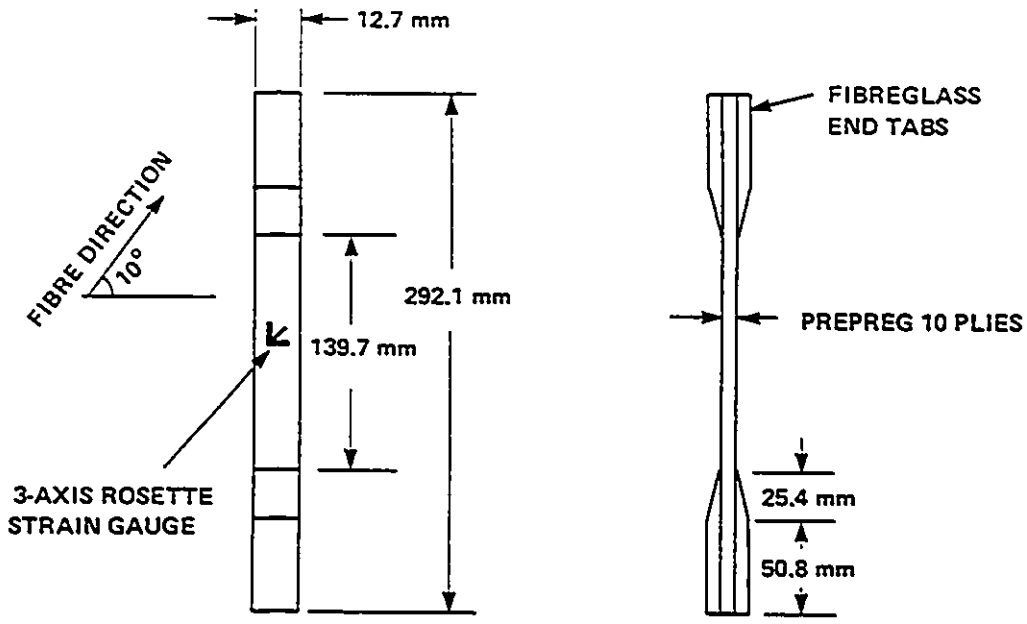

FIGURE 4.8: 10° OFF-AXIS TENSILE SHEAR SPECIMEN

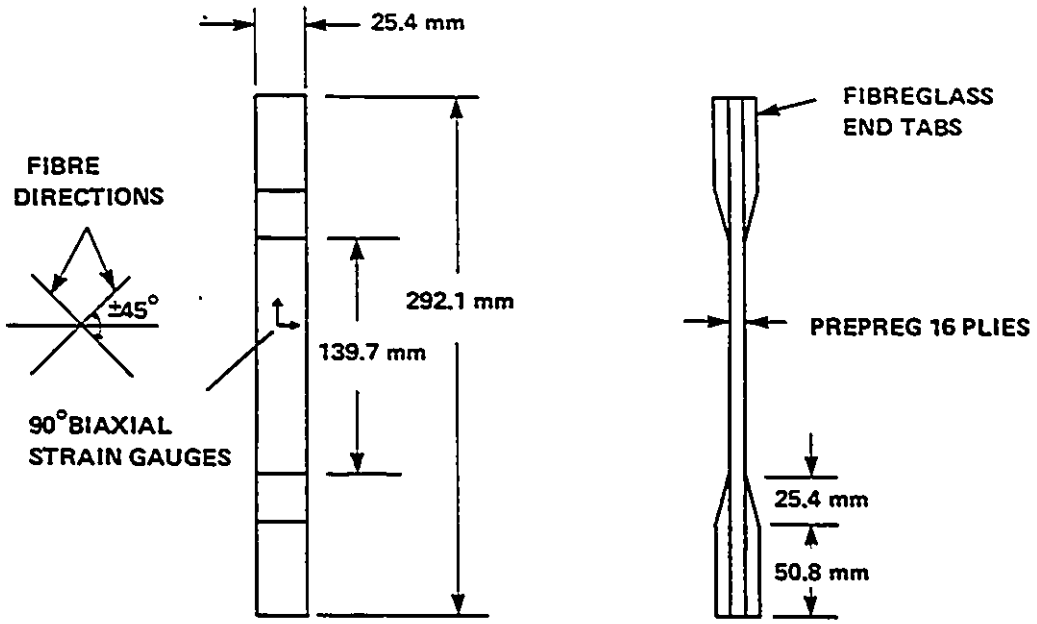

FIGURE 4.9: ±45° OFF-AXIS TENSION SHEAR SPECIMEN

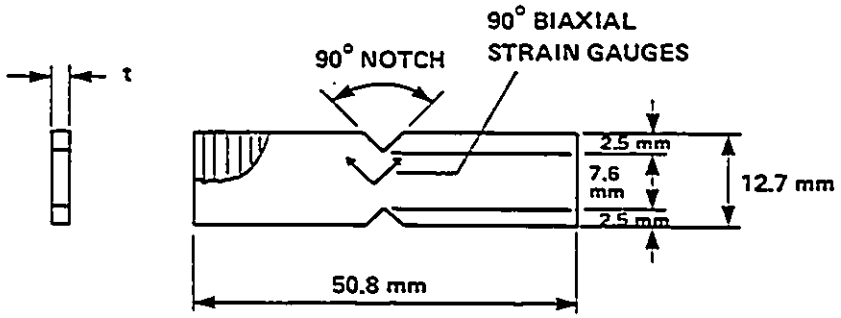

FIGURE 4.10: IOSIPESCU SHEAR SPECIMEN

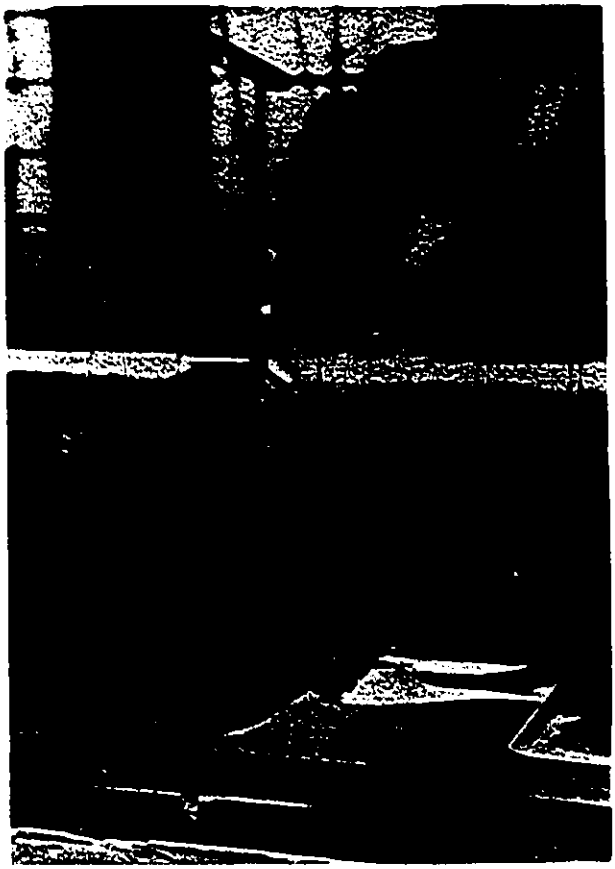

FIGURE 4.11: MACHINING OF THE 90° NOTCH OF MULTIPLE IOSIPESCU SPECIMENS USING A SLITTING SAW

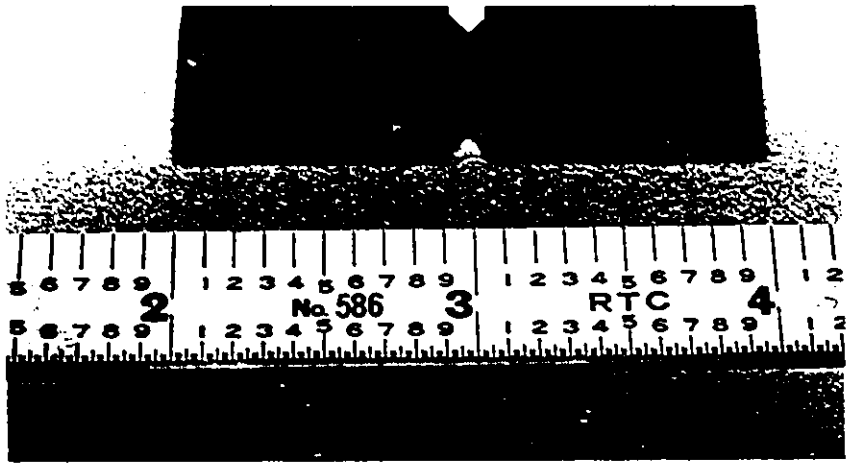

FIGURE 4.12: A TYPICAL MACHINED SPECIMEN

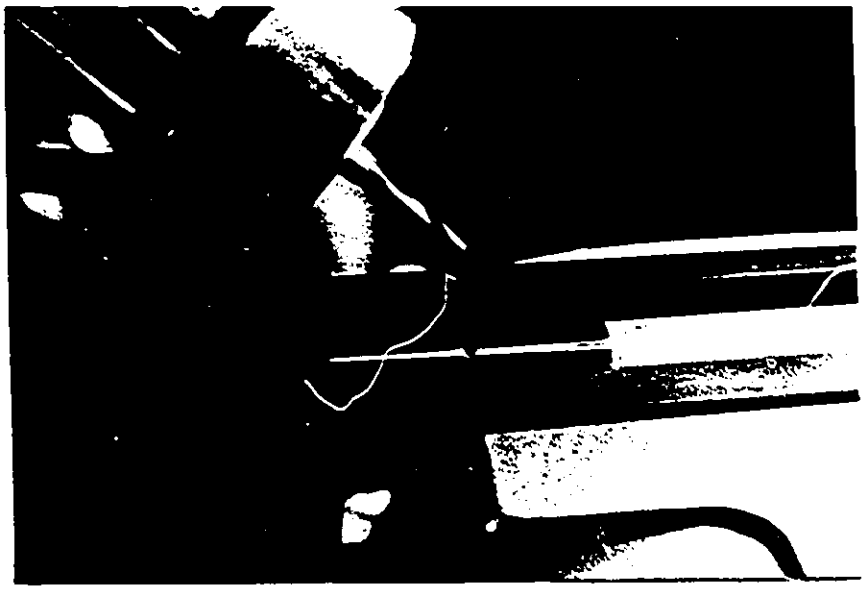

FIGURE 4.13: MACHINING OF THE 90° NOTCH OF MULTIPLE IOSIPESCU SPECIMENS USING A CARBIDE-TIPPED END MILL

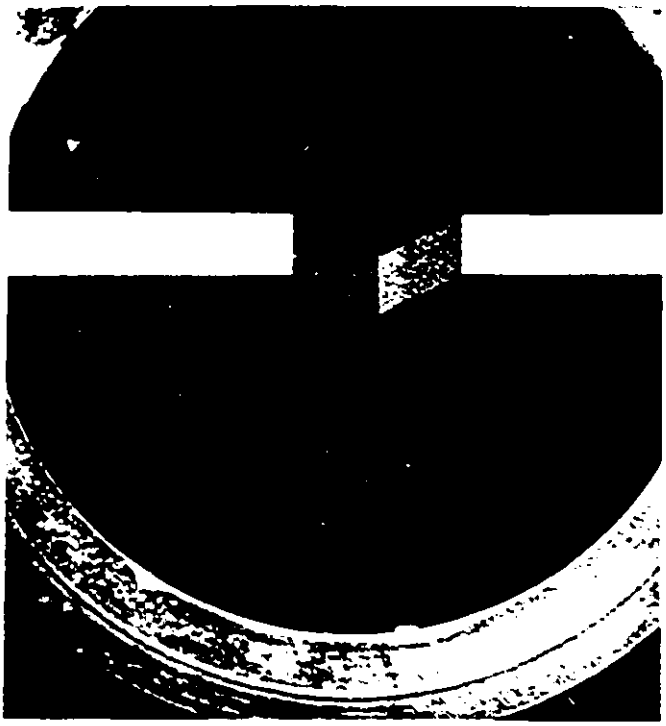

FIGURE 4.14: A TYPICAL MACHINED SPECIMEN

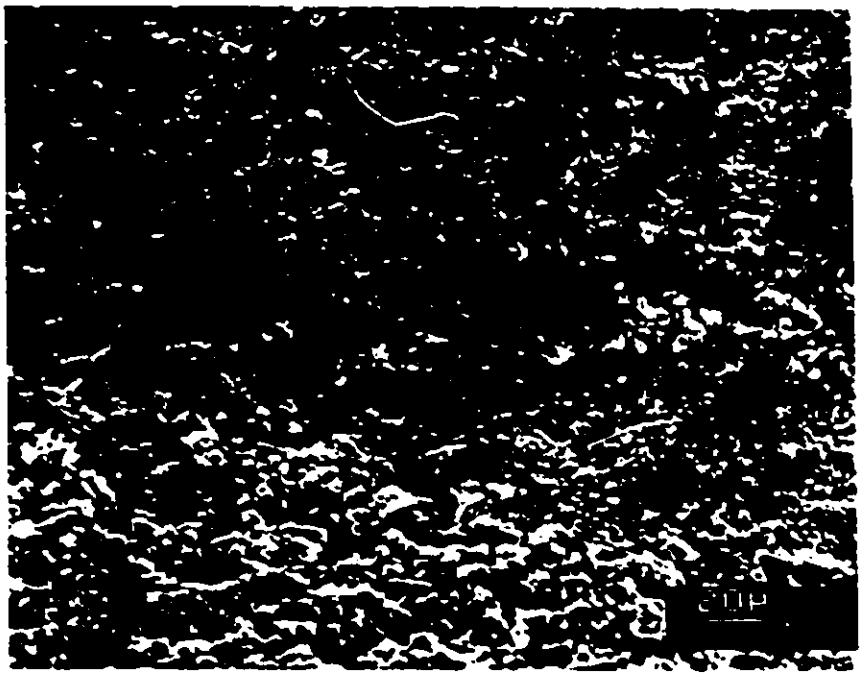

FIGURE 4.15: SCANNING ELECTRON MICROGRAPH OF THE ROOT (VIEWED FROM THE TOP) OF NOTCH PREPARED WITH THE SLITTING SAW (METHOD A)

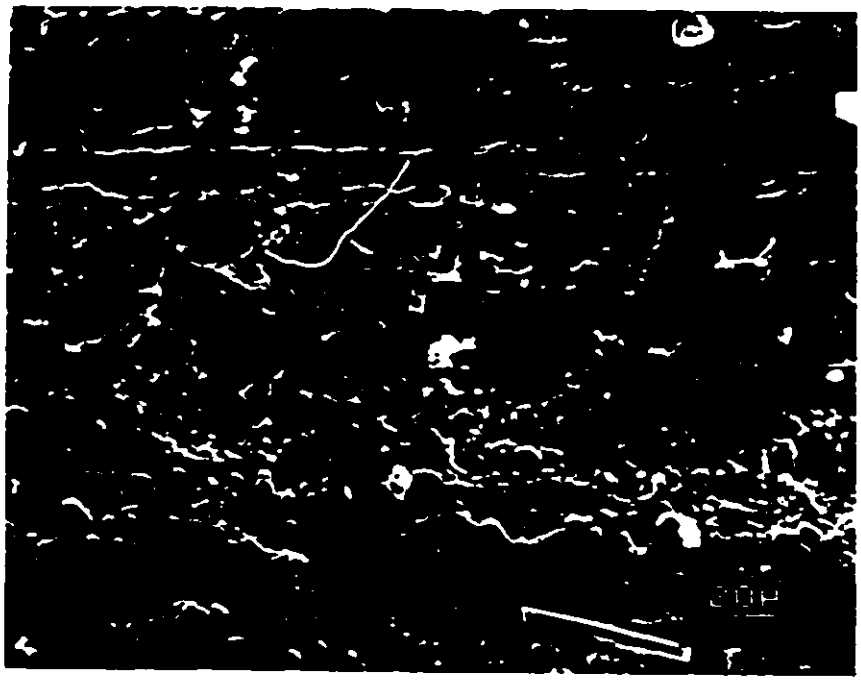

FIGURE 4.16: SCANNING ELECTRON MICROGRAPH OF THE ROOT (VIEWED FROM THE TOP) OF NOTCH PREPARED WITH THE CARBIDE-TIPPED END MILL (METHOD B)

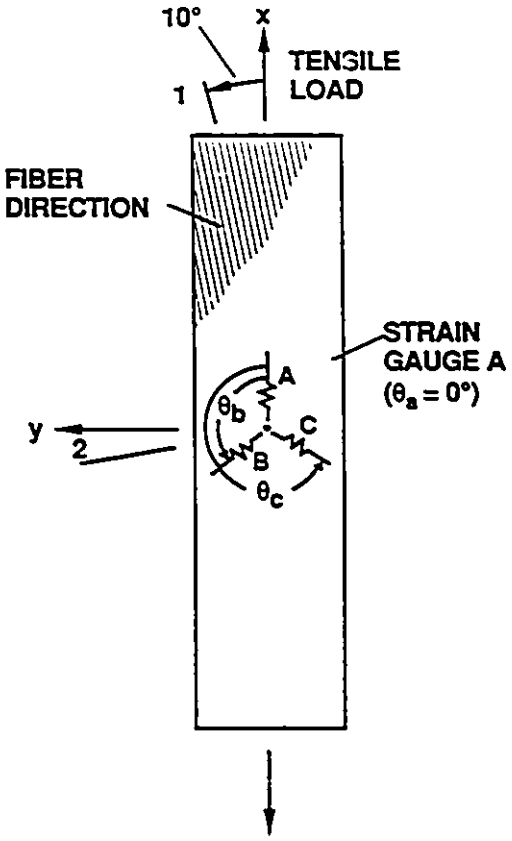

FIGURE 5.1: SCHEMATIC DEPICTING 10° OFF-AXIS TENSION TEST SPECIMEN WITH STRAIN GAUGE POSITIONS

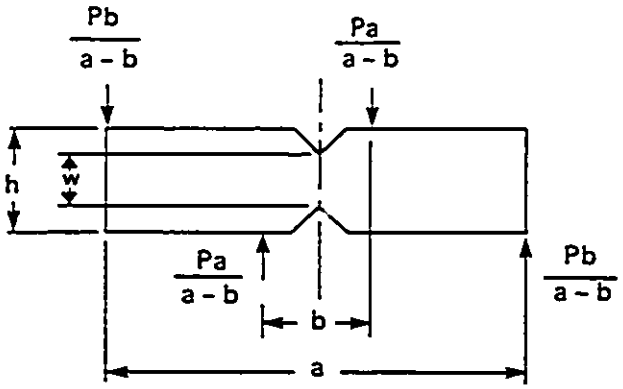

a = 5 1.mm
b = 12.7 mm
w = 7.6 mm

FIGURE 5.2: LOADING DIAGRAM FOR IOSIPESCU SPECIMEN

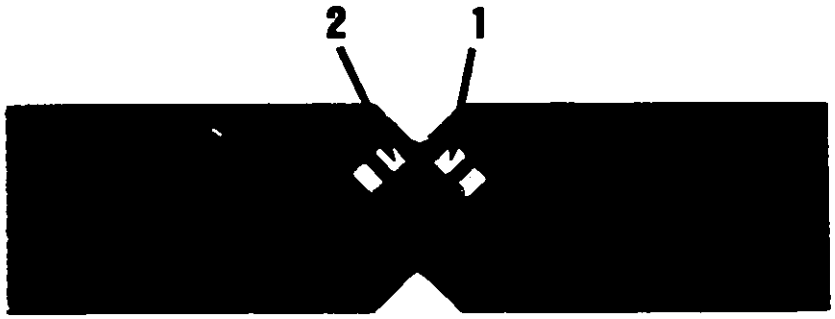

FIGURE 5.3: IOSIPESCU SPECIMEN WITH BIAXIAL STRAIN GAUGES

FIGURE 5.4: A TYPICAL ±45° OFF-AXIS TENSION TEST SET-UP

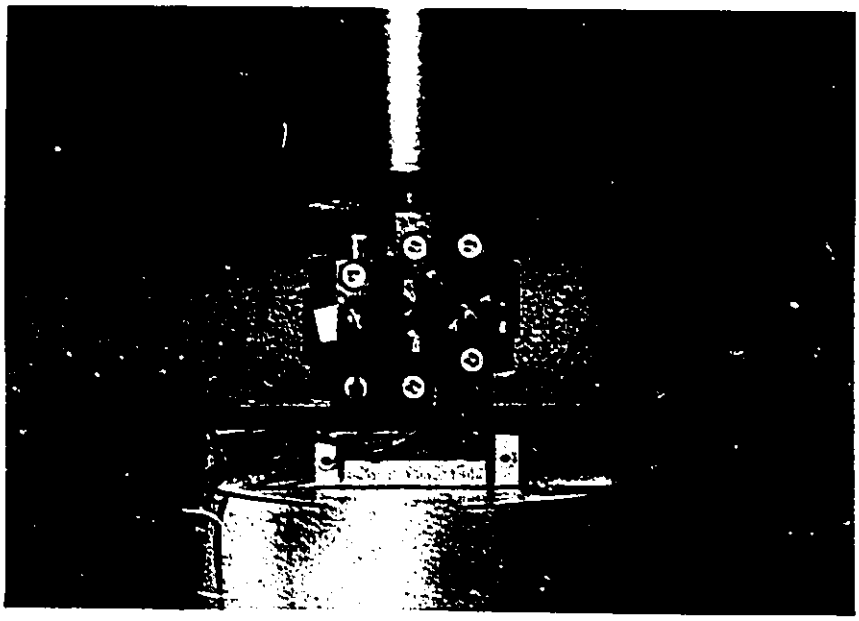

FIGURE 5.5: IOSIPESCU TEST FIXTURE

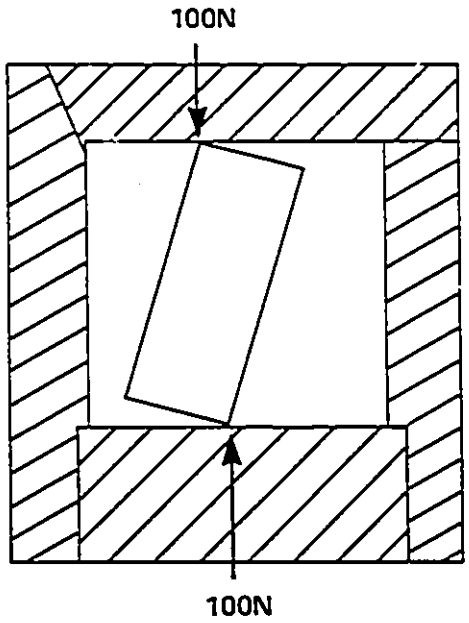

FIGURE 5.6: IMPROPER SEATING OF IOSIPESCU SPECIMEN (CASE 2)

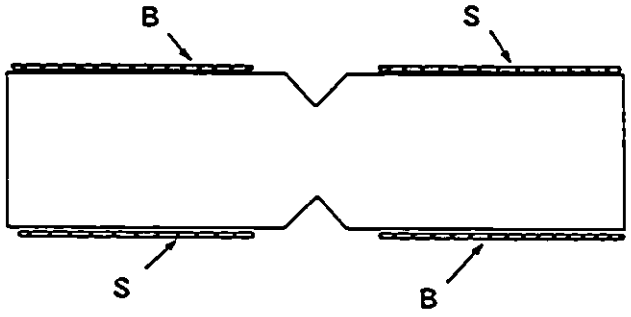

S = STEEL RAZOR BLADE
B = BRASS SHIM

FIGURE 5.7: SHIMMING DETAILS FOR CASES 3 AND 4

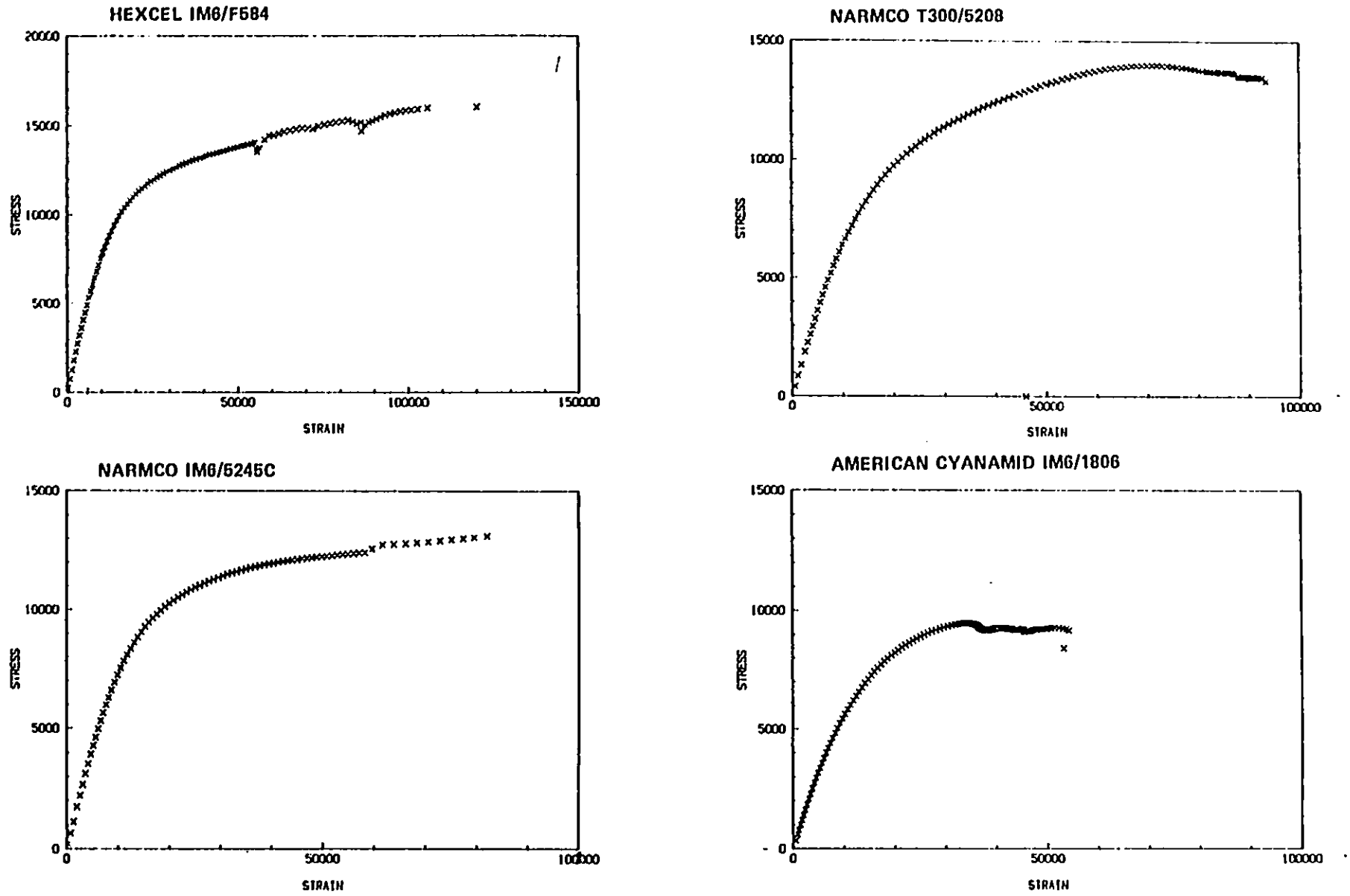

FIGURE 6.1: TYPICAL SHEAR STRESS-STRAIN CURVES OBTAINED FROM A TENSION TEST OF A $[\pm 45°]_{16}$ CARBON/EPOXY SPECIMEN

FIGURE 6.2: TYPICAL FAILED ±45° OFF-AXIS TENSION SHEAR SPECIMENS FROM FOUR COMPOSITE MATERIALS

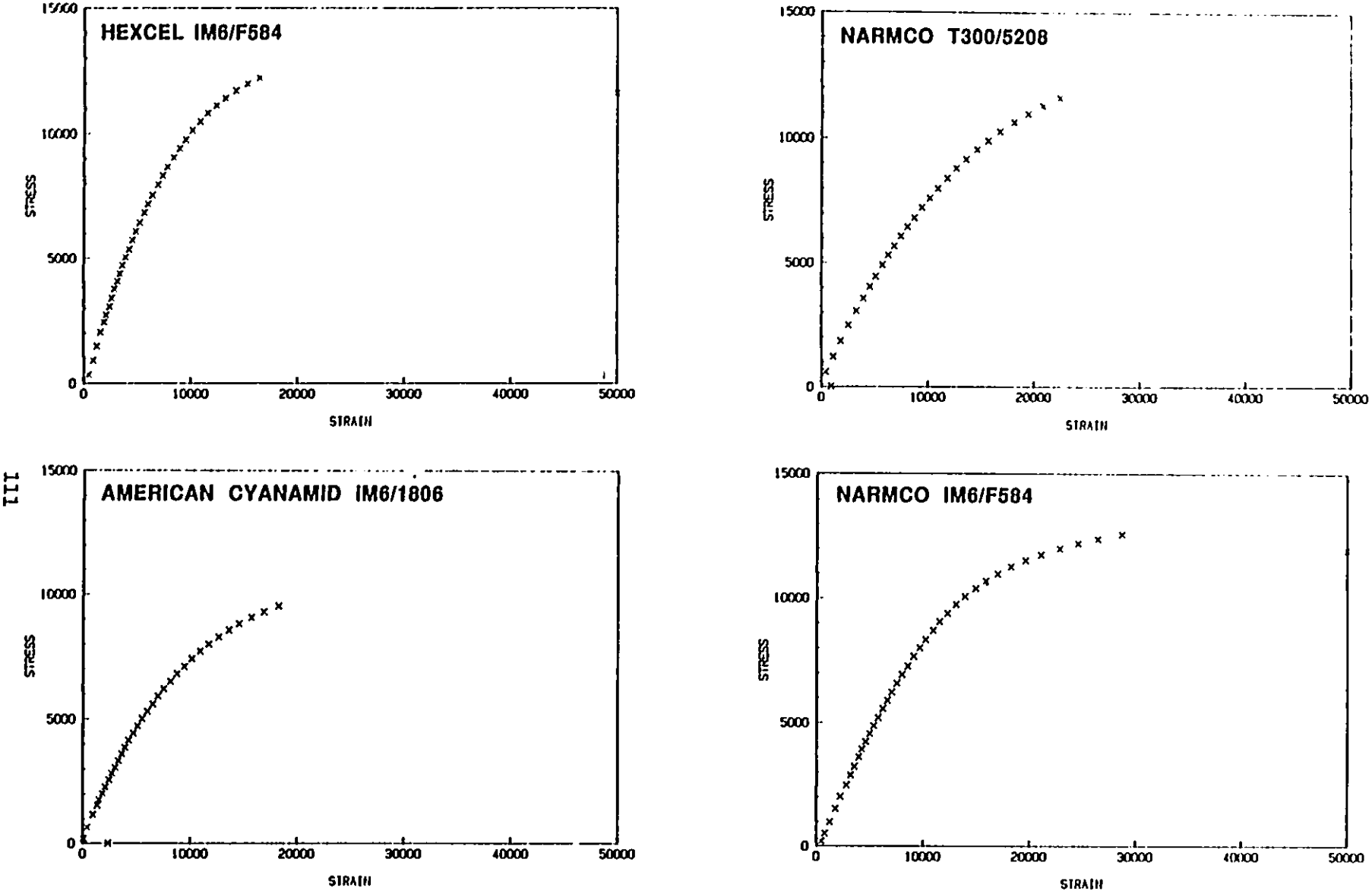

FIGURE 6.3: TYPICAL SHEAR STRESS-STRAIN CURVES OBTAINED FROM A TENSION TEST OF 10° OFF-AXIS SPECIMENS

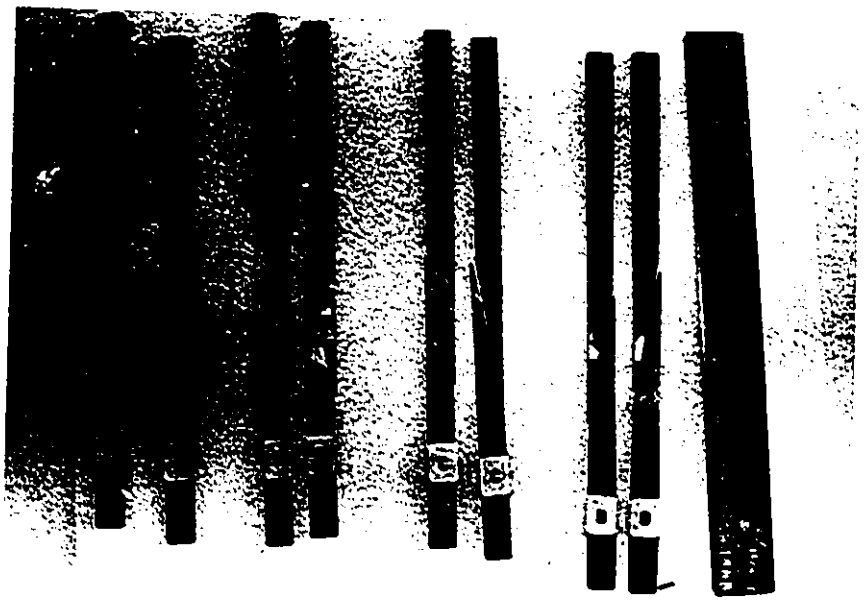

FIGURE 6.4: TYPICAL FAILED 10° OFF-AXIS TENSILE SPECIMENS FROM FOUR MATERIAL SYSTEMS

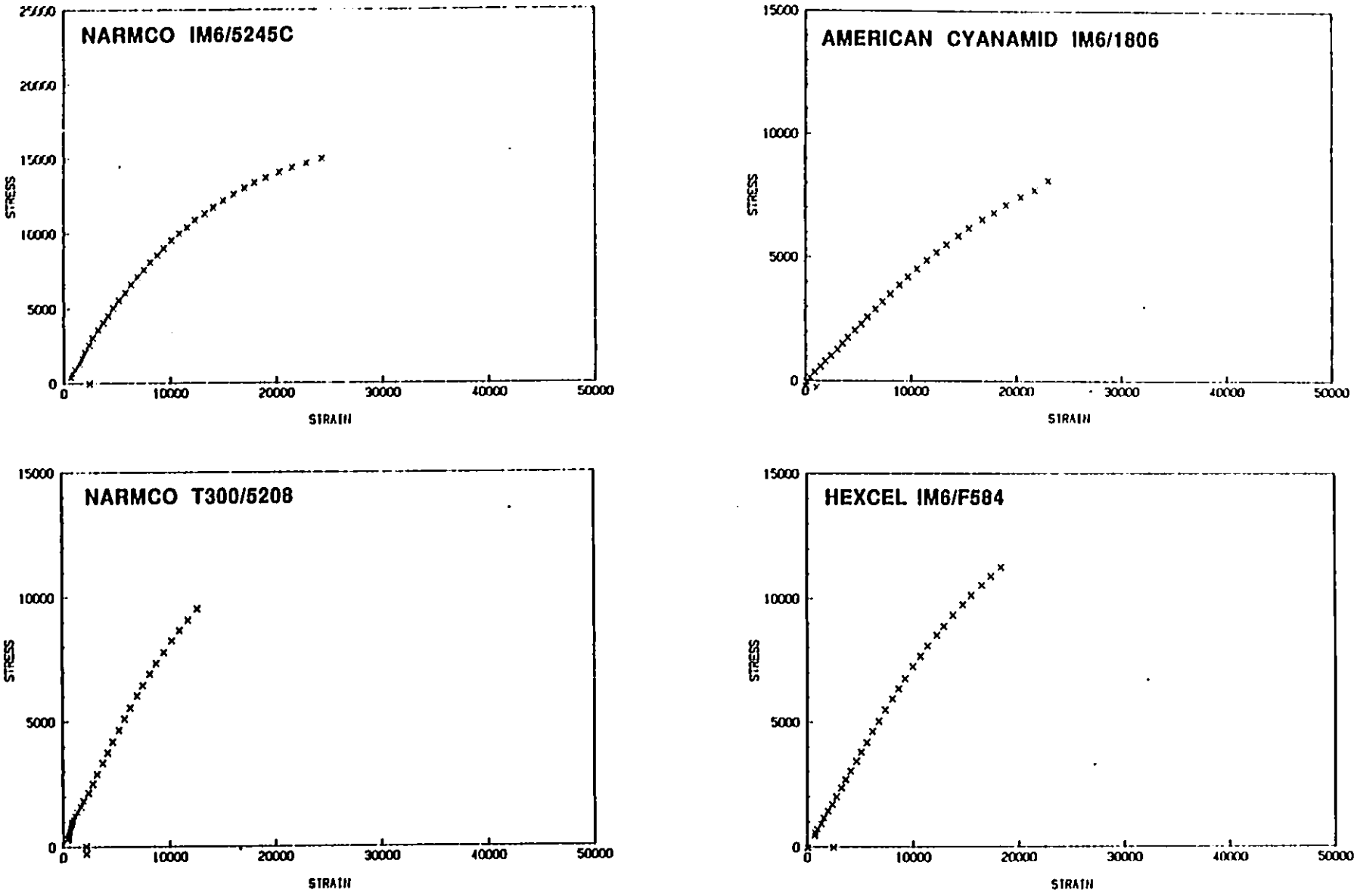

FIGURE 6.5: TYPICAL SHEAR STRESS-STRAIN CURVES OBTAINED FROM A TEST OF IOSIPESCU SHEAR SPECIMENS

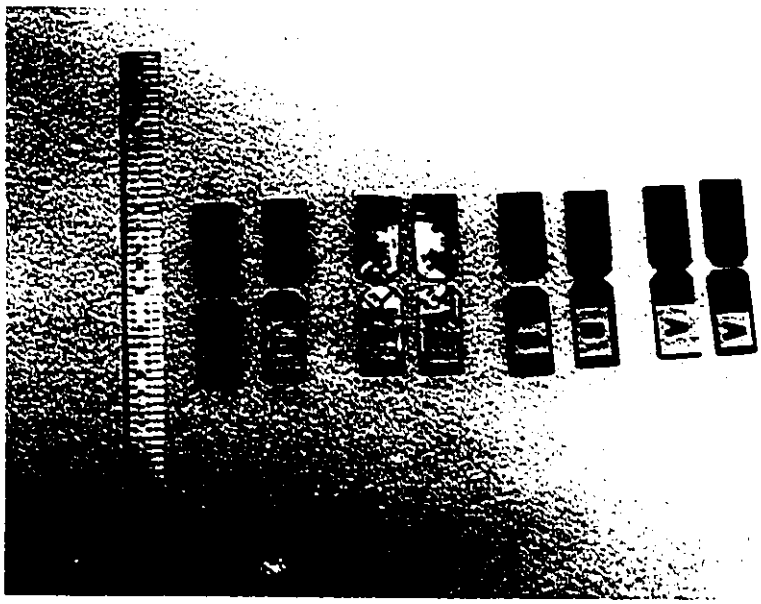

FIGURE 6.6: TYPICAL FAILED IOSIPESCU SHEAR SPECIMENS FROM FOUR COMPOSITE MATERIALS

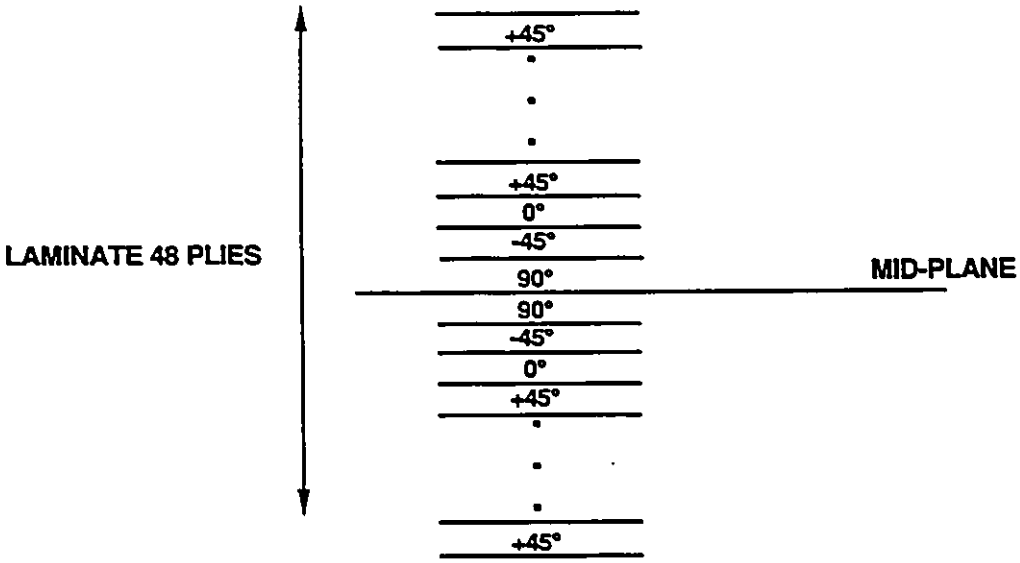

FIGURE 6.7: STACKING SEQUENCE OF A $[+45°/0°/-45°/90°]_{6s}$ LAMINATE

(a) NARMCO T300/5208

(b) AMERICAN CYANAMID IM6/1806

FIGURE 6.8: FRACTOGRAPHS OF IOSIPESCU SPECIMENS FROM NARMCO T300/5208 AND AMERICAN CYANAMID IM6/1806

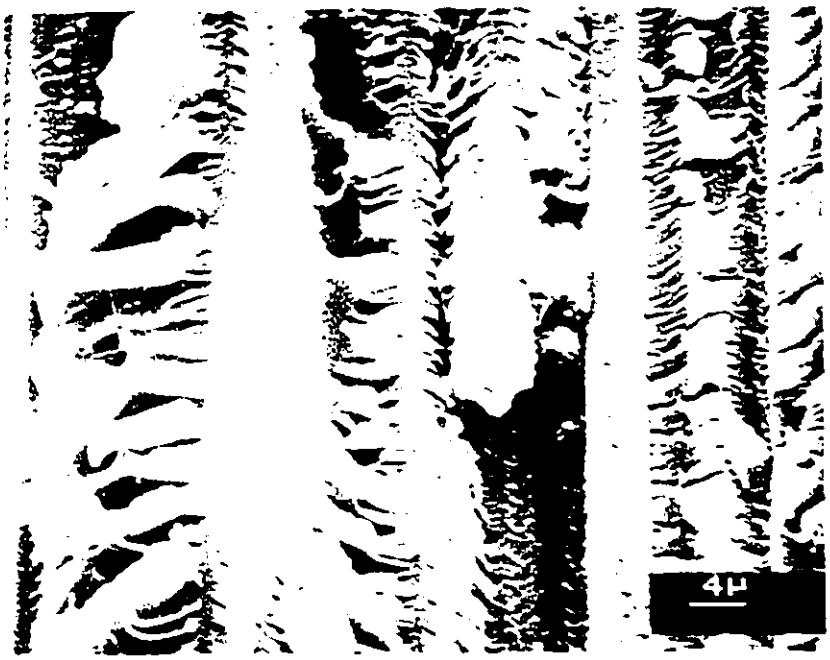

(c) HEXCEL IM6/F584

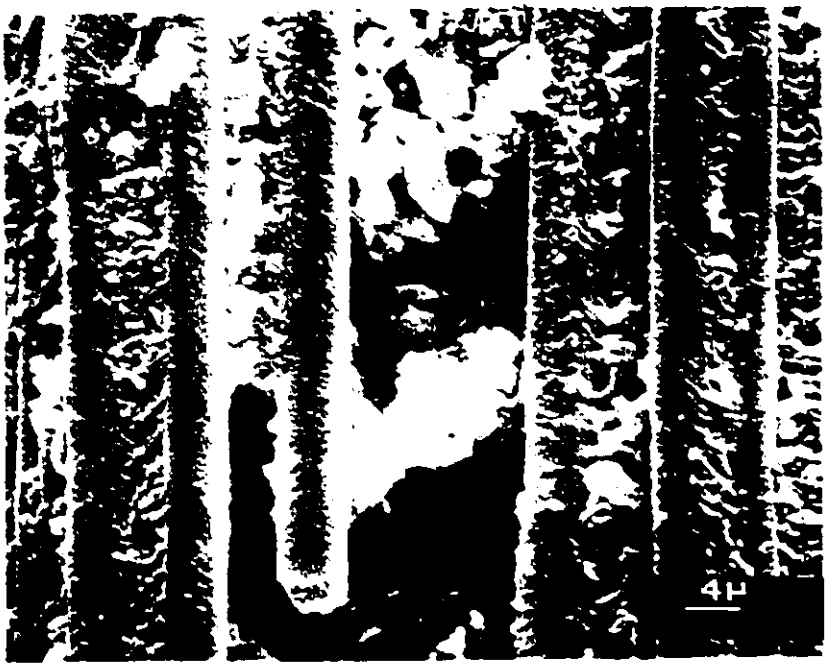

(d) NARMCO IM6/5245C

FIGURE 6.9: FRACTOGRAPHS OF IOSIPESCU SPECIMENS FROM NARMCO IM6/5245C AND HEXCEL IM6/F584

TABLE 2.1

EVALUATION OF IN-PLANE SHEAR TEST METHODS BY DECISION ANALYSIS TECHNIQUE

In-plane shear test method	Criterion													
	Cost of fabrication				Cost of testing				Data producibility		Accuracy of experimental results			
	Material quantity	Processing equipment	Specimen processing	Specimen preparation	Testing equipment	Special fixture	Specimen testing	Auxiliary instrumentation	Strength	Stiffness	Comparison with thin-walled tube experimental results		Total score	Rating
Weighting	20	50	40	40	100	50	50	50	150	150	200			
Rating	(10)	(10)	(10)	(10)	(10)	(10)	(10)	(10)	(10)	(10)	(10)			
Two-rail	7	10	10	6	10	5	10	10	6	7	7		6880	6
Three-rail	6	10	10	7	10	4	10	10	7	7	8		7200	4
45° tensile	9	10	10	10	10	10	10	10	7	8	9		8030	1
10° off-axis	10	10	9	10	10	10	10	10	7	7	9		7860	3
Cross-beam	2	8	7	8	7	7	3	10	6	7	6		5890	9
Picture frame	4	10	10	8	10	6	4	10	7	6	7		6650	7
Thin-walled tube	1	8	2	7	2	2	2	7	10	10	10		6530	8
Slotted-tensile	8	10	10	7	10	3	4	10	8	8	7		6990	5
Iosipescu	9	10	10	10	10	7	10	10	8	8	9		8030	1

TABLE 4.1

MATERIAL PROCUREMENT SPECIFICATIONS

Material Systems	Narmco Rigidite T300/5208	Narmco Rigidite IM6/5245	Hexcel IM6/F584	Cycom IM6/1806
I. Typical Physical properties				
Resin Content (wt. %)	41 ± 3%	34 ± 2%	34 ± 2%	34 ± 2%
Gel time at 350°F (minutes)	28 ± 8	6 ± 2	10 ± 2	10 - 15
Volatile content (wt. %)	2% max.	1% max.	2% max.	1%
Fibre areal weight (g/m^2)	145	145	145	145
Resin flow 100 psi at 300°F	21 ± 6%	low flow	low flow	low flow
Cured thickness (nominal)	5.0 mils	5.1 mils	5.7 mils	5.1
Taped width	12 inch	12 inch	12 inch	12 inch
Out time at room temperature	10 days	10 days	10 days	10 days
II. Typical laminate mechanical properties				
0 degree tensile strength at R.T. (Ksi)	185	380	385	335
0 degree tensile modulus at R.T. (Msi)	21.0	24.7	22.0	24.7
0 degree compressive strength at R.T. (Ksi)	165	234	251	208
0 degree compressive modulus at R.T. (Msi)	19.0	24.0	22.0	24.7
Short beam shear strength at R.T. (Ksi)	13.0	16.1	18.2	16.0
Shipping: The materials must be in sealed polyethylene bags in insulated containers with dry ice refrigeration.				

TABLE 4.2

CURE CYCLES

Material Systems	Narmco Rigidite T300/5208	Narmco Rigidite IM6/5245C	Hexcel IM6/F584	American Cyanamid IM6/1806
1. Initial Pressure	22 inch Hg vacuum	22 inch Hg vacuum 85 psi	22 inch Hg vacuum 100psi	
2. Initial Heat Rise	RT -275°C at 4-6°F/minute	RT -250°F at 3-5°F/minute	RT -350°F at 3-5°F/minute Vent Bag at 150°F	
3. Dwell	60 minutes at 275°F	60 minutes at 250°F	----------	
4. Pressurize	Apply 85-100psi Vent Bag at 20 psi	raise pressure to 100 psi and Vent Bag	----------	
5. Final Heat Rise	275°F-350°F at 4-6°F/minute	250°F-350°F at 3-5°F/minute	----------	
6. Cure	120 minutes at 350°F	120 minutes at 350°F	120 minutes at 350°F	
7. Cool Down	350°F-140°F at 8°F/minute under pressure	350°F-140°F at 8°F/minute under pressure	350°F-140°F at 8°F/minute under pressure	
8. Depressurize	release autoclave pressure	release autoclave pressure	release autoclave pressure	

TABLE 4.3

TEST MATRIX (IN-PLANE SHEAR PROPERTIES)

TEST	TYPE	PLY ORIENTATION	SPECIMEN DIMENSION mm	NOMINAL THICKNESS mm	PROPERTIES	TEST METHOD	TEST REPLICATES
Tension	Shear	$(\pm 45°)_{16_T}$	292.1 by 25.4	2.0	$\frac{\text{Strength } \tau_{12}}{\text{Modulus } G_{12}}$	ASTM D3518-76	10
Tension	Shear	$(10°)_{10_T}$	292.1 by 12.7	1.3	$\frac{\text{Strength } \tau_{12}}{\text{Modulus } G_{12}}$	10° off-axis tensile	10
Compression	Shear	$(0°)_{16_T}$	50.8 by 12.7	2.0	$\frac{\text{Strength } \tau_{12}}{\text{Modulus } G_{12}}$	Iosipescu	10

TABLE 5.1

STRAIN READINGS FOR TRIAL IOSIPESCU SPECIMENS

CASE	LOAD (N.)	STRAIN READING (MICROSTRAIN)			
		GAUGE 1*	GAUGE 2	GAUGE 3	GAUGE 4
1†	160	-1026	453	–	–
2†	120	-348	403	-719	230
3‡	139	-459	309	-488	326
4‡	139	-441	444	-443	464

* Gauges 3 and 4 are back-to-back with gauges 1 and 2, respectively.

† Without shimming

‡ With shimming

TABLE 6.1

NARMCO T300/5208 ±45° TENSILE SHEAR TEST RESULTS

Specimen	Ultimate		at 0.5% strain
	Strength MPa (Ksi)	Strain γ_{12} μmm/mm	Modulus GPa (Msi)
1	94.5 (13.7)	77,663	4.55 (0.66)
2	95.1 (13.8)	99,099	4.83 (0.70)
3	95.1 (13.7)	62,181	4.83 (0.70)
4	94.5 (13.7)	72,564	4.83 (0.70)
5	94.5 (13.7)	76,046	5.04 (0.73)
6	95.1 (13.8)	81,164	4.83 (0.70)
7	93.1 (13.5)	72,326	4.83 (0.70)
8	96.5 (14.0)	89,006	4.97 (0.72)
9	96.5 (14.0)	71,332	5.04 (0.73)
10	92.4 (13.4)	55,161	5.24 (0.76)
Average	94.5 (13.7)	75,654	4.90 (0.71)

TABLE 6.2

AMERICAN CYANAMID IM6/1806 ±45° TENSILE SHEAR TEST

Specimen	Ultimate		at 0.5% strain
	Strength MPa (Ksi)	Strain * γ_{12} μmm/mm	Modulus GPa (Msi)
1	93.8 (13.6)	-	4.35 (0.63)
2	108.9 (15.8)	-	4.00 (0.58)
3	64.1 (9.3)	-	4.28 (0.62)
4	100.0 (14.5)	-	3.72 (0.54)
5	96.5 (14.0)	-	3.51 (0.51)
6	93.8 (13.6)	-	4.00 (0.58)
7	100.7 (14.6)	-	4.00 (0.58)
8	79.3 (11.5)	-	4.00 (0.60)
9	64.1 (9.30)	-	4.55 (0.66)
10	106.2 (15.4)	-	3.72 (0.54)
AVERAGE	90.7 (13.2)	-	4.00 (0.58)

* = Strain Gauges Separated Before Failure

TABLE 6.3

HEXCEL IM6/F584 ±45° TENSILE SHEAR TEST RESULTS

Specimen	Ultimate		at 0.5% strain Modulus
	Strength MPa (Ksi)	Strain * γ_{12} μmm/mm	GPa (Msi)
1	126.9 (18.4)	-	5.86 (0.85)
2	122.0 (17.7)	-	5.72 (0.83)
3	121.3 (17.6)	-	6.62 (0.96)
4	116.5 (16.9)	-	6.07 (0.88)
5	126.9 (18.4)	-	5.52 (0.80)
6	125.5 (18.2)	-	6.14 (0.89)
7	128.2 (18.6)	-	6.00 (0.87)
8	122.0 (17.7)	-	5.67 (0.82)
9	116.5 (16.9)	-	6.07 (0.88)
10	118.6 (17.2)	-	5.79 (0.84)
Average	122.4 (17.8)	-	5.93 (0.86)

* = Strain Gauges Separated Before Failure

TABLE 6.4

NARMCO IM6/5245C ±45° TENSILE SHEAR TEST RESULTS

Specimen	Ultimate		at 0.5% strain
	Strength MPa (Ksi)	Strain * γ_{12} μmm/mm	Modulus GPa (Msi)
1	120.0 (17.7)	-	4.69 (0.68)
2	100.7 (14.6)	-	5.79 (0.84)
3	-	-	-
4	125.5 (18.2)	-	5.65 (0.82)
5	135.8 (19.7)	-	5.38 (0.78)
6	120.0 (17.4)	-	5.66 (0.82)
7	121.3 (17.6)	-	5.66 (0.82)
8	117.9 (17.1)	-	5.31 (0.77)
9	109.6 (15.9)	-	5.79 (0.84)
10	105.5 (15.3)	-	5.72 (0.83)
Average	117.6 (17.1)	-	5.52 (0.80)

* = Strain Gauges Separated Before Failure

TABLE 6.5

NARMCO T300/5208 10° OFF-AXIS TENSILE SHEAR TEST RESULTS

Specimen	Ultimate		at 0.5% strain	
	Strength MPa (Ksi)	Strain γ_{12} μmm/mm	Modulus GPa	(Msi)
1	75.8 (11.0)	17,687	6.07	(0.88)
2	80.0 (11.6)	22,445	6.00	(0.87)
3	82.0 (11.9)	23,873	6.21	(0.90)
4	78.6 (11.4)	22,285	5.86	(0.85)
5	73.8 (10.7)	18,738	5.93	(0.86)
6	72.4 (10.5)	11,404	9.38	(1.36)
7	40.7 (5.9)*	6,232	6.48	(0.94)
8	70.3 (10.2)	11,263	8.14	(1.18)
9	37.2 (5.4)*	3,561	-	
10	62.1 (9.0)	9,065	7.73	(1.12)
Average	74.4 (10.7)	17,095	6.83	(0.99)

* = Excluded (Pre-mature failures)

TABLE 6.6

AMERICAN CYANAMID IM6/1806 10° OFF-AXIS TENSILE SHEAR TEST RESULTS

Specimen	Ultimate		at 0.5% strain	
	Strength MPa (Ksi)	Strain γ_{12} μmm/mm	Modulus GPa	(Msi)
1	59.3 (8.6)	12,951	6.83	(0.99)
2	65.9 (9.5)	18,257	6.35	(0.92)
3	57.9 (8.4)	15,698	5.38	(0.78)
4	64.1 (9.3)	10,872	5.93	(0.86)
5	60.7 (8.8)	14,029	6.62	(0.96)
6	60.0 (8.7)	19,181	5.79	(0.84)
7	61.4 (8.9)	18,357	6.00	(0.87)
8	56.5 (8.2)	17,687	5.24	(0.76)
9	51.7 (7.5)	11,099	6.35	(0.92)
10	55.8 (8.1)	13,292	6.07	(0.88)
Average	59.3 (8.6)	15,142	6.07	(0.88)

TABLE 6.7

HEXCEL IM6/F584 10° OFF-AXIS TENSILE SHEAR TEST RESULTS

Specimen	Ultimate		at 0.5% strain
	Strength MPa (Ksi)	Strain γ_{12} μmm/mm	Modulus GPa (Msi)
1	67.6 (9.8)	11,379	7.73 (1.12)
2	84.1 (12.2)	16,430	8.48 (1.23)
3	88.3 (12.8)	19,629	8.07 (1.17)
4	89.6 (13.0)	19,667	7.73 (1.12)
5	75.2 (10.9)	11,409	9.17 (1.33)
6	86.9 (12.6)	17,644	8.20 (1.19)
7 *	52.4 (7.6)	5,753	—
8	90.3 (13.1)	19,103	8.07 (1.17)
9 *	45.5 (6.6)	8,182	—
10	86.2 (12.5)	28,109	5.45 (0.79)
Average	83.4 (12.1)	17,921	7.86 (1.14)

* = excluded (pre-mature failures)

TABLE 6.8

NARMCO IM6/5245C 10° OFF-AXIS TENSILE SHEAR TEST RESULTS

Specimen	Ultimate		at 0.5% strain
	Strength MPa (Ksi)	Strain γ_{12} μmm/mm	Modulus GPa (Msi)
1	83.4 (12.1)	27,058	5.72 (0.83)
2	90.3 (13.1)	33,022	6.62 (0.96)
3	87.6 (12.7)	43,241	5.45 (0.79)
4	86.9 (12.6)	30,961	5.79 (0.84)
5	87.6 (12.7)	33,247	6.28 (0.91)
6	86.9 (12.6)	28,721	6.28 (0.91)
7	88.3 (12.8)	—	5.93 (0.86)
8	87.6 (12.7)	35,067	5.79 (0.84)
9	82.0 (11.9)	27,674	5.86 (0.85)
10	87.6 (12.7)	28,086	6.69 (0.97)
Average	86.8 (12.5)	31,897	6.00 (0.87)

TABLE 6.9

NARMCO T300/5208 IOSIPESCU SHEAR TEST RESULTS

Specimen	Ultimate		at 0.5% strain
	Strength MPa (Ksi)	Strain γ_{12} μmm/mm	Modulus GPa (Msi)
1	85.5 (12.4)	21,401	3.79 (0.55)
2	—	—	—
3	84.1 (12.2)	21,650	4.69 (0.68)
4	60.7 (8.8)	15,475	4.69 (0.68)
5	68.9 (10.0)	12,699	6.07 (0.88)
6	86.2 (12.5)	23,301	5.10 (0.74)
7	91.0 (13.2)	22,035	6.55 (0.95)
8	100.7 (14.6)	20,687	7.66 (1.11)
9	80.7 (11.7)	18,441	5.72 (0.83)
10	77.2 (11.2)	13,631	7.73 (1.12)
Average	81.7 (11.8)	18,813	5.79 (0.84)

TABLE 6.10

AMERICAN CYANAMID IM6/1806 IOSIPESCU SHEAR TEST RESULTS

Specimen	Ultimate		at 0.5% strain
	Strength MPa (Ksi)	Strain γ_{12} μmm/mm	Modulus GPa (Msi)
1	53.8 (7.8)	20,695	3.38 (0.49)
2	45.5 (6.6)	19,121	2.62 (0.38)
3	62.7 (9.1)	30,596	2.41 (0.35)
4	45.5 (6.6)	13,264	3.72 (0.54)
5	72.4 (10.5)	24,462	2.90 (0.42)
6	49.0 (7.1)	22,469	2.55 (0.37)
7	55.2 (8.0)	16,439	3.93 (0.57)
8	61.4 (8.9)	26,136	2.00 (0.29)
9	70.3 (10.2)	34,574	2.97 (0.43)
10	57.2 (8.3)	23,036	2.90 (0.42)
Average	57.3 (8.3)	23,079	2.97 (0.43)

TABLE 6.11

HEXCEL IM6/F584 IOSIPESCU SHEAR TEST RESULTS

Specimen	Ultimate		at 0.5% strain
	Strength MPa (Ksi)	Strain γ_{12} μmm/mm	Modulus GPa (Msi)
1	77.2 (11.2)	18,331	5.10 (0.74)
2	88.9 (12.9)	23,344	5.17 (0.75)
3	90.3 (13.1)	21,953	6.00 (0.87)
4	114.5 (16.6)	24,288	4.55 (0.66)
5	95.8 (13.9)	23,189	8.28 (1.20)
6	77.2 (11.2)	21,714	6.76 (0.98)
7	77.2 (11.2)	17,058	4.62 (0.67)
8	98.6 (14.3)	25,699	5.86 (0.85)
9	106.9 (15.5)	38,374	5.10 (0.74)
10	94.5 (13.7)	19,356	6.21 (0.90)
Average	93.8 (13.4)	23,330	5.79 (0.84)

TABLE 6.12

NARMCO IM6/5245C IOSIPESCU SHEAR TEST RESULTS

Specimen	Ultimate		at 0.5% strain
	Strength MPa (Ksi)	Strain γ_{12} μmm/mm	Modulus GPa (Msi)
1	82.0 (11.9)	25,871	3.10 (0.45)
2	103.4 (15.0)	24,299	7.31 (1.06)
3	86.2 (12.5)	25,296	4.97 (0.72)
4	106.9 (15.5)	30,955	5.10 (0.74)
5	90.3 (13.1)	28,649	5.72 (0.83)
6	100.0 (14.5)	46,389	4.14 (0.60)
7	103.4 (15.0)	42,154	3.79 (0.55)
8	99.3 (14.4)	39,515	4.48 (0.65)
9	86.2 (12.5)	28,568	2.83 (0.41)
10	97.9 (14.2)	34,623	4.76 (0.69)
Average	95.8 (13.9)	32,632	4.62 (0.67)

TABLE 6.13

ELASTIC CONSTANTS OF FOUR COMPOSITE MATERIALS (CORRECTED TO LAMINATE FIBRE VOLUME)

ELASTIC CONSTANTS	LONGITUDINAL (0) E_{11} GPa AT 0.5% STRAIN	TRANSVERSE (90°) E_{22} GPa AT 0.5% STRAIN	POISSON RATIO ν AT 0.5% STRAIN	SHEAR MODULUS G_{12} GPa AT 0.5% STRAIN		
				IOSIPESCU	±45° TENSILE	10° OFF-AXIS TENSILE
Narmco T300/5208	125.6	7.63	0.33	4.37	3.52	4.75
American Cyanamid IM6/1806	148.7	7.97	0.33	3.07	4.18	6.13
Hexcel IM6/F584	158.8	7.89	0.34	5.42	5.17	7.10
Narmco IM6/5245C	162.9	8.85	0.34	4.96	6.01	6.62

TABLE 6.14

COMPARISONS OF PREDICTED AND MEASURED TENSILE MODULUS $(+45° / 0° / -45° / 90°)_{6S}$ LAMINATES

MATERIAL	TYPES	SHEAR MODULUS USED IN PREDICTION GPa (MSI)	PREDICTED MODULUS AT 0.5% STRAIN GPa (MSI)	MODULUS FROM TESTING AT 0.5% STRAIN GPa (MSI)
T300/5208	a b c	4.4 (0.63) 3.5 (0.51) 4.8 (0.70)	47.9 (6.95) 47.2 (6.85) 48.3 (7.00)	54.4 (7.89) [1.2%]
IM6/1806	a b c	3.1 (0.45) 4.2 (0.61) 6.1 (0.88)	54.8 (7.94) 55.7 (8.08) 57.4 (8.32)	54.3 (7.88) [0.8%]
IM6/F584	a b c	5.4 (0.78) 5.2 (0.75) 7.1 (1.03)	60.0 (8.70) 59.8 (8.67) 61.4 (8.90)	59.6 (8.65) [0.9%]
IM6/5245C	a b c	5.0 (0.72) 6.0 (0.87) 6.6 (0.96)	61.4 (8.90) 62.1 (9.01) 62.7 (9.09)	58.7 (8.51) [0.2%]

a = IOSIPESC U b = ±45° TENSILE c = 10° OFF-AXIS TENSILE

[ ] = COEFFICIENT OF VARIATION

TABLE 6.15

CONSTITUENTS MATERIAL PROPERTIES FOR MICROMECHANIC PREDICTIONS

FIBRES	SHEAR MODULUS G_f (GPa)	POISSON RATIO ν_f
T300	101.6	0.27
IM6	109.4	0.27
MATRIX	**SHEAR MODULUS G_m (GPa)**	**POISSON RATIO ν_m**
5208	1.28	0.35
1806	1.19	0.35
F584	1.53	0.35
5245C	1.22	0.35

TABLE 6.16

A SUMMARY OF PREDICTED SHEAR MODULI FOR EACH MATERIAL USING 7 PREDICTION TECHNIQUES AND TEST RESULTS OF IOSIPESCU SPECIMENS (60% FIBRE VOLUME)

PREDICTED RESULTS				
	T300/5208 (GPa)	IM6/1806 (GPa)	IM6/F584 (GPA)	IM6/5245C (GPa)
STRENGTH OF MATERIALS:	3.13	2.927	3.75	3.0
SEMI-EMPIRICAL: a. b.	6.17 10.20	5.7 9.62	7.24 12.1	5.83 9.85
ELASTICITY: a. b.	4.88 4.89	4.63 4.57	5.82 5.82	4.70 4.68
HALPIN-TSAI	5.25	4.96	6.29	5.07
ADAMS-DONER	5.12	4.76	6.12	4.88
EXPERIMENTAL RESULTS				
IOSIPESCU	4.61	2.93	5.38	4.97

TABLE 6.17

NEAT RESINS AND FIBRES PROPERTIES FOR IN-PLANE SHEAR STRENGTH PREDICTIONS

TYPE	NEAT RESINS				COMPOSITE MATERIALS			
					FIBRES			
	TENSILE MODULUS (E_{11}) GPa	TENSILE STRENGTH (S_{11}) MPa	SHEAR MODULUS (G_m) GPa	SHEAR STRENGTH (S_{12}) MPa	TYPE	SHEAR MODULUS (G_f) GPa	$\frac{\text{FIBRE SHEAR MODULUS}}{\text{RESIN SHEAR MODULUS}}$ (G_f/G_m)	FIBRE VOLUME FRACTION (%)
Narmco 5208	3.4	50.4	1.28	30.2	T300	101.6	$\frac{101.6}{1.28} = 79.4$	74.0
American Cyanamid 1806	3.2	78.0	1.19	46.8	IM6	109.4	$\frac{109.4}{1.19} = 91.9$	68.0
Hexcel F584	4.14	73.1	1.53	43.8	IM6	109.4	$\frac{109.4}{1.53} = 71.5$	69.0
Narmco 5245C	3.3	82.8	1.22	49.7	IM6	109.4	$\frac{109.4}{1.22} = 89.7$	65.0

$S_{12} = 0.6\,S_{11}$

TABLE 6.18

A SUMMARY OF PREDICTED AND EXPERIMENTAL RESULTS OF IN-PLANE SHEAR STRENGTHS

METHOD	PREDICTED RESULTS			
	NARMCO T300/5208 MPa	AMERICAN CYANAMID IM6/1806 MPa	HEXCEL IM6/F584 MPa	NARMCO IM6/5245C MPa
Strength-of-material	30.2	62.9	47.1	57.2
Finite-difference	6.0	15.6	15.9	22.1
TEST	**EXPERIMENTAL RESULTS**			
±45° tensile	94.5	90.7	122.4	117.6
10° off-axis	74.4	59.3	83.4	86.8
Iosipescu	81.7	57.3	93.8	95.8

APPENDIX A

Narmco T300/5208 $G_f = 101.6$ GPa $G_m = 1.28$ GPa $V_f = 0.6$ $V_m = 0.4$

Strength-of-Materials:

$$G_{12} = \frac{G_f G_m}{G_m V_f + G_f V_m}$$

$$= \frac{101.6 \times 1.28}{(1.28)(0.6) + (101.6)(0.4)}$$

$$= \underline{3.13 \text{ GPa}}$$

Semi-Empirical:

a)
$$\frac{1}{G_{12}} = \left[\frac{V_t}{G_f} + \eta_s \frac{V_m}{G_m}\right]$$

$$\eta_s = \frac{1}{2}\left[1 + \frac{G_m}{G_f}\right]$$

$$= \frac{1}{2}\left[1 + \frac{1.28}{101.6}\right]$$

$$= 0.506$$

$$\frac{1}{G_{12}} = \left[\frac{0.6}{101.6} + (0.5)\frac{0.4}{1.28}\right]$$

$$G_{12} = \underline{6.17 \text{ GPa}}$$

b)
$$G_{12} = \frac{G_m}{1 - \sqrt{K_f}\,(1 - G_m/G_f)}$$

$$K_f = 0.785$$

$$G_{12} = \frac{1.28}{1 - \sqrt{0.785}\,(1 - 0.0126)}$$

$$= \underline{10.2 \text{ GPa}}$$

Elasticity:

a)
$$G_{12} = \left[\frac{G_f(1 + C) + G_m(1 - C)}{G_f(1 - C) + G_m(1 + C)}\right]$$

$$C = V_f$$

$$G_{12} = \left[\frac{101.6\ (1.6) + 1.28\ (0.4)}{101.6\ (0.4) + 1.28\ (1.6)}\right] 1.28$$

$$= \underline{4.88 \text{ GPa}}$$

b) $$G_{12} = (1 - C)G_m \frac{2G_f - (G_f - G_m)V_m}{2G_m + (G_f - G_m)V_m} + \frac{(G_f + G_m) - (G_f - G_m)V_m}{(G_f + G_m) + (G_f - G_m)V_m}$$

where C = 0 corresponds to isolated fibres

$$G_{12} = 1.28 \left[\frac{2 \times 101.6 - (101.6 - 1.28)0.4}{2 \times 1.28 + (101.6 - 1.28)0.4}\right]$$

$$= \underline{4.89 \text{ GPa}}$$

c) Halpin-Tsai:

$$\frac{G_{12}}{G_m} = \frac{1 + \xi\eta V_f}{1 - \eta V_f}$$

$$\eta = \frac{(G_f/G_m - 1)}{(G_f/G_m + \xi)}$$

$$\xi = 1 + 40\ V_f^{10}$$

$$= 1 + 40(0.6)$$

$$= 1.243$$

$$\eta = \left[\frac{101.6/1.28 - 1}{101.6/1.28 + 1.243}\right]$$

$$= 0.97$$

$$\frac{G_{12}}{G_m} = \frac{1 + (0.97)(1.243)(0.6)}{1 - (0.97)(0.6)}$$

$$= 4.1$$

$$G_{12} = \underline{5.25 \text{ GPa}}$$

<u>American Cyanamid IM6/1806</u> $G_f = 109.4$ GPa $G_m = 1.19$ GPa $V_f = 0.4$

Strength-of-Materials:

$$G_{12} = \frac{G_f G_m}{G_m V_f + G_f V_m}$$

$$= \frac{109.4 \times 1.19}{1.19 \times 0.6 + 109.4 \times 0.4}$$

$$= \underline{2.93 \text{ GPa}}$$

Semi-Empirical:

a) $$\frac{1}{G_{12}} = \left[\frac{V_f}{G_f} + \eta_s \frac{V_m}{G_m}\right]$$

$$\eta_s = \frac{1}{2}\left[1 + \frac{G_m}{G_f}\right]$$

$$= \frac{1}{2}\left(1 + \frac{1.19}{109.4}\right)$$

$$= \underline{0.505}$$

$$\frac{1}{G_{12}} = \left[\frac{0.6}{109.4} + 0.505\ \frac{0.4}{1.19}\right]$$

$$= \underline{5.71\ \text{GPa}}$$

b)
$$G_{12} = \frac{G_m}{1 - \sqrt{K_f}(1 - G_m/G_f)}$$

$$K_f = 0.785$$

$$G_{12} = \frac{1.19}{1 - \sqrt{0.785}\ \left(1 - \frac{1.19}{109.4}\right)}$$

$$= \underline{9.62\ \text{GPa}}$$

Elasticity:

a)
$$G_{12} = \left[\frac{G_f + (1 + C) + G_m(1 - C)}{G_f(1 - C) + G_m(1 + C)}\right] G_m$$

$$C = V_f$$

$$G_{12} = \left[\frac{109.4\ (1 + 0.6) + 1.19\ (1 - 0.6)}{109.4\ (1 - 0.6) + 1.19\ (1 + 0.6)}\right] 1.19$$

$$= \underline{4.63\ \text{GPa}}$$

b)
$$G_{12} = (1 - C)G_m\ \frac{2G_f - (G_f - G_m)V_m}{2G_m + (G_f - G_m)V_m} + CG_f\ \frac{(G_f + G_m) - (G_f - G_m)V_m}{(G_f + G_m) + (G_f - G_m)V_m}$$

C = 0 corresponds to isolated fibres

$$G_{12} = 1.19\ \left[\frac{2 \times 109.4 - (109.4 - 1.19)\ 0.4}{2 \times 1.19 + (109.4 - 1.19)\ 0.4}\right]$$

$$= \underline{4.57\ \text{GPa}}$$

c) Halpin-Tsai:

$$\frac{G_{12}}{G_m} = \frac{1 + \xi\ \eta\ V_f}{1 - \eta\ V_f}$$

$$\eta = \frac{(G_f/G_m - 1)}{(G_f/G_m + \xi)}$$

$$\xi = 1 + 40\ V_f^{10}$$

$$= 1 + 40(0.6)^{10}$$

$$= 1.243$$

$$\eta = \left[\frac{109.4/1.19 - 1}{109.4/1.19 + 1.243}\right]$$

$$= 0.976$$

$$\frac{G_{12}}{G_m} = \frac{1 + (0.976)(1.243)(0.6)}{1 - (0.976)(0.6)}$$

$$G_{12} = \underline{4.96 \text{ GPa}}$$

Hexcel IM6/F584 $G_f = 109.4$ GPa $G_m = 1.53$ GPa $V_f = 0.6$ $V_m = 0.4$

Strength-of-Materials:

$$G_{12} = \frac{G_f}{G_m V_f + G_f V_m}$$

$$= \frac{109.4 \times 1.53}{1.53 \times 0.6 + 109.4 \times 0.4}$$

$$= \underline{3.75 \text{ GPa}}$$

Semi-Empirical:

a)

$$\frac{1}{G_{12}} = \left[\frac{V_f}{G_f} + \eta_s \frac{V_m}{G_m}\right]$$

$$\eta_s = \frac{1}{2}\left(1 + \frac{G_m}{G_f}\right)$$

$$= \frac{1}{2}\left(1 + \frac{1.53}{109.4}\right)$$

$$= 0.507$$

$$\frac{1}{G_{12}} = \left[\frac{0.6}{109.4} + 0.507\ \frac{0.4}{1.52}\right]$$

$$G_{12} = \underline{7.24 \text{ GPa}}$$

b)

$$G_{12} = \frac{G_m}{1 - \sqrt{K_f}\ (a - G_m/G_f)}$$

$$K_f = 0.785$$

$$G_{12} = \frac{1.53}{1 - \sqrt{0.785}\ (1 - 0.014)}$$

Elasticity:

a) $$G_{12} = \left[\frac{G_f(1 + C) + G_m(1 - C)}{G_f(1 - C) + G_m(1 + C)}\right] G_m$$

$$C = V_f$$

$$= \left[\frac{109.4\ (1 + 0.6) + 1.52\ (0.4)}{109.4\ (0.4) + 1.53\ (1.6)}\right] 1.53$$

$$= \underline{5.82\ \text{GPa}}$$

b) $$G_{12} = (1 - C)\ G_m \frac{2G_f - (G_f - G_m)V_m}{2G_m + (G_f - G_m)V_m} + CG_f \frac{(G_f + G_m) - (G_f - G_m)V_m}{(G_f + G_m) + (G_f - G_m)V_m}$$

where C = 0 corresponds to isolated fibre

$$G_{12} = 1.53 \left[\frac{2 \times 109.4 - (109.4 - 1.53)\ 0.4}{2 \times 1.53 + (109.4 - 1.53)\ 0.4}\right]$$

$$= \underline{5.82\ \text{GPa}}$$

c) Halpin-Tsai:

$$\frac{G_{12}}{G_m} = \frac{1 + \zeta\ \eta\ V_f}{1 - \eta\ V_f}$$

$$\eta = \frac{(G_f/G_m - 1}{(G_f/G_m + \zeta}$$

$$\xi = 1 + 40\ V_f^{10}$$

$$= 1 + 40\ (0.6)^{10}$$

$$= 1.243$$

$$G_{12} = \frac{1 + (0.969)(1.243)(0.6)}{1 - (0.969)(0.6)}$$

$$G_{12} = \underline{6.29\ \text{GPa}}$$

Narmco IM6/5245C $G_f = 109$ GPa $G_m = 1.22$ GPa $V_f = 0.6$ $V_m = 0.4$

Strength-of-Materials:

$$G_{12} = \frac{G_f G_m}{G_m V_f + G_f V_m}$$

$$= \frac{109.4 \times 1.22}{1.22 \times 0.6 + 109.4 \times 0.4}$$

$$= \underline{3.0 \text{ GPa}}$$

Semi-Empirical:

a)
$$\frac{1}{G_{12}} = \left[\frac{V_f}{G_f} + \eta_s \frac{V_m}{G_m}\right]$$

$$\eta_s = \frac{1}{2}\left(1 + \frac{G_m}{G_f}\right)$$

$$= \frac{1}{2}\left(1 + \frac{1.22}{109.4}\right)$$

$$= 0.506$$

$$\frac{1}{G_{12}} = \left[\frac{0.6}{109.4} + 0.506\ \frac{0.4}{1.22}\right]$$

$$= 5.83 \text{ GPa}$$

b)
$$G_{12} = \frac{G_m}{1 - \sqrt{K_f}\,(1 - G_m/G_f)}$$

$$K_f = 0.785$$

$$G_{12} = \frac{1.22}{1 - \sqrt{0.785}\,(1 - 0.011)}$$

$$= \underline{9.85 \text{ GPa}}$$

Elasticity:

a)
$$G_{12} = \left[\frac{G_f(1 + C) + G_m(1 - C)}{G_f(1 - C) + G_m(1 + C)}\right] G_m$$

$$C = V_f$$

$$G_{12} = \left[\frac{109.4\ (1 + 0.6) + 1.22\ (1 - 0.6)}{109.4\ (1 - 0.6) + 1.22\ (1 + 0.6)}\right] 1.22$$

$$= \underline{4.70 \text{ GPa}}$$

b) $$G_{12} = (1 - C)\, G_m \frac{2G_f - (G_f - G_m)V_m}{2G_m + (G_f - G_m)V_m} + CG_f \frac{(G_f + G_m) - (G_f - G_m)V_m}{(G_f + G_m) + (G_f - G_m)V_m}$$

where C = 0 corresponds to isolated fibres

$$G_{12} = 1.22 \left[\frac{2 \times 109.4 - (109.4 - 1.22)\ 0.4}{2 \times 1.22 + (109.4 - 1.22)\ 0.4}\right]$$

$$= \underline{4.68 \text{ GPa}}$$

c) Halpin-Tsai:

$$\frac{G_{12}}{G_m} = \frac{1 + \zeta \eta V_f}{1 - \eta\, V_f}$$

$$\eta = \frac{(G_f/G_m - 1}{(G_f/G_m + \zeta}$$

$$\xi = 1 + 40V_f^{10}$$

$$\xi = 1 + 40\ (0.6)^{10}$$

$$= 1.243$$

$$\eta = \left[\frac{109.4/1.22 - 1}{109.4/1.22 + 1.243}\right]$$

$$= 0.975$$

$$\frac{G_{12}}{G_m} = \frac{1 + \xi\eta\ V_f}{1 - \eta V_f}$$

$$= \frac{1 + (0.975)(1.243)(0.6)}{1 - (0.975)(0.6)}$$

$$G_{12} = \underline{5.07 \text{ GPa}}$$

APPENDIX B

I. Strength-of-Materials Approach:

$$\tau_{12} = \frac{S_{ms}}{SCF}$$

where S_{ml} = ultimate tensile strength of matrix

S_{mc} = ultimate shear strength of matrix

$S_{ms} = 0.6\ S_{ml}$ (estimated)

SCF = stress concentration factor

$$= \frac{1 - V_f[1 - (G_m/G_f)]}{1 - (4V_f/\pi)^{\frac{1}{2}}[1 - (G_m/G_f)]}$$

V_f = fibre volume fraction

Narmco T300/5208 $S_{ms} = 30.2$ MPa $V_f = 0.7$ $G_m/G_f = 0.0126$

$$SCF = \frac{1 - 0.74\ (1 - 0.0126)}{[1 - (4 \times 0.74/\pi)]^{\frac{1}{2}}\ (1 - 0.0126)}$$

$$= \frac{0.27}{(0.24)\ (0.99)} = \frac{0.27}{0.23} = 1.1$$

$$\tau = \frac{30.2}{1.1} = 30.2 \text{ MPa}$$

American Cyanamid IM6/1806 SMS = 46.8 $V_f = 0.68$ $G_m/G_f = 0.0113$

$$SCF = \frac{1 - 0.68\ (1 - 0.0113)}{[1 - (4 \times 0.68/\pi)]^{\frac{1}{2}}\ (1 - 0.0113)}$$

$$= \frac{0.27}{(0.37)(0.99)} = \frac{0.27}{0.36} = 0.74$$

$$\tau = \frac{46.8}{0.74} = \underline{62.9 \text{ MPa}}$$

Hexcel IM6/F584 $S_{mg} = 43.8$ $V_f = 0.69$ $G_m/G_f = 0.0141$

$$SCF = \frac{1 - 0.69\ (1 - 0.0141)}{[1 - (4 \times .69/\pi)]^{\frac{1}{2}}\ (1 - 0.0141)}$$

$$= \frac{0.32}{(0.35)(0.99)} = 0.93$$

$$\tau_{12} = \frac{43.8}{0.93} = \underline{47.1 \text{ MPa}}$$

Narmco IM6/5245C $S_{ms} = 49.7$ $V_f = 0.65$ $G_m/G_f = 0.0113$

$$SCF = \frac{1 - 0.65\ (1 - 0.0113)}{\left[1 - (4 \times .65/\pi)^{\frac{1}{2}}\right]\ (1 - 0.0113)}$$

$$= \frac{0.357}{(0.415)(0.99)} = 0.87$$

$$\tau = \frac{49.7}{0.87} = \underline{57.2\ \text{MPa}}$$

II. Advanced Method Approach:

Narmco T300/5208 at $G_f/G_m = 79.4$ and 74% fibre volume

From Figure 3.9 SCF = 5

$$\tau = \frac{30.2}{5} = 6.04\ \text{MPa}$$

American Cyanamid IM6/18.6 at $G_f/G_m = 91.9$ and 68% fibre volume

From Figure 3.9 SCF = 3

$$\tau = \frac{46.8}{3} = 15.6\ \text{MPa}$$

Hexcel IM6/F584 at $G_f/G_m = 71.5$ and 69.9% fibre volume

From Figure 3.9 SCF = 2.75

$$\tau = \frac{43.8}{2.75} = 15.9\ \text{MPa}$$

Narmco IM6/5245C at $G_f/G_m = 89.7$ and 65% fibre volume

From Figure 3.9 SCF = 2.25

$$\tau = \frac{49.7}{2.25} = 22.1\ \text{MPa}$$